PAIGE NOEL MCKEON

paige.mckeon@som.umaryland.edu

EDUCATION

B.S. in Behavioral and Systems Neuroscience
Michigan State University (MSU)
Lyman Briggs Residential College
East Lansing, MI
August 2013 – May 2017

Ph.D. in Molecular Medicine
University of Maryland School of Medicine (UMSOM)
Graduate Program in Life Sciences
Molecular Medicine Program
Thesis Advisor: Brian N. Mathur, Ph.D.
Baltimore, MD
August 2017 – June 2023

HONORS, AWARDS, & MEMBERSHIPS

Feb 2023	AAAS Mass Media Science and Engineering Fellowship Semi-Finalist
2020-2022	Research Society on Alcoholism (RSA) Student Membership
Sept 2022	DC Science Writers Association (DCSWA)
Sept 2022	National Association of Science Writers (NASW)
March 2022	Association for Women in Science (AWIS) Student Membership
March 2022	Clearest Data Presentation Award (UMSOM Neuroscience Mini-Retreat)
August 2019	Graduate Student Association Travel Award
2013-2017	Dean's Honors List at Michigan State University
2013-2017	Academic Scholar's Program (ASP) at Michigan State University
2014-2015	Distinguished Member Award for Neuroscience Club at Michigan State University

RESEARCH EXPERIENCE

Ph.D. Research
Thesis Advisor: Brian N. Mathur, Ph.D.
Department of Pharmacology
University of Maryland School of Medicine
Investigating Mechanisms of Ethanol Reward in the Nucleus Accumbens
2018 – Present

Ph.D. Rotation Research
Mentor: Dennis Sparta, Ph.D.
Department of Anatomy and Neurobiology
University of Maryland School of Medicine
June 2018 – Aug 2018

Ph.D. Rotation Research
Mentors: Claire Fraser, Ph.D.; Sylvia Beurmann Ph.D.
Institute for Genome Sciences
University of Maryland School of Medicine
April 2018 – June 2018

Ph.D. Rotation Research
Mentor: Brian N. Mathur, Ph.D.
Department of Pharmacology
University of Maryland School of Medicine
Dec 2017 – Mar 2018

Mentored Undergraduate Research
Mentors: William Atchison, Ph.D.; Rosa Jaiman, Ph.D.
Michigan State University Department of Pharmacology and Toxicology
"MeHg-induced Cytotoxicity through Vesicular Release of Glutamate in Mouse Primary Cerebellar and Cortical Astrocytes Culture"
June 2015 – May 2017

Mentored Undergraduate Research
Mentors: Alexandra Burt, Ph.D.; Brooke Slawinksi Ph.D.
Michigan State University Twin Registry
"Neuroticism moderates the relationship between fear of crime and quality of life"
Dec 2014 – May 2015

PUBLICATIONS

McKeon PN, Patton MH, Padgett KE, Abel, E, Sheats, S, Mathur BN. The rewarding properties of ethanol are mediated by BDNF signaling in the nucleus accumbens core. *In preparation.*

McKeon PN*, Bunce GW*, Patton MH, Chen R, Mathur BN. (2022). Cortical control of striatal fast-spiking interneuron synchrony. The Journal of Physiology. 600(9), 2189–2202.

McKeon PN*, Mathur BN. (2021). On location for cannabinoid control of multimodal behavior. Neuron. 109(9): 1416-1418.

Girven KS, Aroni S, Navarrete J, Marino RAM, **McKeon PN**, Cheer JF, Sparta DR. (2021). Glutamatergic input from the insula to the ventral bed nucleus of the stria terminalis controls reward-related behavior. Addiction Biology. 26(3): e12961.

Patton MH, Padgett KE, **McKeon PN**, Qadir H, Patton MS, Mu C, Roberts BM, Mathur BN. (2019). TrkB-dependent disinhibition of the nucleus accumbens is enhanced by ethanol. Neuropsychopharmacology. 44(6): 1114-1122.

Patton MH, Padgett KE, **McKeon PN**, Lu SG, Abrams TW, Mathur BN. (2019). An Aplysia-like synaptic switch for rapid protection against ethanol-induced synaptic inhibition in a mammalian habit circuit. Neuropharmacology. 144: 1-8.

ORAL AND POSTER PRESENTATIONS

Sept 2018-23	Biannual Lab Meetings (UMSOM), *Oral Presentations*
Mar 2023	Program in Neuroscience Recruitment Symposium, *Poster Presentation*
Nov 2022	Molecular Medicine Program (UMSOM) Seminar, *Oral Presentation*
Oct 2022	Gordon Research Conference, *Poster Presentation*
Oct 2022	Gordon Research Seminar, *Poster Presentation*
Oct 2022	Gordon Research Seminar, *Oral Presentation*
Jun 2022	Research Society on Alcoholism, *Poster Presentation*
Jun 2022	Program in Neuroscience (UMSOM) Retreat, *Poster Presentation*
Mar 2022	Program in Neuroscience (UMSOM) Mini Retreat, *Poster Presentation*
June 2019	Research Society on Alcoholism, *Poster Presentation*
June 2019	Program in Neuroscience (UMSOM) Retreat, *Poster Presentation*
June 2018	Program in Neuroscience (UMSOM) Retreat, *Poster Presentation*
Mar 2017	The Annual Meeting of the Society of Toxicology, *Poster Presentation*
Nov 2016	Integrative Pharmacological Sciences Training Program Grant Retreat (MSU), *Poster Presentation*
Oct 2016	Michigan Society of Toxicology, *Poster Presentation*
Aug 2016	Bridge to Ph.D. in Neuroscience Summer Program (MSU), *Oral Presentation*
Aug 2016	Mid-Michigan Symposium for Undergraduate Research Experience (MSU), *Poster Presentation*
May 2015	Undergraduate Research and Arts Forum (MSU), *Poster Presentation*

TEACHING EXPERIENCE

Jan-May 2017	Neuroscience Lab (NEU 311L) at MSU – *Learning Assistant*
Sep-Dec 2016	Capital Area Literacy Coalition's Read to Succeed Program – *Tutor*
Jul-Aug 2016	Bridge to Ph.D. in Neuroscience Summer Program at MSU - *Trained Undergraduate Participants*

Abstract

Title of Dissertation: Less is more: alcohol weakens inhibitory signaling to strengthen striatal complex output

Paige McKeon, Doctor of Philosophy, 2023

Dissertation directed by: Brian Mathur, PhD, Associate Professor, Department of Pharmacology

The striatal complex critically integrates a variety of inputs to regulate the motivation to perform, and the performance of, discrete action sequences executed under goal-directed and habitual strategies. Drugs of abuse such as alcohol target the striatal complex, strengthening associations between rewards and external cues and, over time, shifting intake from being goal-oriented toward compulsively automated. Our work herein examines alcohol targeting of the striatal complex under two different conditions: under the first condition, we ultimately aim to determine if and how alcohol alters the firing of a GABAergic cellular population called fast-spiking interneurons (FSIs) known to regulate striatal output to mediate habitual behaviors. To that end, we uncover a novel mechanism mediating FSI synchronous firing. Under the second condition, we examine how acute alcohol exposure influences the experience of reward. Alcohol strengthens a form of inhibitory plasticity in the NAc that is mediated by brain derived neurotrophic factor (BDNF) signaling, but whether this interaction regulates alcohol reward is unknown. We here discover the sources of BDNF that drive this form of plasticity and further find that simulating BDNF-releasing afferents *in vivo* is rewarding to mice. We also find that alcohol and BDNF may interact in vivo to mediate reward. As such, these findings point to a novel mechanism for alcohol reward: BDNF signaling at inhibitory synapses in the NAc.

Less is more: alcohol weakens inhibitory signaling to strengthen striatal complex output

by

Paige N. McKeon

Dissertation submitted to the Faculty of the Graduate School of the
University of Maryland, Baltimore in partial fulfillment
of the requirements for the degree of
Doctor of Philosophy
2023

Dedication

To my parents Matt and Beth.

Many thanks to:

My thesis committee: Drs. Thomas Blanpied, Mary Kay Lobo, Alexandre Medina de Jesus, Paul Shapiro, and Dennis Sparta for their thoughtful feedback on my thesis and all their support. Special thanks to Drs. Mary Kay Lobo and Alexandre Medina de Jesus for their comments and edits as readers of this dissertation.

My qualifying exam committee: Drs. Todd Gould, Alexandre Medina de Jesus, Paul Shepard, and Jeffrey Winkles for their support during what was the scariest hurdle of this entire process.

Drs. Claire Fraser and Dennis Sparta for taking me on as a rotation student.

Dr. Toni Antalis, director of the Molecular Medicine Program, and Dr. William Randall, director of the Toxicology Program (to which I was admitted before it disbanded). Their support meant a lot to me in the first couple years of grad school as I struggled through coursework.

Chelsea Leonard for her assistance and guidance as the Academic Service Specialist for the Molecular Medicine Program.

Garrett Bunce, co-first author to the publication in Chapter 2 and a literal actual computational modeling wizard.

Mathur lab members I've known: Dr. Mike White, Dr. Kara Cover, Chaoqi Mu, Willa Kerkhoff, Dr. Michael Patton, Dr. Houman Qadir, Morgan Heckman, Abby Lieberman, Brent Stewart, Maxwell Madden, Alli Siclair, Kat Pizano, and Tomi Oladunni.

Mathur lab members past and present for their contributions to this dissertation: Dr. Bradley Roberts, Ellie Abel, Sam Sheats, and especially Dr. Mary Patton who set all these projects in motion and whose guidance over email, well-organized notebooks, and dropbox files were pivotal to my understanding of these projects when I first started out.

A special thanks to Mathur lab alumna and close friend Katie Padgett who not only contributed to the projects herein, but who also took me under her wing during my Mathur lab rotation and taught me most of my first techniques. I'll always cherish the memories of us hoovering Big Mac meals whilst patch clamping together.

Massive thank you to my family and all my other friends for the ways you've been there for me during one of the greatest endeavors of my life; for putting up with me during my low lows but also being there to help celebrate the high highs along the way. Especially Sara, who was my roommate for most of the time I've been in this program (and through a pandemic!). I almost certainly would not have made it this far without her friendship and support. Thank you.

And of course the biggest thanks of all goes to my mentor Dr. Brian Mathur. His passion for science exploration and appreciation for the wonderful stories that rigorous experimentation creates immediately drew me to his lab. And his patience, constructive feedback, and encouragement of me to believe in and challenge myself have helped me grow not only as a scientist and critical thinker, but also as a person.

Table of Contents

Figures

Abbreviations

6-OHDA	6-hydroxydopamine
AA	Alcoholics anonymous
AAV	Adeno-associated virus
aCSF	Artificial cerebrospinal fluid
AMPA	A-amino-3-hydroxy-5-methyl-4-isoxazolepropionic acid
AP	Action potential
AUD	Alcohol use disorder
BAC	Blood alcohol concentration
BDNF	Brain-derived neurotrophic factor
BLA	Basolateral amygdala
CB1	Cannabinoid type 1 receptor
CBP	CREB-binding protein
CeA	Central amygdala
CHI	Cholinergic interneuron
ChR2	Channelrhodopsin
CIE	Chronic intermittent exposure
CPP	Conditioned place preference

CREB	cAMP-response element binding protein
CTX-B	Cyclotraxin B
DID	Drinking in the Dark
D1R	Dopamine 1-like receptor
D2R	Dopamine 2-like receptor
D3R	Dopamine 3 receptor
DAT	Dopamine transporter
DLS	Dorsolateral striatum
DMS	Dorsomedial striatum
eCB	Endocannabinoid
eGFP	Enhanced green fluorescent protein
eIPSC	Electrically-evoked inhibitory postsynaptic current
eLFS	Electrical low frequency stimulation
EPSC	Excitatory postsynaptic current
ERK	Extracellular signal-regulated kinase
EtOH	Ethanol
EPSC	Excitatory postsynaptic current
eYFP	Enhanced yellow fluorescent protein

fMRI	Functional magnetic resonance imaging
FSI	Fast-spiking interneuron
GABA	Gamma-aminobutyric acid
IHC	Immunohistochemistry
iLTD	Inhibitory long-term depression
i.p.	Intraperitoneal
IPSC	Inhibitory postsynaptic current
LED	Light-emitting diode
LFS	Low frequency stimulation
LH-MFB	Lateral hypothalamus-medial forebrain bundle
LSD-1	Lysine-specific histone demethylase 1
LTD	Long-term depression
LTP	Long-term potentiation
LTSI	Low-threshold spiking interneuron
MAPK	Mitogen-activated protein kinase
mPFC	Medial prefrontal cortex
mRNA	Messenger ribonucleic acid
MSN	Medium spiny projection neuron

NAc	Nucleus accumbens
Npas4	Neuronal Per Arnt Sim domaine protein 4
NMDA	N-methyl-D-aspartic acid
NMDG	N-methyl-D-glucamine
n.s.	Not significant
oIPSC	Optically-evoked inhibitory postsynaptic current
OFC	Orbitofrontal cortex
oLFS	Optical low frequency stimulation
P75NTR	p75 neurotrophin receptor
PFA	Paraformaldehyde
PFC	Prefrontal cortex
PKA	Protein kinase A
plPFC	Prelimbic prefrontal cortex
PV	Parvalbumin
PVT	Paraventricular thalamus
RACK1	Receptor for activated C kinase 1
RMP	Resting membrane potential
SD	Standard deviation

SEM	Standard error of the mean
SSI	Somatostatin interneuron
TH	Tyrosine hydroxylase
TrkB	Tyrosine receptor kinase B
Val66Met	Valine 66 to methionine mutation
VTA	Ventral tegmental area

Chapter 1: Introduction

At the heart of preclinical and clinical investigations towards developing treatments for alcohol use disorder (AUD) lies two questions: why do people drink alcohol? And why do some people drink so much that they develop AUD?

To address these unknowns, an understanding of the brain circuitry, cell types, and integration of circuits that regulate alcohol intake across stages of alcohol use, misuse, and addiction is critical.

1.1 The striatal complex

The striatal complex of the basal ganglia integrates a variety of diverse inputs to enable the motivation to perform, and the performance of, discrete action sequences executed under goal-directed and habitual strategies. It can be divided into two functionally discrete regions: the dorsal striatum, which controls motor sequences and cognitive functions, and the ventral striatum, which regulates motivated behaviors (Chen et al., 2020; Alexander et al., 1986; Wichman and Delong, 1996). The wide variety of behaviors encompassed by striatal activity can be attributed to the fact that it is innervated by excitatory glutamatergic motor, sensory, associative, and limbic cortices (Hunnicutt et al., 2016; Alexander et al., 1986; Haber, 2016). The dorsal striatum contains the caudate nucleus (dorsomedial striatum or DMS) and putamen (dorsolateral striatum or DLS; Alexander et al., 1986; Middleton and Strick, 2000). The ventral striatum contains the nucleus accumbens (NAc) and olfactory tubercle (Russo et al., 2010; Grueter et al., 2012). The NAc can be even further segregated into the NAc core and NAc shell, with the core

bearing more similarity to the dorsal striatum and the shell more often compared to the amygdala (Zahm and Brog, 1992; Groenewegen et al., 1999). Cell types expressed in dorsal and ventral striata are relatively consistent (Gerfen, 1992; Nicola et al., 2000; Stuber et al., 2012). The predominant neuron population expressed in the striatal complex is inhibitory (GABAergic) medium spiny projection neurons (MSNs; Hedreen and Holm, 1992). MSNs are generally classified into two subgroups based on whether they release dynorphin or enkephalin as well as whether they express dopamine 1- or 2-like receptors (D1R and D2R, respectively; Gerfen, 1992; Gerfen and Surmeier, 2011). Interneurons are also contained within the striatum. Providing potent GABAergic control over MSNs are parvalbumin-expressing, fast-spiking interneurons (FSIs) and low threshold-spiking interneurons (LTSIs), but there are also modulatory cholinergic interneurons (CHIs, also known as tonically active neurons or TANs; Kita et al., 1990; Kawaguchi, 1993; Tepper and Bolam, 2004; Chuhma et al., 2011; Ribeiro et al., 2019). MSNs may also target each other via inhibitory synapses (Taverna et al., 2007), though this is much more likely to occur in dorsal striatum than ventral striatum (Chuhma et al., 2011). Powerful activation of glutamatergic inputs onto dorsal and ventral striatum MSNs is required to drive MSNs to fire due to the powerful inhibition from GABAergic interneurons, which act as a sort of filter for extraneous excitation.

1.2 Reward and goal-directed behavior circuitry

Initiation and continuation of approach towards rewarding stimuli as well as avoidance of aversive stimuli is mediated by the integration of a variety of inputs by NAc MSNs (Salamone and Correa, 2002; Pezze and Feldon, 2004; Klawonn and Malenka,

2018). It is canonically accepted that MSNs expressing D1R activate the “direct” pathway by targeting the ventral pallidum to inhibit GABAergic ventral tegmental area (VTA) neurons to mediate motivated behaviors, while MSNs expressing D2R activate the “indirect” pathway by inhibiting the VTA directly to regulate either suppression of satiety or aversion (Hikida et al., 2010; Sesack and Grace, 2010; Xia et al., 2011; Tai et al., 2012; Hikida et al., 2013; Yamaguchi et al., 2015; Nguyen et al., 2018; Sandoval-Rodriguez et al., 2023; Nakanishi et al., 2014; Volkow and Morales, 2015). However, while much remains unknown about how NAc MSN output is controlled in the regulation of reward and aversion, these output pathways are highly disputed (White and Hiroi, 1991; Kupchik et al., 2015; Soares-Cunha et al., 2016; Kupchik and Kalivas, 2017; Soares-Cunha et al., 2020; Soares-Cunha et al., 2022; Zhou et al., 2022; Da Cunha et al., 2012; Soares-Cunha et al., 2016). More specifically: while the VTA does seem predominantly innervated by D1R MSNs, ~50% of D1R MSNs also target the ventral pallidum along with D2R MSNs (Lu et al., 1998; Kupchik et al., 2015; Soares-Cunha et al., 2020). Furthermore, a separate subpopulation of MSNs expressing both D1R and D2R exists along a ventromedial gradient from 7.3 to 14.6% in NAc core and shell, respectively (Surmeier et al., 1996; Gagnon et al., 2017).

Much has been revealed about the intricacies of NAc circuitry through optogenetics (Britt et al., 2012; Stuber et al., 2012), immunohistochemistry (Phillipson and Griffiths, 1985), and tracing studies (Friedman et al., 2002). Excitatory glutamatergic inputs into the NAc come from amygdala, prefrontal cortex (PFC), ventral hippocampus, and thalamus (Phillipson and Griffiths, 1985; Friedman et al., 2002; Britt et al., 2012; also summarized in Sesack and Grace, 2010) and the strength of these synapses can be modulated by VTA

dopamine neurons (Stuber et al., 2012; Nicola et al., 2000; Yu et al., 2019). Dopaminergic (modulatory) and GABAergic (inhibitory) inputs from the VTA also target the NAc. Interestingly, VTA dopaminergic inputs display heterogeneity, with some co-releasing glutamate or GABA onto MSNs in addition to dopamine (Stuber et al., 2010; Tecuapetla et al., 2010; Tritsch et al., 2014). The timing and concentration of dopamine released from the VTA depends upon a balance between vesicular release, dopamine transporter (DAT) reuptake, and diffusion (Rice and Cragg, 2008). Dopamine neurons can control their own activity as well, by inhibiting themselves via D2R auto-receptor signaling (Ford, 2014). Presynaptic D2R activation on dopamine neurons also controls DAT functioning by increasing its activity (Lee et al., 2007). Glutamatergic projections can reciprocally modulate VTA dopamine neuron activity, inhibiting dopamine release via ionotropic glutamate receptors (kainite, AMPA, or NMDA; Avshalumov et al., 2008; Yavas and Young, 2017) or via activation of metabotropic receptors if synaptic overflow of glutamate occurs due to high intensity stimulation (Zhang and Sulzer, 2004; Yavas and Young, 2017). But glutamate can also activate dopamine terminals, as others have seen that optogenetic activation of glutamatergic prefrontal cortex inputs drives dopamine release (Mateo et al., 2017). Serotonin is another monoamine in the NAc, but its effects are dissociable from dopamine. Dopamine reduces MSN responses to excitatory transmission from the paraventricular thalamus (PVT) only, while serotonin reduces MSN responses to the PVT, basolateral amygdala (BLA) and ventral hippocampus (Muramatsu et al., 1998; Mathur et al., 2011; Christoffel et al., 2021).

The overarching understanding about the NAc as an integration center for these inputs is that the glutamatergic inputs encode environmental stimuli including contexts,

cues, and internal states, and the dopaminergic input reinforces these signals (Charara and Grace, 2003; Day et al., 2007; Stuber et al., 2008; Brown et al., 2011; Flagel et al., 2011; Pennartz et al., 2011; Britt et al., 2012). All glutamatergic inputs innervate MSN subpopulations relatively equally (Li et al., 2018) and activation of each glutamatergic input reinforces instrumental behavior as does direct optogenetic activation of NAc MSNs, suggesting that perhaps the amount of glutamate released is more important to consider than the specific projection releasing glutamate (Britt et al., 2012). However, this is contradicted by a tracing study finding that afferents from NAc MSNs to the ventral pallidum receive no synaptic contact with prefrontal cortex and ventral hippocampus (Papp et al., 2012) and others associating hippocampus activation to contextual information, the amygdala to emotionally salient events, and the PFC with cue value (Everitt and Wolf, 2002; Kelley, 2004; Pennartz et al., 2011; Russo and Nestler, 2013). Measuring synaptic strength of these inputs has also revealed some discrete specificity, though there is disparity between studies about exactly how the projections differ in synaptic strength onto MSN subpopulations. Deroche and Yocky find that excitatory synaptic strength from the amygdala is greatest on D1R MSNs while PFC and hippocampus strength is greater on D2R MSNs (2021), yet others using similar approaches find that there are stronger inputs from hippocampus onto D1R MSNs due to more synaptic connections on D1R MSN dendrites (MacAskill et al., 2012; Scudder et al., 2018). It is possible these disparities are due to slight differences in experimental strategies, namely viral injection locations. Ultimately though, it is agreed that synaptic plasticity occurring at glutamatergic projections into the NAc is a crucial mechanism by which particularly salient stimuli, such

as drugs of abuse, strengthen NAc output (Schotanus and Chergui, 2008; Sun et al., 2008; Kheirbek et al., 2009; Schmidt and Pierce, 2010; Wolf and Ferrario, 2010; Schultz, 2011).

GABAergic innervation of NAc MSNs comes predominantly from other MSNs and interneuron populations within the NAc, as previously mentioned. The role of GABA signaling in the NAc and its interplay with other systems is largely unknown. Interneurons also rely on excitation from PFC, amygdala, ventral hippocampus, and VTA (Qi et al., 2016; Yu et al., 2017; Scudder et al., 2018; Trouche et al., 2019), though their integration of these inputs is far stronger than that of MSNs (Wright et al., 2017; Yu et al., 2017; Scudder et al., 2018). FSIs are the major source of inhibition in the NAc (Qi et al., 2016; Wright et al., 2017; Yu et al., 2017; Schall et al., 2021). Contradictory optogenetic studies (Qi et al., 2016 versus Chen et al., 2019, for example) unpacking the behavioral consequences of NAc FSI activation ultimately point to the fact that FSIs, which are typically uncoordinated during reward-seeking tasks (Berke, 2008), may be difficult to examine experimentally without using broad network activation or inhibition (Covey and Yocky, 2021). LTSIs also provide inhibitory control over both D1R and D2R MSNs (Scudder et al., 2018) following activation from the same excitatory inputs as FSIs and MSNs (Ribeiro et al., 2019). While LTSIs do not modulate NAc output nearly as strongly as FSIs, addiction studies have revealed that their activation enhances the strength of reward experienced by drugs of abuse (Smith et al., 2017; Ribeiro et al., 2019).

CHIs, a source of the neurotransmitter acetylcholine and another source of glutamate, are activated from all the same extra- and intra-striatal projections as the other neurons described, however, they are not targeted by FSIs or other CHIs (Guo et al., 2015). But interestingly, they are predominantly targeted by inhibitory axons (Gonzales and

Smith, 2015). Acetylcholine released from CHIs targets ionotropic nicotinic receptors and metabotropic muscarinic receptors (Gonzales and Smith, 2015). CHIs can directly or indirectly excite external NAc targets via nicotinic receptors on dopaminergic, glutamatergic, or GABAergic neurons (Nelson et al., 2014; Mateo et al., 2017) or through targeting of muscarinic receptors on internal GABA sources (Abudukeyoumu et al., 2019). Feedforward excitation via potentiation of glutamate signaling or inhibition via potentiation of GABA signaling is also possible (Witten et al., 2010; Mateo et al., 2017). CHIs also control dopamine release in the NAc, directly eliciting dopamine release both *ex vivo* and *in vivo* (Zhou et al., 2002; Exley and Cragg, 2008; Mateo et al., 2017). This may be dependent upon the rate of dopamine neuron activity, whereby low firing rate enables facilitation of dopamine release (Mateo et al., 2017). However, high dopamine neuron firing rate, which is associated with reward-seeking behaviors, is associated with suppression of dopamine release by acetylcholine activity (Collins et al., 2016; Collins et al., 2019). Acetylcholine from CHIs also can activate glutamatergic PFC inputs in the NAc, which can facilitate dopamine release from VTA (Mateo et al., 2017). The role of CHIs in reward is ultimately unclear, or otherwise it is complicated. Optogenetics studies have revealed they can suppress (Witten et al., 2010), facilitate (Lee et al., 2016) or have no effect (Witten et al., 2010) on cocaine conditioned place preference (CPP), as an example. See **Figure 1.1** for a circuit map diagram of neurotransmission integration in the NAc.

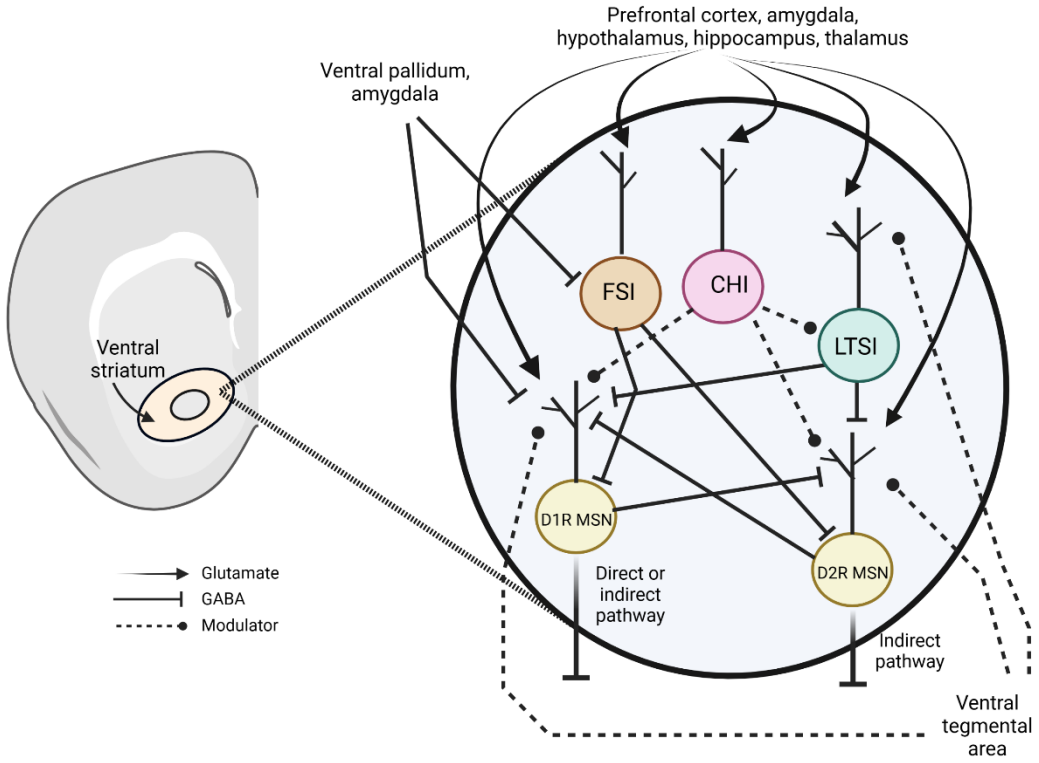

Figure 1.1 Ventral striatum integration of neurotransmission. Left: Location of ventral striatum depicted in a hemisected mouse brain slice. Right: Magnification into ventral striatum depicts integration of inputs onto cell subpopulations. Glutamate is released onto all cell subpopulations within the ventral striatum from the prefrontal cortex, amygdala, hypothalamus, hippocampus, and thalamus. The ventral pallidum and amygdala serve as extrinsic sources of GABA. Fast-spiking interneurons (FSIs) and low threshold-spiking interneurons (LTSIs) release GABA onto both subpopulations of medium spiny neurons (MSNs). MSNs may also inhibit each other. Cholinergic interneurons (CHIs) release acetylcholine onto LTSIs and both subpopulations of MSNs to modulate their activity. MSN subpopulations are characterized by expression of dopamine 1- or 2-like receptors (D1R and D2R, respectively) and their output can activate either the direct pathway (D1R MSNs) or the indirect pathway (both D1R and D2R MSNs). The ventral tegmental area is a source of dopamine for the ventral striatum, but can also co-release glutamate or GABA (see **Figure 1.3** for more detail).

While dopamine receptor expression on MSNs as the mediator of output pathways in the NAc is disputed, this is less so the case in both medial and lateral regions of the dorsal striatum; MSNs expressing D1R are heavily associated with "direct" pathway activation, targeting GABAergic substantia nigra reticulata and the internal segment of the globus pallidus neurons, while those expressing D2R are associated with the "indirect" pathway, targeting GABAergic external segment of the globus pallidus neurons (Gerfen and Wilson; 1996; Gertler et al., 2008; Matamales et al., 2009; Valjent et al., 2009; Bertrain-Gonzalez et al., 2010; Kravitz et al., 2010; Sesack and Grace, 2010 Chuhma et al., 2011; Gerfen and Surmeier, 2012). It is generally understood that both DMS and DLS receive glutamatergic input from thalamus (particularly the intralaminar thalamic nuclei; Smith et al., 2004) and cortex (Groenewegen et al., 1999; Heilbronner et al., 2016). But recent studies have revealed that inputs may be more discrete than previously thought. The weight of inputs onto D1R and D2R differ whereby D1R MSNs receive afferents primarily from secondary motor, visual, and cingulate cortices and D2R MSNs receive inputs primarily from primary motor and sensory cortices as well as the thalamus (Lu et al., 2021). The posterior DMS also may integrate inputs differently than other regions of DMS; prelimbic cortex and BLA inputs both target this region, but only plastic events at prelimbic cortex inputs onto D1R MSNs are critical for goal-directed learning (Fisher et al., 2020). However, the BLA also targets the prelimbic cortex and must be activated for the goal-directed learning mediated by prelimbic-D1R MSN plasticity (Fisher et al., 2020). The FSIs of the dorsal striatum are expressed in a gradient, whereby stronger concentrations of FSIs can be seen in the DLS as compared to the DMS (Schlosser et al., 1999; Luk and Sadikot; 2001;Tepper and Bolam, 2004). FSIs may be more heterogeneous in the dorsal

striatum than in the NAc; it was recently discovered that FSIs in the DMS have increased excitability as compared to DLS FSIs and that only DLS FSIs receive excitatory input from the cingulate cortex (Monteiro et al., 2018).

Dopamine is released into the dorsal striatum from the substantia nigra as well as the lateral VTA (Bolam et al., 2000; Haber et al., 2000; Lerner et al., 2015). It is well supported that dopamine release in the NAc and DMS facilitates the formation of goal-directed, flexible cognition and behavior (Grospe et al., 2018; Wang et al., 2020; van der Merwe et al., 2023), although others have seen that dopamine signaling in the DMS is critical for the development of compulsive reward seeking (Seiler et al., 2022). Similar to the NAc, dopamine release mediates plastic events at glutamatergic inputs onto striatal MSNs (Graybiel, 2008; Surmeier et al., 2007; Wickens et al., 2009; Lovinger, 2010). In the context of behavioral tasks, dopamine can induce long-term potentiation (LTP) and long-term depression (LTD) in D1R- or D2R-expressing MSNs, respectively, to allow the basal ganglia to disinhibit thalamocortical neurons (Frank, 2005). Dopamine activation of D1R facilitates glutamate receptor trafficking thus enhancing excitability of those cells, in opposition to that of D2R activation (Snyder et al., 2000; Sun et al., 2005; Hallet et al., 2006; Gerfen and Surmeier, 2012). LTSIs in the DMS are anatomically close in proximity to dopamine afferents and directly prevent optogenetic induction of dopamine release via activation of $GABA_B$ receptors, thus locally gating dopamine release into the DMS *in vitro* (Holly et al., 2022). *In vivo*, dopamine sensor imaging during operant learning reveals that LTSIs modulate striatal dopamine dynamics (Holly et al., 2022).

Glutamate signaling in the DMS is needed for efficient shifting in response patterns due, at least in part, to its elevation of acetylcholine from CHIs (Palencia and Ragozzino,

2006). CHIs in the DMS are in fact critical for the ability to be behaviorally flexible and less compulsive (Aoki et al., 2015; Martos et al., 2017). It is unclear if these findings are due to the glutamate or the acetylcholine released by CHIs (Bradfield et al., 2013; Prado et al., 2017). But genetically silencing acetylcholine and not glutamate release impairs behavioral flexibility, promotes habit formation, and causes maladaptive eating in mice (Favier et al., 2020). Perhaps pointing to a mechanism, blocking acetylcholine signaling in the DMS is associated with diminished dopamine efflux (Threlfell et al., 2012; Favier et al., 2020). However, this contradicts with other work demonstrating that in both dorsal striatum and NAc, acetylcholine release by CHIs inhibits electrically-evoked dopamine release (Cachope et al., 2012; Foster et al., 2014; Shin et al., 2017). Reciprocally, dopamine signaling modulates acetylcholine release from CHIs in a striatal subregion-specific manner; midbrain dopamine neurons drive pauses in DMS firing mediated by D2R activation while mediating robust bursts in DLS CHIs due to glutamate co-release and activation of muscarinic glutamate receptors (Cai and Ford, 2018). Notably, despite the short bursts in activity in the DMS, the frequency of CHI to MSN neurotransmission is higher in DMS (Cai and Ford, 2018). See **Figure 1.2** for a circuit map depiction of neurotransmission integration in the dorsal striatum,

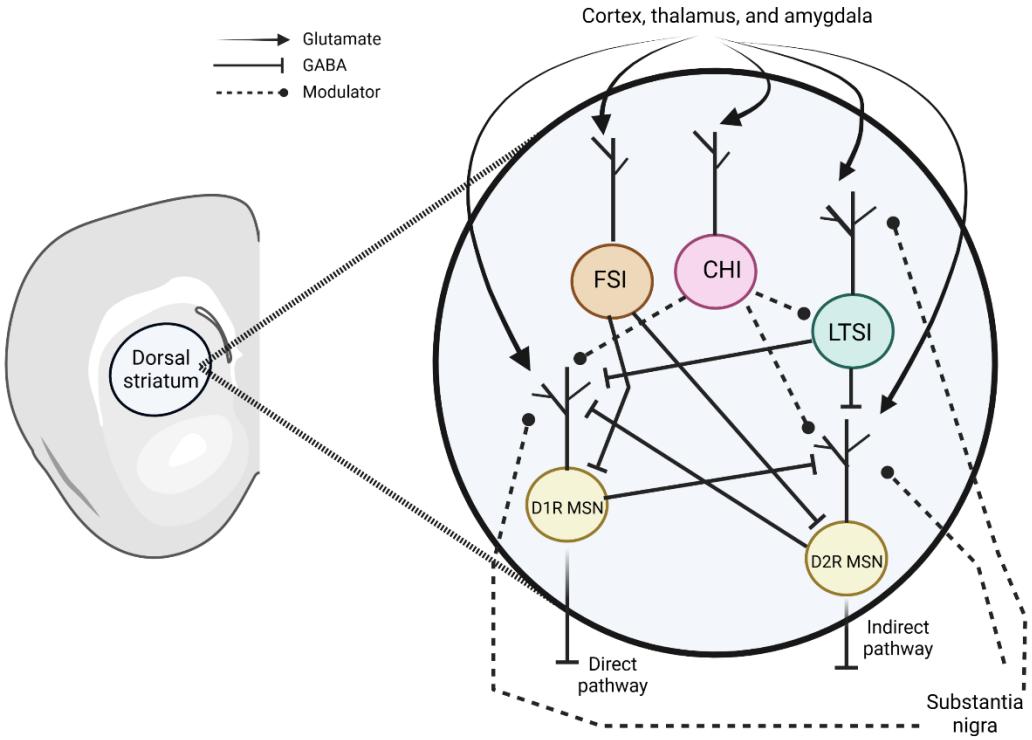

Figure 1.2 Dorsal striatum integration of neurotransmission. Left: Location of dorsal striatum depicted in a hemisected mouse brain slice. Right: Magnification into dorsal striatum depicts integration of inputs onto cell subpopulations. Glutamate is released onto all cell types within the striatum from regions of cortex, thalamus, and amygdala. Fast-spiking interneurons (FSIs) and low threshold-spiking interneurons (LTSIs) release GABA onto both subpopulations of medium spiny neurons (MSNs). MSN subtypes also inhibit each other. Cholinergic interneurons (CHIs) release acetylcholine onto LTSIs and both subpopulations of MSNs to modulate their activity. Dopamine is released from the substantia nigra into the striatum. MSN subpopulations are characterized by expression of dopamine 1- or 2-like receptors (D1R and D2R, respectively) and their output can activate either the direct (D1R MSN) or indirect (D2R MSN) pathways.

1.3 Alcohol hijacks circuitry subserving motivated behavior

One hypothesis is that people drink alcohol because it feels good; alcohol is known to have powerfully rewarding properties. A recent imaging study in humans demonstrated that acute administration of a high (0.8 g/kg) dose of alcohol significantly increases connectivity from reward-related regions to sensory and motor cortices (Han et al., 2021). Others have found that adolescent and young adult social drinkers who subjectively find alcohol more rewarding drink more and have an increased risk of alcohol misuse (Allen et al., 2021; Morris et al., 2016; Jünger et al., 2017; King et al., 2011). Furthermore, those who find alcohol initially more rewarding have a higher likelihood of later developing AUD (King et al., 2021).

Binge drinking, a goal-directed, motivated drinking pattern that raises blood alcohol concentration (BAC) above 0.08 g/dL of blood, is heavily correlated with increased risk of subsequent AUD development (Ehlers et al., 2022; Crews et al., 2019) and in and of itself leads to serious health repercussions (Jünger et al., 2017). Reciprocally, those with AUD symptomology are more likely to binge drink; a study looking at rate of alcohol consumption in early drinkers (aged 16-24) found that participants with more AUD symptoms reached peak BAC and drink numbers as compared to controls (Carpenter et al., 2019).

Human and rodent studies support the theory that aberrant neural plasticity and reactivity may exist prior to AUD onset. Binge drinkers have heightened resting state functional connectivity of networks subserving reward (NAc and DMS) and salience (orbitofrontal cortex and anterior cingulate cortex) as compared to light drinkers who can more easily control their consumption (Arienzo et al., 2020), suggesting that alcohol

aberrantly enhances output of these networks. Furthermore, binge drinkers who are otherwise healthy have increased reactivity of their NAc to reward receipt as compared to non-binge drinkers, though they have less functional connectivity from NAc to the dorsal anterior cingulate cortex suggesting this heightened activity is due to deficient regulation upon receipt of rewards (Crane et al., 2017). These human imaging studies have opened doors to investigations into neurotransmitter and peptide signaling systems through which alcohol may do this. Alcohol has a plethora of molecular targets, enabling it to modulate a wide variety of neurotransmitter systems and cellular populations in discrete circuits driving different symptoms of alcohol misuse and AUD (see reviews: Abrahao et al., 2017; Lovinger, 2008; Lovinger and Roberto, 2013; Lovinger and Abrahao, 2018; Egervari et al., 2021; Brenner et al., 2020).

To unravel how brain circuitry is targeted by alcohol to aberrantly drive binge consumption, rodent models are used. The predominant focus of preclinical research investigations is alcohol interactions with glutamate signaling in the NAc. The findings altogether suggest that both acute and chronic alcohol exposures enhance excitatory transmission strength in the NAc to increase its output, albeit in different ways. Elevated levels of glutamate in the NAc support excess ethanol consumption (Griffin 3rd et al., 2014) and alcohol-preferring strains of mice have elevated basal glutamate levels as compared to alcohol-avoiding mice following repeated exposure to alcohol (Kapasova and Szumlinski, 2008). Following a combined chronic alcohol use and alcohol vapor chamber exposure procedure, mice have enhanced glutamate activity at ventral hippocampal projections targeting NAc D1R MSNs due to insertion of glutamatergic AMPA receptors into these synapses (Kircher et al., 2019).

To gain an understanding of how alcohol influences the ability of the NAc to function as a circuit integration center, Kolpakova and colleagues (2021) utilized a dual wavelength optogenetic approach so that they could stimulate two circuits (PFC and BLA afferents in the NAc) at once on the same slice. This revealed that while both projections target the same populations of MSNs, NAc MSNs prioritize information from the PFC. Binge drinking alters this by strengthening BLA inhibition of PFC inputs (Kolpakova et al., 2021). Furthermore, *in vivo* optogenetic stimulation of the BLA but not the pPFC suppresses escalation of alcohol binge drinking in mice (Kolpakova et al., 2021). Many others support the theory that alcohol intake potentiates DMS glutamatergic transmission and inhibition of this attenuates alcohol-seeking (Wang et al., 2010; Wang et al., 2012; Ma et al., 2017; Roltsch Hellard et al., 2019).

Yet there are lines of evidence suggesting otherwise. Pharmacologically or chemogenetically increasing activation of the NAc core diminishes binge-like consumption of alcohol but not other fluids (Purohit et al., 2018; Pozhidayeva et al., 2020). Providing the first evidence for bidirectional control of NAc core and binge-like drinking, pharmacologically diminishing NAc core activity effectively increases drinking (Purohit et al., 2018). This disparity in the literature may be because these latter studies utilized global activation or inactivation of NAc activity, neglecting the ability of alcohol to act in a synapse specific manner.

This synapse specificity is also seen in the DMS. Excessive alcohol consumption in rats increases ionotropic glutamate receptors at the corticostriatal projection (a postsynaptically expressed mechanism) and increases the probability of glutamate release from the BLA (a presynaptic mechanism; Ma et al., 2017). Presynaptic D1R and D2Rs on

cortical afferents in the DMS are differentially targeted by alcohol, demonstrating even more intricate interactions of alcohol with this system. Postsynaptic D1R MSNs that are targeted by glutamatergic corticostriatal afferents expressing D2R have stronger responses to these afferents than postsynaptic D2R MSNs and excessive alcohol intake induces a long-term potentiation at the cortico-D1R MSN synapse, strengthening this projection (Lu et al., 2019). This is supported by other findings suggesting that D1R MSNs are mediators of alcohol consumption, while D2R MSN activation is negatively associated with drinking (Cheng et al., 2017; Cheng and Wang, 2019; Roltsch Hellard et al., 2019). Furthermore, alcohol consumption increases NMDA receptor expression on D1R MSNs and optogenetic inhibition of D1R MSNs diminishes operant lever presses for alcohol in addition to the amount of alcohol consumed (Roltsch Hellard et al., 2019). Conversely, DMS long-term depression (LTD) induced optogenetically increases operant alcohol intake in a D2R-dependent manner (Roltsch Hellard et al., 2019). Pointing to a potential mechanism, others have found that activation of postsynaptic, but not presynaptic, D2R inhibits corticostriatal transmission in an endocannabinoid (eCB)-dependent manner (Lu et al., 2019). Even concentrations of ethanol associated with mild intoxication can significantly alter plasticity in corticostriatal circuits mediating goal-directed behavior, impairing NMDA-dependent LTP dose dependently in the DMS and promoting LTD at higher concentrations (Yin et al., 2007).

Differences in inhibitory neurotransmission are highly underexplored as they relate to alcohol use in the striatum, and thus the narrative is less complete. In other brain regions, acute alcohol enhances GABAergic signaling by acting directly as an agonist at $GABA_A$ receptors or by inducing GABA release (Siggins et al., 2005; Kelm et al., 2011). Evidence

for alcohol enhancing GABA neurotransmission largely points to indirect modulation via other signaling systems, namely those that act via presynaptic G protein-coupled receptors (reviewed in Kelm et al., 2011). In the DLS, acute ethanol inhibits stimulus-evoked inhibitory neurotransmission (Blomeley et al., 2011) and weakens the strength of inhibition from FSIs and MSNs onto other MSNs, thus disinhibiting DLS output (Patton et al., 2016). In the NAc, GABA from the VTA almost exclusively targets CHIs to enable reinforcement of reward behavior (Al-Hasani, et al., 2021), but beyond these studies not much is known. This gap in knowledge must be addressed moving forward in alcohol research, as it could point to novel treatment strategies and targets.

There are many ongoing investigations pursuing a better understanding of aberrant modulation of other neurotransmitter systems in the NAc and DMS by alcohol (see reviews: Lovinger, 1997; Narahashi et al., 2001; Lovinger, 2008; Nam et al., 2013, Abrahao et al., 2017; Lovinger and Alvarez, 2017; Chouhan et al., 2020). The aforementioned eCB-mediated LTD in the NAc that is dependent upon metabotropic glutamate receptor signaling (Lu et al., 2019) is eliminated following exposure to drugs of abuse (delta9-tetrahydrocannabinol: Mato et al., 2005; cocaine: McCutcheon et al., 2011), and blocking these glutamate receptors suppresses drug seeking in a CB1-dependent manner (cocaine: Li et al., 2018). Genetic deletion or pharmacologically blocking dopamine 3 receptors (D3R, a D2-like receptor) increases expression of $GABA_A$ receptors (Leggio et al., 2015), which inhibits voluntary alcohol consumption due to the resultant elevated strength of inhibitory neurotransmission in the NAc (Leggio et al., 2019). A primary focus in the literature currently is the signaling interplay between dopamine 3 receptor (D3R), RACK1/BDNF, and GABA. Ethanol consumption is substantially higher

in wildtype mice as compared to D3R knockout mice, and treating wildtypes with a D3R antagonist lowers their consumption (Leggio et al., 2014). Blocking BDNF signaling with an antagonist diminishes ethanol intake and lowers D3R expression in wildtypes and blocking signaling via D3R with buspirone also diminishes ethanol consumption culminating in the understanding that increased D3R together with increased RACK1/BDNF expression reinforce ethanol consumption (Leggio et al., 2014). This supports another finding that acute systemic administration of alcohol activates H-Ras, a protein activated downstream of TrkB that alcohol directly targets, in the NAc, as does operant self-administration of alcohol (Hamida et al., 2012). Genetic knockdown or pharmacological inhibition of NAc H-Ras reduces ethanol consumption alone as compared to other solutions and attenuates goal-directed seeking for alcohol (Hamida et al., 2012).

BDNF as a positive regulator of alcohol reward and consumption is supported. BDNF signaling disinhibits the NAc and alcohol enhances this disinhibition (Patton et al., 2019; see **Figure 1.3**). A study looking at BDNF mRNA levels in the VTA and terminal areas of the mesolimbic dopaminergic circuits of alcohol-preferring and -avoiding rats found that it was increased in the amygdala and VTA and diminished in the hippocampus of alcohol-preferring as compared to alcohol-avoiding rats with a trend for increased expression in the NAc, as well (Raivio et al., 2014). Following an acute administration of ethanol (1.5 and 3 g/kg), they further found that ethanol modulates BDNF levels in a region-specific manner, whereby it diminishes dose-dependently in the hippocampi of both rat types and significantly increases in the VTA of only alcohol-preferring rats at the higher dose (Raivio et al., 2014). Ethanol also induces region-specific changes in a time-dependent manner, whereby significantly variable levels of BDNF mRNA are seen in

hippocampus, amygdala, frontal cortex, and NAc depending on the timepoint (ranging from 90 min to 24 h) of analysis (Raivio et al., 2014).

Yet still others find that BDNF regulates controlled or diminished intake of ethanol (Logrip et al., 2008; Haun et al., 2018). And interestingly, in what appears to be contradictory to Hamida (2012), Leggio (2014), and their colleagues, others have determined that BDNF/RACK1 signaling may serve as a protective, homeostatic mechanism for attenuating elevated responding for ethanol and that reduction in BDNF levels augments ethanol consumption (McGough et al., 2004; Jeanblanc et al., 2006). A prediction that follows from these findings is that BDNF signaling through TrkB is required for BDNF-mediated reduction in voluntary ethanol consumption, and this is indeed the case (Jeanblanc et al., 2006). These oppositional findings demonstrate the need for further investigation into the role of BDNF in alcohol reward and consumption.

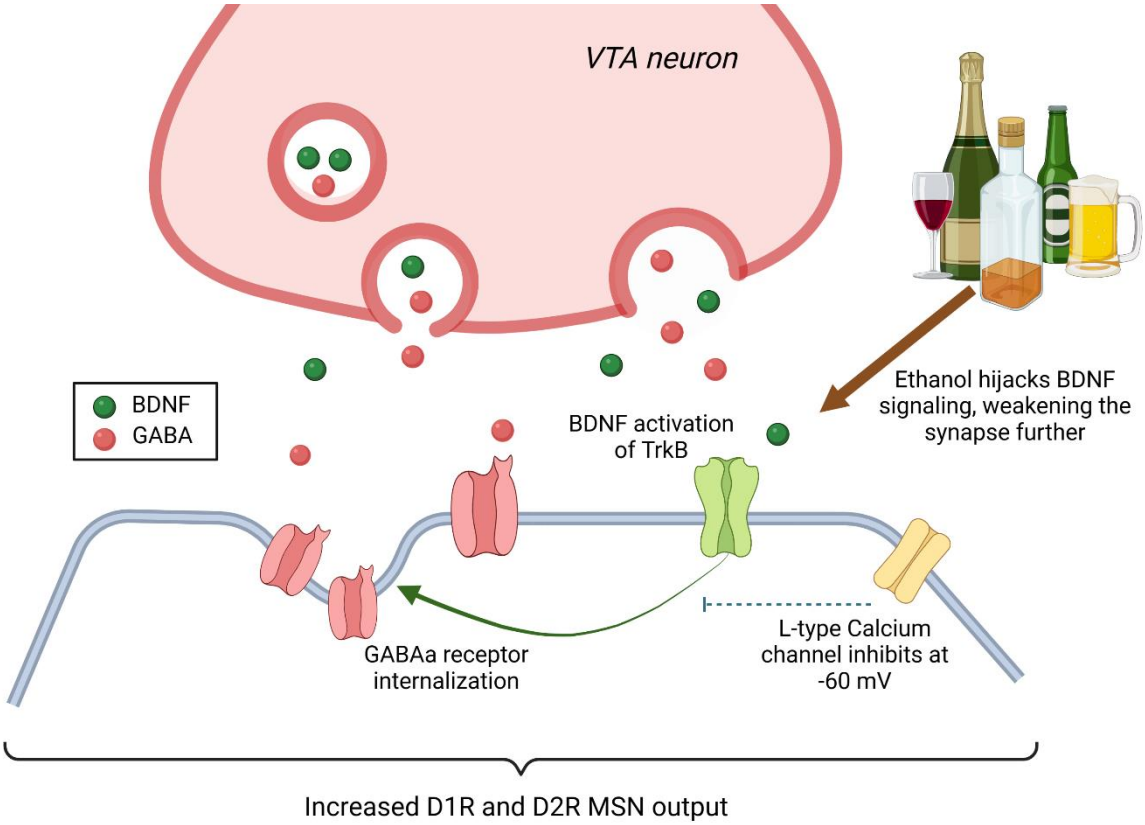

Figure 1.3 Summary of brain-derived neurotrophic factor (BDNF)-mediated disinhibition of the nucleus accumbens (NAc). Dopaminergic ventral tegmental area (VTA) neurons corelease dopamine, GABA, and BDNF onto D1R and D2R MSNs in the NAc. BDNF activates its canonical postsynaptic receptor tyrosine receptor kinase B (TrkB), initiating a signaling cascade culminating in dynamin phosphorylation. Thus, the weakening of GABAergic synapses that is observed is due to $GABA_A$ receptor internalization. Calcium entry through L-type voltage-gated calcium channels inhibits $GABA_A$ internalization when the voltage of the MSN is relatively depolarized (-60 mV). Ethanol targets BDNF signaling via TrkB to augment NAc disinhibition.

1.4 Alcohol, BDNF, and reward

Conflicting lines of evidence in the exploration of the role of BDNF in elevated alcohol consumption raise the question: what is the role of BDNF in natural reward? Activation of TrkB via exogenous intrastriatal infusion of BDNF minimizes response preservation to an initial strategy for obtaining a reward, thereby facilitating faster strategy shifting for receipt of a reward (D'Amore et al., 2013). Examination of the role of lysine-specific histone demethylase 1 (LSD1; an enzyme that positively regulates BDNF expression) in the lateral hypothalamus-medial forebrain bundle (LH-MFB) of rats further supports the idea that BDNF positively modulates the experience of reward and reward reinstatement. LSD1-driven increases in BDNF expression are critical in rats conditioned to press for self-stimulation, which is rewarding (Sagarkar et al., 2021). Notably, exogenous delivery of BDNF reinstates lever pressing in rodents with prior Lsd1 siRNA administration, which on its own blocks LSD1 and inhibits lever press activity (Sagarkar et al., 2021). In a molecular investigation on dopamine signaling in NAc D1R MSNs and its regulation of reward-related behavior via downstream signaling activation of mitogen-activated protein kinase (MAPK), investigators discovered that MAPK phosphorylates Neuronal Per Arnt Sim domain protein 4 (Npas4) to increase its interaction with CREB-binding protein (CBP), thereby increasing the transcriptional activity of Npas4 at the BDNF promoter to enhance reward-related learning and memory (Funahashi et al., 2019).

The BDNF genetic mutation most heavily studied in relation to the drastic shift in the experience of reward as it relates to a variety of diseases is a nonsynonymous single nucleotide polymorphism in the BDNF gene (valine 66 to methionine; Val66Met), which results in a decrease of BDNF release and impacts the signaling of reward processing

neurotransmitters such as serotonin, dopamine, and glutamate (Ninan et al., 2010; Terracciano et al., 2010; Pattwell et al., 2012; Galvin et al., 2015; Hao et al., 2017; Jing et al., 2017; Cash et al., 2021). Recent fMRI research in humans reveals that Val66Met carriers show no activation to monetary gains and a blunted dopamine response to placebo analgesic, supporting BDNF as a mediator of reward by suggesting that less dopamine release correlates with lower sensitivity to reward (Pecina et al., 2014). Other fMRI research has looked into reactivity of the amygdala, a brain region critical for emotional processing and salience, in individuals carrying Val66Met as compared to controls with regards a variety of behavioral phenotypes including reward dependence during an emotional face-masking task (Redlich et al., 2020). Overall, higher BDNF methylation is associated with higher amygdala reactivity, with no significance between carriers of the mutant gene and controls (Redlich et al., 2020). Moreover, BDNF methylation is positively associated with harm avoidance and negatively associated with novelty seeking (Redlich et al., 2020). In a meta-analysis of 60 drug abusers (30 heroin, 30 methylamphetamine) and 52 healthy controls, researchers found a positive association between BDNF promoter methylation and a variety of addictive phenotypes in those abusing drugs as compared to controls (Xu et al., 2016).

But it is important to note that negative associations between BDNF and reward in other contexts exist. While BDNF may mediate responses to cocaine, BDNF may in other circumstances reduce intake of morphine and cocaine (Graham et al., 2009; Lobo et al., 2010; Koo et al., 2012). BDNF also contributes to symptomology of major depressive disorder (Eisch et al., 2003; Berton et al., 2006; Bakusic et al., 2021). Many of these studies reveal discrete synapse specificity, with BDNF differentially targeting D1R and D2R

MSNs. For example, BDNF release from the VTA onto D1R MSNs in the NAc strengthens GABAergic tone and reduces morphine and cocaine reward (Koo et al., 2012). Furthermore, chronic social defeat stress (a measure of stress susceptibility, which is associated with depression) is mediated by BDNF signaling through D2R MSNs in the NAc (Pagliusi et al., 2022). Interestingly though, BDNF signaling through D1R MSNs protects against social stress (Pagliusi et al., 2022). While this could theoretically indirectly enable individuals to better enjoy rewards in social environments, the higher expression level of TrkB receptors on D2R MSNs suggests that they are preferentially targeted by BDNF (Lobo et al., 2010; Baydyuk et al., 2011).

Circuit-specific investigations in rodent models have elucidated more complexity to the system, as they demonstrate that BDNF may act differentially depending on the circuit in which it is released. For instance, following 3-day intra-cranial injection schedules of a cannabinoid receptor agonist in specific brain regions of rats, various effects on the reward experience occur (Navabpour et al., 2021). Intra-central amygdala (CeA) and intra-medial prefrontal cortex injections both elevate BDNF levels in the hippocampus, yet activation of cannabinoid receptors in the CeA result in a conditioned place preference while resulting in a conditioned place aversion when activated in the medial prefrontal cortex (Navabpour et al., 2021).

Studies investigating how co-use of drugs promotes continual concurrent use provide further insight into the relationship between alcohol reward and BDNF. Those consuming alcohol often use and abuse it with other drugs; one example is that of nicotine and alcohol. Over 85% of those with AUD are estimated to also be smokers (Falk et al., 2006; Grant et al., 2015; Saha et al., 2018). Investigators recently examined

neuroadaptations in the mesolimbic pathways of rats following ethanol and nicotine exposure via direct cannulation into the posterior VTA (Waeiss et al., 2010). While their main finding was that only ethanol and nicotine together triggered release of glutamate, dopamine, and BDNF into the NAc, they also notably found that exogenously administering BDNF through cannula prior to drug exposure was sufficient to enhance the reinforcing properties of ethanol alone in the NAc (Waeiss et al., 2010). This suggests that either BDNF signaling itself or another signaling system that converges with BDNF signaling may mediate ethanol reward.

One prediction that follows from all these disparate findings is that midbrain BDNF enables associations with negative stimuli, which makes it critical for memories of potentially rewarding or aversive stimuli, but in the contexts of depression or high stress, BDNF signaling establishes abnormal associations even with nonthreatening stimuli (Nestler and Carlezon, 2006). However, this explanation does not account for why BDNF is observed as a reinforcer of reward in some lab settings.

At the very least, it is evident that BDNF signaling is context dependent. Similarly, with drugs of abuse: context matters (age of consumption, associations between environment and drug use, how the drug is administered, etc.), thus it follows that this context dependence of drug use may be attributable to modulation of the BDNF system under different conditions by alcohol. Much work is needed for a better understanding of the relationship between BDNF and reward under different contexts, and whether this may be attributable to its interplay with other neurotransmitter systems. We herein investigate the relationship between BDNF interplay with neurotransmitter systems in the NAc and ethanol to address some of these gaps in knowledge.

1.5 Habitual consumption of alcohol

Repeated expression of any goal-directed behavior eventually gives way to automated behavior; this is associated with the transition from flexible circuitry in the basal ganglia to inflexible circuitry associated with habits (Graybiel, 2008; Lipton et al., 2019). As repeated alcohol exposure continues over time, habit formation is facilitated (Everitt et al., 2001; Graybiel, 2005). The high sensitivity of the brain to acute alcohol exposure and binge alcohol consumption makes it unsurprising that as repeated bouts of binging occur, brain circuits quickly adapt in ways that are hard to reverse. Not only does chronic alcohol use drive habitual consumption of ethanol, but it also accelerates habitual responding for natural rewards such as sucrose (Lesscher et al., 2010; Sjoerds et al.,2013; Corbit et al., 2012). Interestingly, the extent of habitual decision making can even predict relapse in alcohol-dependent individuals (Sebold et al., 2014; Duka et al., 2017; Sebold et al., 2017).

Circuit mechanisms mediating this behavioral shift are studied at length in rodents. This habitual consumption is associated with a shift in activation from the DMS to the DLS, and many have explored how exactly this shift occurs during alcohol intake. The orbitofrontal cortex (OFC) seems pivotal in this behavioral shift; ensembles of neurons in OFC, DMS, and DLS display different activities depending on whether an action is goal-directed or habitual, with DMS and OFC becoming more engaged and DLS less active during goal-directed actions (Gremel and Costa, 2013). Interestingly, the magnitude of OFC neuronal activity correlates with the level of goal-directed behavior (Gremel and Costa, 2013).

DLS lesion studies demonstrate that habitual behavior is not established in the absence of the DLS (Yin et al., 2004; Yin et al., 2006). In pursuit of a more direct,

mechanistic understanding of how the DLS drives habitual behaviors, many researchers have focused on dopamine and glutamate (Wickens et al., 2007; Belin-Rauscent et al., 2012; Corbit et al., 2014). Whether and how alcohol modulates the strengths of corticostriatal inputs onto DMS and DLS MSNs over time to weaken cognitive flexibility and strengthen salience signal learning has drawn much research attention. To this end, a computational model of corticostriatal interactions performing concurrent goal-directed learning and habit learning was recently developed (Barnett et al., 2023). In this model, learning processes were distinguished by creating a distinction between PFC → DMS-mediated learning, reliant upon reward-prediction error signals, and premotor cortex → DLS-mediated learning, supported by salience signals. Following poor outcome representation in the PFC, the efficacy of goal-directed learning was diminished and DLS-mediated stimulus-response associations were strengthened (Barnett et al., 2023). This suggests that altering executive control by impairing PFC output enhances cognitive inflexibility.

But the fact that the basal strength of inhibition in the DLS is twice that of the DMS suggests that DLS MSNs are under a stronger inhibitory tone and less sensitive to glutamatergic synaptic changes (Wilcox et al., 2014). Acute alcohol exposure diminishes the strength of inhibition onto MSNs (from FSIs and other MSNs; Patton et al., 2016) and repeated alcohol exposure causes differential changes in sensitivity to GABAergic transmission in the DLS and DMS, whereby it enhances inhibitory tone in the DMS and diminishes it in the DLS (Wilcox et al., 2014). Furthermore, following chronic ethanol consumption in a voluntary drinking paradigm, spontaneous glutamatergic transmission in the dorsal striatum is unchanged, while spontaneous GABA release is more frequent

(Wilcox et al., 2014). Altogether these findings demonstrate that it is likely that multiple coincident mechanisms through which alcohol targets the dorsal striatum exist. The potency of the inhibitory network in the DLS and the substantial evidence that alcohol targets GABAergic sources in the DLS makes these sources critically important to study.

FSIs in the DLS are essential for the behavioral shift towards compulsivity. Beyond their aforementioned higher expression level in the DLS as compared to the DMS, what makes this cell population so critically important in the context of AUD is that it is directly targeted by alcohol and other psychoactive drugs (Wiltschko et al., 2010; Blomeley et al., 2011; Patton et al., 2016) and causally linked to habitual responding for sucrose (O'Hare et al., 2017). Furthermore, ablation of FSIs in the DLS reduces ethanol consumption and attenuates habitual ethanol intake (Patton et al., 2021).

FSIs co-activate to enhance their modulation of striatal output, which enables them to organize as ensembles to encode rapid, discrete action speed (Roberts et al., 2019) and drive balanced MSN network activity (Damodaran, 2014). It is accepted as canon that this co-activation occurs via gap junction formation between FSIs (Koos and Tepper, 1999; Lau et al., 2010; Zhang et al., 2014). However, connexin-36, the pore forming protein that creates gap junctions (Cummings et al., 2008), declines in expression from development into adulthood (Bruzzone et al., 1996; Belluardo et al., 2000) and investigations into other mechanisms that may exist to mediate this co-activation are lacking. The striatum is a site of functional convergence; while corticostriatal projections may be topographically organized, they also can overlap (Malach and Graybiel, 1986; Gerfen, 1989; Flaherty and Graybiel, 1991; Parthasarathy et al., 1992; Flaherty and Graybiel, 1993; Flaherty and Graybiel, 1995; Brown et al., 1998; Takada et al., 1998; Hoffer and Alloway, 2001). As

the striatum is the input nucleus of the basal ganglia, it makes sense that anatomical data reveals reciprocally connected cortical regions target the striatum with densely overlapping arborizations (Yeterian and Van Hoesen, 1978; Flaherty and Graybiel, 1993). Moreover, functionally distinct motor and somatosensory cortices converge in striatum (Flaherty and Graybiel, 1993). Corticostriatal terminals may target MSNs, shaping their output directly, (Kemp and Powell, 1971; Frotscher et al., 1981; Dube et al., 1988; Wilson, 1995; Wilson and Kawaguchi, 1996), but the literature also supports convergence of cortical afferents onto FSIs (Lapper et al., 1992; Bennett and Bolam, 1994). In fact, anatomical studies have revealed that there is denser arborization of cortical convergence onto FSIs, with nearly half their total population targeted dually by both motor and sensory cortical terminals (Ramanathan et al., 2002). In many cases, an individual FSI may be targeted by multiple cortical axons (Ramanathan et al., 2002). Convergent excitation onto inhibitory cell populations has been seen to drive synchrony in other brain regions leading to feedforward inhibition in a similar manner to that of FSIs onto MSNs (Wang et al., 2019). Altogether these findings suggest a role for the anatomically demonstrable convergence of cortical excitation onto FSIs as a mediator of their synchrony, but investigations into this are lacking in the literature.

1.6 Specific Aims

Though it is established that FSIs are targeted by ethanol and necessary for acquisition of habitual consumption of the drug, there are gaps in knowledge about how this small population of neurons can so potently modulate striatal output via their targeting of MSNs and whether this mechanism may stand as a target for alcohol in the progression

of AUD. We know that FSIs functionally organize as ensembles in adult animals (Roberts et al., 2019) and that the ability of FSIs to co-activate enhances their modulation of striatal output through temporal summation. This is largely thought to be enabled by FSI-FSI electrical coupling (Koos and Tepper, 1999; Lau et al., 2010; Zhang et al., 2014), yet mechanisms underlying FSI synchrony have not been investigated in adult mice. Understanding how FSIs modulate striatal output is highly informative towards work investigating aberrant modulation of FSIs by drugs of abuse, such as alcohol and we herein provide whole-cell patch-clamp and computational modeling data to enable a better comprehension of this.

To address gaps in knowledge about FSI network activity and how this small population of neurons in the dorsal striatum is able to exert such powerful influence over MSNs to enable the habit formation and compulsivity, this thesis begins with the following aims:

1. **Determine the FSI-FSI electrical coupling rate in adult mice. (Chapter 2)**
2. **Determine whether integration of cortical inputs into the DLS occurs differentially on FSIs and MSNs. (Chapter 2)**
3. **Determine whether integration of convergent excitatory inputs (from cortex) may serve as a mechanism for synchronous cellular network activity (Chapter 2).**

The latter half of my thesis investigates a novel mechanism mediating the rewarding properties of alcohol, which those who regularly misuse alcohol may have heightened sensitivity to. Determining the role of BDNF signaling in the progression of

AUD is critical to furthering our understanding of how alcohol modulates the brain over time to aberrantly drive certain behaviors. Moreover, conflicting findings in the literature on the role of BDNF in reward indicate the need for further investigations into how BDNF modulates midbrain circuitry. Our lab is the first to investigate inhibitory plasticity in the NAc as well as its and its relationship to reward. As such, the work herein is highly novel and essential towards the advancement of broadening neuroscientific understanding for how alcohol modulates NAc inhibitory plasticity in a behaviorally relevant manner.

4. **Determine the source of BDNF necessary and sufficient for driving inhibitory NAc plasticity (Chapter 3).**
5. **Stimulate BDNF afferents in the NAc *in vivo* and determine whether it is rewarding (Chapter 3).**
6. **Determine whether BDNF afferent stimulation interacts with ethanol *in vivo* to support the rewarding properties of ethanol. (Chapter 3).**

Chapter 2: Cortical control of striatal fast-spiking interneuron synchrony

Abstract

Inhibitory fast-spiking interneurons in the dorsal striatum regulate actions and action strategies, including habits. Fast-spiking interneurons are widely believed to synchronize their firing due to the electrical synapses formed between these neurons. However, neuronal modeling data suggest convergent cortical input may also drive synchrony in fast-spiking interneuron networks. To better understand how fast-spiking interneuron synchrony arises, we performed dual whole-cell patch clamp electrophysiology experiments to inform a simple Bayesian network modeling cortico-fast-spiking interneuron circuitry. Dual whole-cell patch clamp electrophysiology revealed that while responsivity to corticostriatal input activation was high in fast-spiking interneurons, few of these neurons exhibited electrical coupling in adult mice. In simulations of a cortico-fast-spiking interneuron network informed by these data, the degree of glutamatergic cortical convergence onto fast-spiking interneurons significantly increased fast-spiking interneuron synchronization while manipulations of electrical coupling between these neurons exerted relatively little impact. These results suggest that the primary source of functional coordination of fast-spiking interneuron activity in adulthood arises from convergent corticostriatal input activation.

2.1 Introduction

The dorsal striatum is the entry point for the processing of cortical information by the basal ganglia, which regulates action learning and control (Gerfen and Surmeier, 2011; Klaus et al. 2019). The dorsolateral region of the striatum (DLS) is required for

automatizing actions (Yin and Knowlton, 2006). Drugs of abuse, including alcohol, target the DLS to facilitate habit learning (Hopf et al., 2010; Lesscher et al., 2010; Corbit et al., 2012; Depoy et al., 2013) and the extent of habitual decision making predicts relapse in alcohol-dependent individuals (Sebold et al., 2014; Duka, 2017; Sebold et al. 2017). This underscores the role of the DLS (putamen in humans) in addiction. Given that alcohol modulates excitatory input to the striatum from the cortex (Cui et al., 2011; Depoy et al., 2013; Ma et al., 2018; Munoz et al., 2018), understanding how the DLS processes excitatory cortical input is critical for devising strategies to curb compulsive alcohol use.

A defining feature of the DLS is the enrichment of GABAergic, parvalbumin expressing fast-spiking interneurons (FSIs; Kita et al., 1990; Kawaguchi, 1993). While FSIs represent only ~1% of the total striatal neuronal population (Luk and Sadicot, 2001), they are targeted by alcohol and other psychoactive drugs (Wiltschko et al., 2010; Blomeley et al., 2011; Patton et al., 2016), causally linked to habitual responding for sucrose (O'Hare et al., 2017), and required for compulsive ethanol consumption (Patton et al., 2021). FSIs are driven to fire action potentials primarily by cortical glutamatergic input (Gittis et al., 2010). Upon cortical activation, FSIs provide potent inhibitory, GABAergic control over neighboring medium spiny projection neurons (MSNs), thus forming a feedforward inhibitory microcircuit governing striatal output (Kita et al., 1990; Bennett and Bolam, 1994; Koos and Tepper, 1999; Tepper et al., 2004; Mallet et al., 2005).

FSIs functionally organize as ensembles in adult animals (Roberts et al., 2019). The ability of FSIs to co-activate enhances their modulation of striatal output through temporal summation, and is largely thought to be enabled by FSI-FSI electrical coupling (Koos and Tepper, 1999; Lau et al., 2010; Zhang et al., 2014). Dual electrophysiological recordings

of FSIs in juvenile acute brain slices show that the electrical synapse connection rate between FSIs is roughly 30% (Koos and Tepper, 1999). Removal of electrical synapses between FSIs in a striatal network model assuming a similar electrical synaptic connectivity rate significantly alters the balanced firing of MSN subpopulations, providing *in silico* evidence for a functional role of FSI-FSI connectivity (Damodaran et al., 2014). However, connexin-36, the pore forming protein enabling electrical coupling between FSIs (Cummings et al., 2008), declines in expression throughout development into adulthood (Bruzzone et al., 1996; Belluardo et al., 2000). This suggests that electrical coupling concomitantly declines into adulthood. Yet, exploration of FSI-FSI electrical coupling and other regulators of FSI-FSI synchrony in adulthood is lacking.

Computational network modeling - using adolescent FSI-FSI electrical coupling rates - suggests that FSI-FSI coupling may actually decrease FSI firing, but this effect is abolished under conditions of coincident cortical input onto electrically coupled FSIs (Hjorth et al., 2009). This would suggest that FSIs are sensitive detectors to synchronized input from the cortex. Considering the anatomical findings that demonstrate broad areas of cortex converge onto FSIs, while focal areas of cortex synapse onto MSNs (Ramanathan et al., 2002), we herein further explore *in silico* how convergent cortical input onto FSIs contributes to FSI synchrony using adult mouse cortico-FSI chemical and FSI-FSI electrical synaptic properties derived experimentally *ex vivo*. We find that FSIs exhibit high responsivity to cortical input and rarely electrically couple in adult mouse brain slices. Applying these data to a computational model, we provide evidence that increasing the convergence of cortical input onto FSIs drives FSI-FSI synchrony more reliably than FSI-

FSI electrical synapses. This provides a possible means by which FSIs synchronize in the face of decreasing FSI-FSI electrical coupling in adulthood.

2.2 Methods

All procedures were performed in accordance with the United States Public Health Service Guide for Care and Use of Laboratory Animals and were approved by the Institutional Animal Care and Use Committee at the University of Maryland School of Medicine. All animal procedures used in this study are compliant with the ethical principles of the Journal of Physiology. Mice were housed with littermates (2-5 per cage) under a 12-hr light/dark cycle (lights on at 0700 hours, off at 1900 hours) with *ad libitum* access to food and water. To enable visualization of parvalbumin-expressing FSIs for electrophysiological recordings, *Pvalb-cre* (Tanahira et al., 2009) mice were crossed with *tdTomato* reporter mice (Ai9(RCL-tdT)). This allowed for selective expression of *tdTomato* fluorophore in cre-recombinase-expressing neurons (*Pvalb-cre* x *floxedTdTomato;* "Pv-tdT"; Madisen et al., 2010). Both male and female Pv-tdT mice were on a C57BL/6 background and aged 6-36 weeks old at the time of surgery.

2.2.1 Stereotaxic surgery and viral vectors. At the time of surgery, mice were anesthetized with isoflurane (induction 5%; maintenance 1-2%) and placed into a stereotaxic frame (David Kopf Instruments). A heating pad was used to maintain body temperature and mineral oil was applied to the eyes. Carprofen (5 mg/kg) was injected subcutaneously for analgesia. Breathing rate of the mice was monitored and toe pinches were delivered throughout the duration of the surgical procedure to ensure mice were properly anesthetized. To target cortical afferents into the striatum for optogenetic

stimulation in acute slices, 250 nL of viral construct expressing channelrhodopsin and enhanced yellow fluorophore protein under the human synapsin 1 gene promoter (AAV5-hSyn-ChR2-eYFP; UPenn) was pressure injected into the primary (+1.78 mm AP, ±1.2 mm ML from bregma, -0.8 mm DV from brain surface) and secondary motor cortices (+1.18 mm AP, ±1.25 mm ML from bregma, -0.75 mm DV from brain surface) of Pv-tdT mice. Following bilateral viral injections, the scalps of the mice were sutured together with aliphatic polymers monofilament Blue nonabsorbable suture and the mice were singly housed in cages for 3 days of recovery. During the first day of recovery, lidocaine was applied to the head wound and carprofen (5 mg/kg) was administered subcutaneously. Carprofen (5 mg/kg) was administered for another two days of recovery before mice were rehoused with their cagemates.

2.2.2 Acute slice preparation. Following >6 weeks post viral transfection surgery, Pv-tdT mice expressing ChR2 in the primary and secondary motor cortices were deeply anesthetized with isoflurane (vaporized, 5%). Their heads were decapitated and their brains were immediately extracted and submerged in 95% oxygen, 5% carbon dioxide (carbogen)-bubbled ice cold cutting solution (in mM: 194 sucrose, 30 NaCl, 4.5 KCl, 1 $MgCl_2$, 26 $NaHCO_3$, 1.2 NaH_2PO_4, and 10 D-glucose). Extracted brains were sliced at 250 μm with a vibratome (Leica VT 1200) and transferred to carbogen-bubbled artificial cerebrospinal fluid (aCSF; in mM: 124 NaCl, 4.5 KCl, 2 $CaCl_2$, 1 $MgCl_2$, 26 $NaHCO_3$, 1.2 NaH_2PO_4, and 10 D-glucose). Brain slices containing the DLS were incubated at 32.4 °C for 30 min before they were removed and stored at room temperature until recordings were performed. For mice over four months old, a modified critical protective recovery slicing protocol was used (Ting et al., 2014; Ting et al., 2018): following deep

anesthesia with isoflurane (vaporized, 5%), mice were transcardially perfused with a high N-methyl-D-glucamine (NMDG) aCSF solution (in mM: 92 NMDG, 2.5 KCl, 1.25 NaH_2PO_4, 30 $NaHCO_3$, 20 HEPES, 25 glucose, 0.5 $CaCl_2$, 10 $MgCl_2$, pH=7.2-7.4, 300-310 mOsm). Following rapid decapitation, brains were removed and then sliced at 250 μm in this NMDG-containing aCSF and incubated at 33 °C for 12 minutes before being transferred to a 4-(2-hydroxyethyl)-1-piperazineethanesulfonic acid (HEPES)-containing aCSF solution for the remainder of the day (in mM: 92 NaCl, 2.5 KCl, 1.25 NaH_2PO_4, 30 $NaHCO_3$, 20 HEPES, 25 glucose, 2 $CaCl_2$, 2 $MgCl_2$, pH 7.2-7.4, 300-310 mOsm).

2.2.3 Whole cell patch-clamp electrophysiology. To record, brain slices were hemisected, and transferred to a recording bath where they were perfused throughout recording with carbogen-bubbled aCSF (29–31 °C) via gravity perfusion. tdT-positive FSIs in the dorsal striatum were visualized and targeted for whole cell current clamp recordings through the epifluorescent light path illuminated by a mercury bulb lamp (X-Cite series 120Q). All whole-cell experiments were recorded using borosilicate glass pipettes (resistances ranging from 2–5MΩ) filled with a potassium-based internal solution (in mM: 126 K-Gluconate, 4 KCl, 10 HEPES, 4 ATP-Mg, 0.3 GTP-Na, and 10 Phosphocreatine; osmolarity ranging from 290-295 mOsm; pH 7.3). Cells were voltage (-60 mV) or current clamped using a MultiClamp 700B amplifier (Molecular Devices) and Clampex 10.4.1.4 software (Molecular Devices) was used for data acquisition. All recordings were filtered at 2 kHz and digitized at 10 kHz.

Electrical coupling between FSIs was determined by injecting current steps into one of a pair of FSIs and observing whether the FSI not receiving a current injection depolarized. FSI and MSN maximum firing rate was determined by increasing current step

injections into the cells. Resting membrane potentials were recorded after correcting for the liquid junction potential (15.7 mV) as per the Nernst-Planck equation (Barry, 1994; Marino et al. 2014). Action potential thresholds were determined by injecting a gradual ramp of current into cells and recording the voltage at which they first detonated an action potential. These voltage values were also corrected for the liquid junction potential. The probability "P" of an FSI or MSN firing in response to cortical input was calculated at a variety of frequencies (1, 10, 20 Hz) by averaging the number of FSI or MSN action potentials elicited by 10 pulses of blue light (4 ms pulse width, 470 nm) over the course of 10 sweeps. To control for viral expression differences between animals, action potential firing fraction values were averaged across animals and statistical significance between cell types was determined by an unpaired *t* test. Of note, FSI-FSI GABAergic synapses were intact during all recordings, as picrotoxin was not included in the recording solution. For all experimental groups, n is defined as individual neurons recorded from multiple *in vitro* brain slices from at least 4 mice.

All reagents for slice electrophysiology cutting and recording solutions were purchased from Sigma-Aldrich. All drugs were purchased from Tocris Bioscience.

2.2.4 Computational Model. The model consists of two basic parameters. The first parameter is the number of FSI neurons in the circuit, which is manually defined by *n*. Each FSI received the same number of inputs, which is defined by the number of FSIs, (i.e. if there are 10 FSIs, each FSI received input from 10 cortical neurons). The second parameter is the value of "convergence". Convergence was defined as the number of independent cortical neurons that target a given FSI. We quantified the percent of convergence as:

$$C\% = \frac{(n^2 - c)}{n(n-1)} \quad (1)$$

Where n is the number of FSIs in the circuit and c is the number of cortical neurons in the circuit. Cortical connectivity was determined randomly for simulations where the percent convergence ranged between 0% and 100%, but controlled so that no FSI received multiple inputs from the same cortical neuron. Following determination of the percent convergence and cortico-FSI connectivity, we then determined the number of lateral, electrical synaptic connections shared between FSIs. This was defined by the equation:

$$\lambda = \frac{x}{n^2 - n} \quad (2)$$

Where λ is the rate of lateral connections, x is the total number of lateral connections, and n is the number of FSIs in the circuit. Determination of which FSIs shared lateral connections was random, and each connection was treated as bidirectional.

In the cortical layer, cortical neurons possessed an action potential firing probability of 0.005, which was kept homogeneous across all neurons to maintain a low baseline firing rate of roughly 5 Hz. The likelihood of an FSI firing an action potential was defined by the following equation:

$$p(FSI_n)(i,t) = \frac{p_{max} - p_0}{n} i + \frac{p(FSI_n)(i,(t-1))}{\tau} + \Sigma\, cc * p(FSI_{gap})_n \quad (3)$$

Where p_{max} is the likelihood of an FSI to fire given all inputs are active; this was determined experimentally to be 0.7 from slice electrophysiology data (see Results). p_0 is defined as the likelihood an FSI fires an action potential given no synaptic input onto the FSI, which is equivalent to the baseline firing rate. *i* is the number of cortical neurons that fired onto an individual FSI. This generated a linear tuning curve in response to increasing cortical stimulation. We approximated FSI dependence on cortical input as a line based off

slice electrophysiology findings (*see Results*). $p(FSI_n)\big(i,(t-1)\big)$ is the probability of firing in the previous time bin, decayed by a rate of τ, which was modelled based off the average τ for FSIs from our electrophysiology findings (see Results). cc is the coupling coefficient, or the strength of lateral electrical synaptic connections, between FSIs. This was determined experimentally to be 0.03 on average (*see Results*). Lastly, $p(FSI_{gap})_n$ is the firing probability of the n^{th} FSI connected to the FSI of interest. This term when multiplied by the coupling coefficient and summed across all FSIs that are electrically connected with the FSI of interest defines how electrically connected FSIs influence one another during the time interval. This equation was also kept uniform across FSIs, and each parameter was kept constant. Both cortical neurons and FSIs had an absolute refractory period of 1 ms.

Each simulation consisted of a 1s trial with each sampling bin size being 1ms. Individual trials either received synchronous input or did not, depending on the experiment. For simulations with synchronous input, we increased the probability of cortical neuron firing to approximately 1 at a frequency of 10Hz. Thus, at 50ms, 150ms, 250ms, 350ms, 450ms, 550ms, 650ms, 750ms, 850ms, and 950ms the probability of a cortical neuron to fire became 1, thereby generating synchronous input onto the FSIs. We deem this an approximation as in some instances these time intervals were timed with a cortical neuron's refractory period.

To assess the network for synchrony, we calculated the cross correlation for each neuron and then averaged this across the population. This was repeated 20 times with a new network, where any random parameters were redrawn. To control for changes in neural firing, neural spike trains were shuffled and the cross-correlation of the shuffled

spike trains was subtracted out (Damadoran et al., 2014). Additionally, to confirm that values chosen for these simulations were not biasing our interpretation we performed several parameter scans of relevant parameters that would influence FSI firing. Parameter scans were done by simulating a single network structure, where all connectivity had been determined and kept the same across simulations, then relevant parameters were varied. Following the simulations cross-correlations were calculated and values at 0s lag, when synchrony will be at its maximum were plotted.

2.3 Results

2.3.1 Fast-spiking interneuron (FSI) electrical coupling.

We performed dual current-clamp recordings of FSIs expressing a fluorescent reporter that were no more than 200 μm apart from n = 78 pairs and found that only ~8% (n = 6) of FSI pairs exhibited electrical coupling (**Figure 2.1a, b,** and **c**). The strength of these connections as measured by their coupling coefficients ranged from 0.0006 to 0.0789 (**Figure 2.1d**). The highest value for current injection per cell pair varied depending on when the maximum firing rate was achieved.

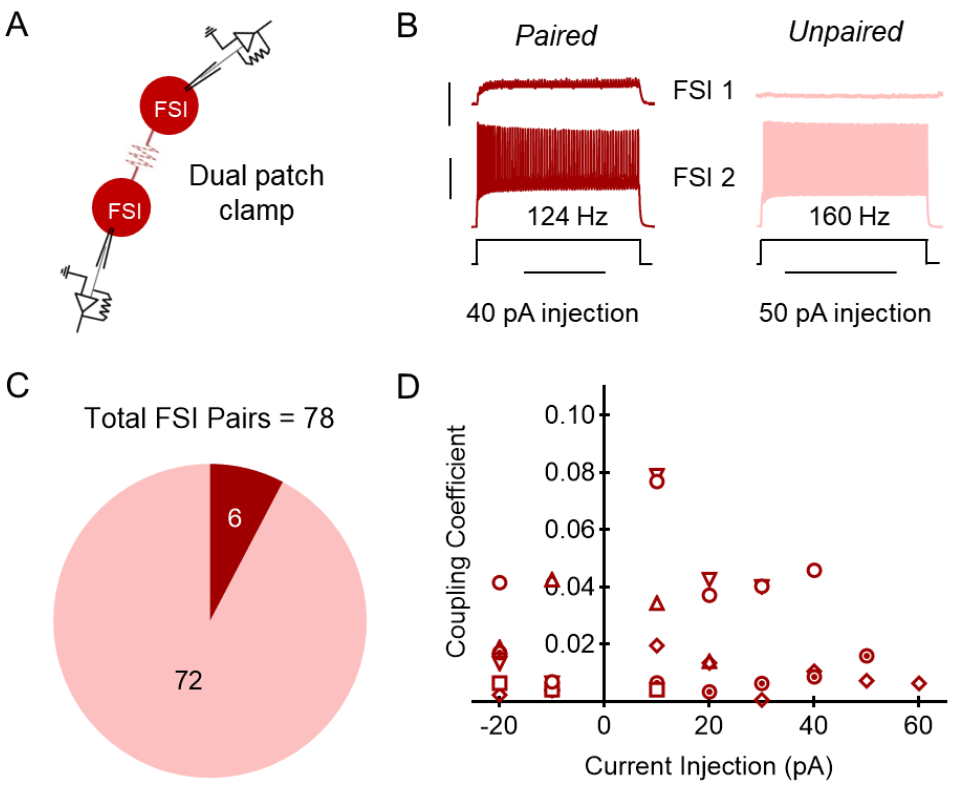

Figure 2.1. Fast-spiking interneuron (FSI) electrical coupling. A: Schematic of dual FSI recordings. B: Representative traces of paired and unpaired FSI paired recording responses to current injection into one FSI (FSI 2 in schematic). Current injection magnitude listed per FSI pair refers to last injection before FSI 2 was too depolarized to elicit an action potential. Scale bars: 5 mV (red trace)/30 mV (black trace), 1 s. C: 6 of 78 FSI pairs were electrically coupled (red) while 72 of 78 pairs were detectably un-paired (pink). D: Coupling coefficients for each FSI pair in the scatterplot. Each symbol is representative of a pair of FSIs (six symbols for six pairs).

2.3.2. FSI and medium spiny projection neuron (MSN) action potential (AP) firing in response to corticostriatal activation.

Next, we gathered empirical corticostriatal synaptic data in order to inform our subsequent network modeling methodology. Because we sought to understand whether increasing the frequency of convergent cortical input onto FSIs may drive their coordinated firing, we calculated the probability "P" of an FSI firing in response to cortical input at a variety of frequencies (1, 10, 20 Hz) across 10 sweeps. Primary and secondary motor cortices (M1 and M2, respectively) directly innervate both FSIs and MSNs (Ramanathan et al., 2002). FSIs are thought to synchronize their activity in vivo, while MSNs are not (O'Hare et al., 2017). Thus, we compared cortical input onto FSIs versus MSNs. To do this, we performed dual whole cell patch clamp recordings of FSIs and MSNs while activating M1/M2 input optogenetically. To distinguish between FSIs and MSNs, we utilized maximum firing rate as a measure (**Figure 2.2a** and **b**). Consistent with known differences between the cell types, FSIs demonstrated a higher firing rate compared to MSNs (**Figure 2.2c**; maximum firing rate in Hz for MSNs: 55.95 ± 8.372, for FSIs: 183.30 ± 65.01; n= 20 MSNs, n = 24 FSIs; $t = 9.53$, $p < 0.0001$; unpaired t test). To ensure healthy cellular recordings for both FSIs and MSNs, we measured resting membrane potentials (RMPs; **Figure 2.2d**; in mV for MSNs: -51.480 ± 29.2, for FSIs: -55.14 ± 6.521; n= 26 MSNs, n = 23 FSIs; $t = 0.587$, $p = 0.560$; unpaired t test) and action potential (AP) thresholds (Fig 2d; in mV for MSNs: -27.10 ± 11.27, for FSIs: -22.84 ± 6.806; n = 25 MSNs and n = 20 FSIs; $t = 1.454$, $p = 0.153$; unpaired t test), with a correction of 15.7 mV for liquid junction potential, and found that neither of which were statistically different. We found that FSI AP discharge followed an M1/M2 cortical afferent optogenetic 10 Hz light pulse train more faithfully than MSN

AP firing across several light intensities (**Figure 2.2e - h**; AP firing fraction for MSNs at 0.4 mW: 0.0 ± 0.0, for FSIs: 0.17 ± 0.39, n = 13 MSNs, n = 12 FSIs, p > 0.999; AP firing fraction for MSNs at 2.2 mW: 0.10 ± 0.31, for FSIs: 0.45 ± 0.15, n = 9 MSNs, n = 10 FSIs, p = 0.142; AP firing fraction for MSNs at 3.8 mW: 0.13 ± 0.24, for FSIs: 0.84 ± 0.41, n = 13 MSNs, n = 12 FSIs, p = 0.005; AP firing fraction for MSNs at 6.3 mW: 0.13 ± 0.24, for FSIs: 0.84 ± 0.41, n = 13 MSNs, n = 12 FSIs, p = 0.002; Kruskal-Wallis ANOVA). This effect was also observed with other light pulse frequencies, including 1 Hz (**Figure 2.2i**; AP firing fraction of MSNs at 0.4 mW: 0.0 ± 0.0, for FSIs: 0.08 ± 0.29, n = 13 MSNs, n = 12 FSIs, p > 0.999; AP firing fraction for MSNs at 2.2 mW: 0.11 ± 0.33, for FSIs: 0.34 ± 0.47, n = 9 MSNs, n = 12 FSIs, p = 0.202; AP firing fraction for MSNs at 3.8 mW: 0.09 ± 0.28, for FSIs: 0.58 ± 0.44, n = 13 MSNs, n = 12 FSIs, p = 0.009; AP firing fraction for MSNs at 6.3 mW: 0.12 ± 0.30, for FSIs: 0.76 ± 0.37, n = 13 MSNs, n = 12 FSIs, p = 0.001; Kruskal-Wallis ANOVA) and 20 Hz (**Figure 2.2j**; AP firing fraction of MSNs at 0.4 mW: 0.0 ± 0.0, for FSIs: 0.17 ± 0.38, n = 13 MSNs, n = 12 FSIs, p = 0.678; AP firing fraction for MSNs at 2.2 mW: 0.02 ± 0.05, for FSIs: 0.55 ± 0.56, n = 9 MSNs, n = 10 FSIs, p = 0.018; AP firing fraction for MSNs at 3.8 mW: 0.04 ± 0.05, for FSIs: 0.72 ± 0.48, n = 13 MSNs, n = 12 FSIs, p = 0.006; AP firing fraction for MSNs at 6.3 mW: 0.05 ± 0.06, for FSIs: 0.86 ± 0.42, n = 13 MSNs, n = 12 FSIs, p = 0.001; Kruskal-Wallis ANOVA).

Figure 2.2. FSI and medium spiny projection neuron (MSN) action potential (AP) firing in response to corticostriatal activation. A: Representative trace of the firing rate of an FSI in response to a current injection of 40 pA. Scale bars: 40 mV, 500 ms. B: Representative trace of the firing rate of an MSN in response to a current injection of 40 pA. Scale bars: 40 mV, 500 ms. C: FSIs (n = 24) demonstrate a faster maximum firing rate compared to MSNs (n = 20 cells). **** $p < 0.0001$, as per unpaired t test. All data represented as mean + SD. D: Action potential (AP) thresholds and resting membrane potentials (RMP) are not significantly different for MSNs (AP threshold n = 25 cells; RMP n = 26 cells) and FSIs (AP threshold n = 20 cells, RMP n = 23 cells). Voltage values are corrected for liquid junction potential (15.7 mV). AP threshold $p = 0.153$ and RMP $p = 0.560$, as per unpaired t test. Data are represented as mean ± SD. E: Schematic of dual FSI and MSN recordings while optogenetically activating corticostriatal inputs. F: Representative trace of dual current clamp recordings from FSIs in response to 470 nm 10 Hz optogenetic stimulation (AAV-ChR2) of cortical inputs. Scale bars: 30 mV, 10 ms. G: Representative trace of dual current clamp recordings from MSNs in response to 470 nm 10 Hz optogenetic stimulation (AAV-ChR2) of cortical inputs. Scale bars: 30 mv, 10 ms. H: The fraction of 470 nm 10 Hz light pulses that elicited APs for FSIs is not significantly greater than for MSNs at light intensities of 0.4 (n = 13 MSNs, n = 12 FSIs; $p > 0.999$) or 2.2 mW (n = 9 MSNs, n = 10 FSIs; $p = 0.142$), but is significantly greater for FSIs than for MSNs at light intensities of 3.8 (n = 13 MSNs, n = 12 FSIs; **$p = 0.005$) and 6.3 mW (n = 13 MSNs, n = 12 FSIs; **$p = 0.002$). Statistical values were determined using Kruskal-Wallis ANOVA. Data represented as mean + SD. I: The AP firing fraction of FSIs in response to 1 Hz 470 nm light pulses is not significantly greater than MSNs at 0.4 (n = 13 MSNs, n = 12 FSIs; $p > 0.999$) or 2.2 mW (n = 9 MSNs, n = 10 FSIs; $p = 0.202$), but is significantly greater for FSIs than for MSNs at 3.8 (n = 13 MSNs, n = 12 FSIs; **$p = 0.009$) and 6.3 mW (n = 13 MSNs, n = 12 FSIs; ***$p = 0.001$) light intensities. Statistical values were determined using Kruskal-Wallis ANOVA. Data represented as mean + SD. J: The fraction of 20 Hz 470 nm light pulses that elicited APs in FSIs is not significantly higher than for MSNs at 0.4 mW (n = 13 MSNs, n = 12 FSIs; $p = 0.678$), but is significantly higher for FSIs than for MSNs at 2.2 (n = 9 MSNs, n = 10 FSIs; *$p = 0.018$), 3.8 (n = 13 MSNs, n = 12 FSIs; **$p = 0.006$) and 6.3 mW (n = 13 MSNs, n = 12 FSIs; ***$p = 0.001$) intensities. Statistical values were determined using Kruskal-Wallis ANOVA. Data represented as mean ± SD.

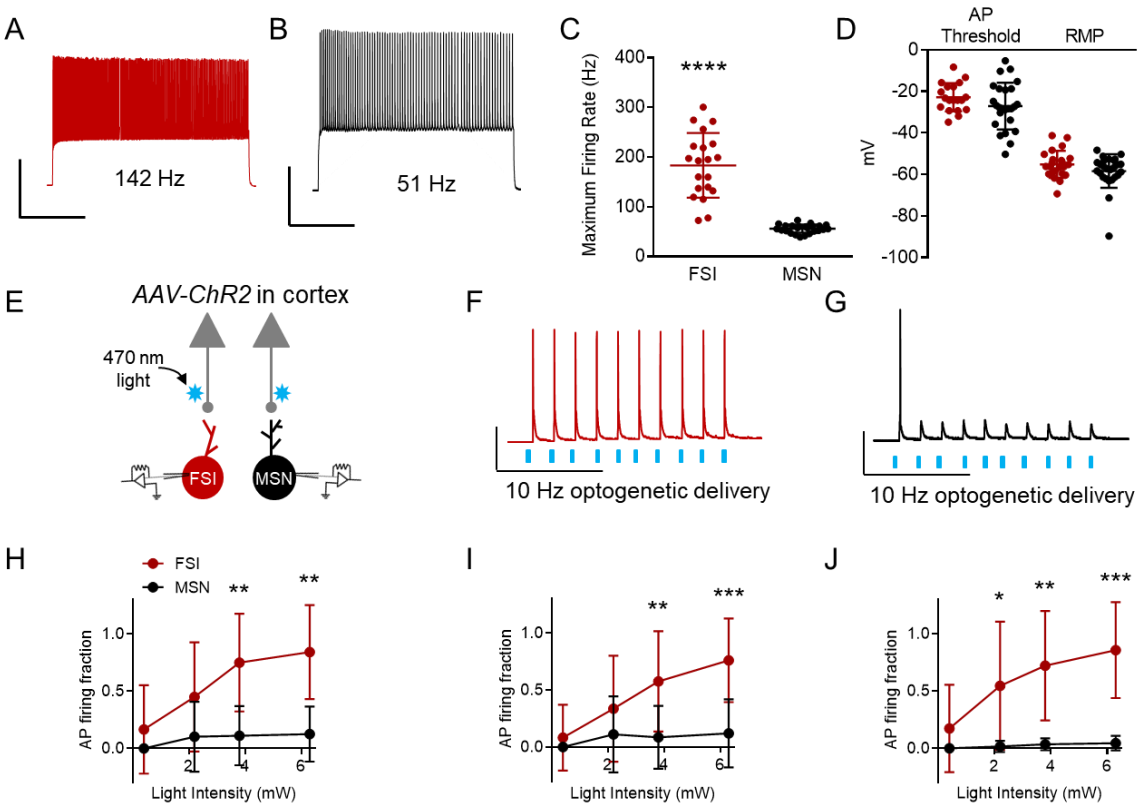
A
142 Hz
B
51 Hz
C
Maximum Firing Rate (Hz)
400
300
200
100
0
****
FSI
MSN
D
AP Threshold
RMP
mV
0
-20
-40
-60
-80
-100
E
AAV-ChR2 in cortex
470 nm light
FSI
MSN
F
10 Hz optogenetic delivery
G
10 Hz optogenetic delivery
H
FSI
MSN
**
**
AP firing fraction
1.0
0.5
0.0
2
4
6
Light Intensity (mW)
I
**
***
AP firing fraction
Light Intensity (mW)
J
*
**
***
AP firing fraction
Light Intensity (mW)

2.3.3 Model architecture and simulation flow.

To further investigate the role of FSI-FSI electrical synapse connectivity on FSI synchrony using our experimentally-derived empirical data, we generated a simple probabilistic neural circuit with two layers: (i) an independent cortical layer and (ii) a layer of FSI neurons dependent on cortical and FSI input (**Figure 2.3**; see Methods for details). **Figure 2.3a** and **b** display the two extremes for an example case of 3 FSIs, whereby **figure 2.3a** shows 0% convergence, and **figure 2.3b** depicts 100% convergence.

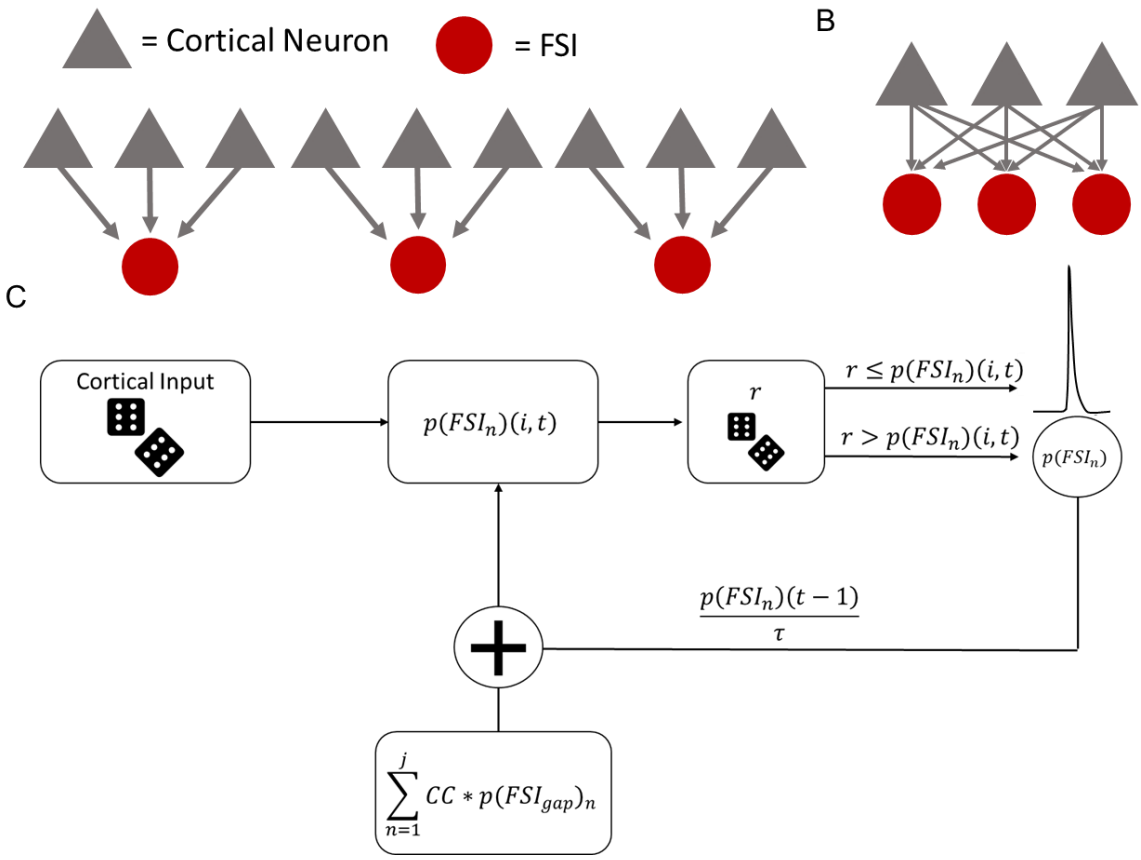

Figure 2.3. Model architecture and simulation flow. A. A completely independent network has a number of cortical neurons equal to the number of FSI neurons squared. B. A completely convergent network has as many cortical neurons as FSI neurons. C. Cortical activity is drawn independently and randomly on each time bin. Then, the downstream FSI integrated the number of inputs it received to determine the likelihood to fire an action potential. To simulate neural variability, random noise is added by drawing a number from a distribution to determine if the neuron fired an action potential or it did not. If the neuron did fire, it then entered a refractory period. If the neuron did not fire an action potential, the probability to fire is stored and decayed by the time constant (τ) for the next iteration.

2.3.4 Simulations reveal that convergent cortical input induces higher levels of FSI-FSI synchrony compared to electrical synapse FSI-FSI connections.

Simulations of the model depicted in the flow diagram represented in **Figure 2.3c** show that FSIs exhibit more synchronous activity under the cortically convergent model than the FSI-FSI laterally electrical synapse connected model whether cortical input is synchronous or asynchronous (**Figure 2.4**). With an n = 10 FSIs, the convergent model shows increased synchrony as assessed by the number of coincidently detected FSI-FSI action potential firing occurrences compared to the laterally connected model, regardless of whether cortical input was synchronous (**Figure 2.4a**) or asynchronous (**Figure 2.4b**). However, peak occurrences were higher in FSIs in the convergent model with synchronous input compared to asynchronous input. We repeated this for n = 5 (**Figure 2.4c** and **d**) and n = 50 (**Figure 2.4e** and **f**). When input was synchronous, FSIs exhibited lower occurrences in the lateral model compared to the convergent model (**Figure 2.4a, c,** and **e**). When input was asynchronous, FSIs again exhibited lower occurrences in the laterally connected model compared to the convergent model (**Figure 2.4b, d,** and **f**). In the simulations with synchronous input, both the convergent model and the laterally connected model exhibited peak occurences in the cross correlegram at 0 ms. This effect has been observed in previous models and is an artifact when the input is itself synchronous (Damadoran et al., 2014).

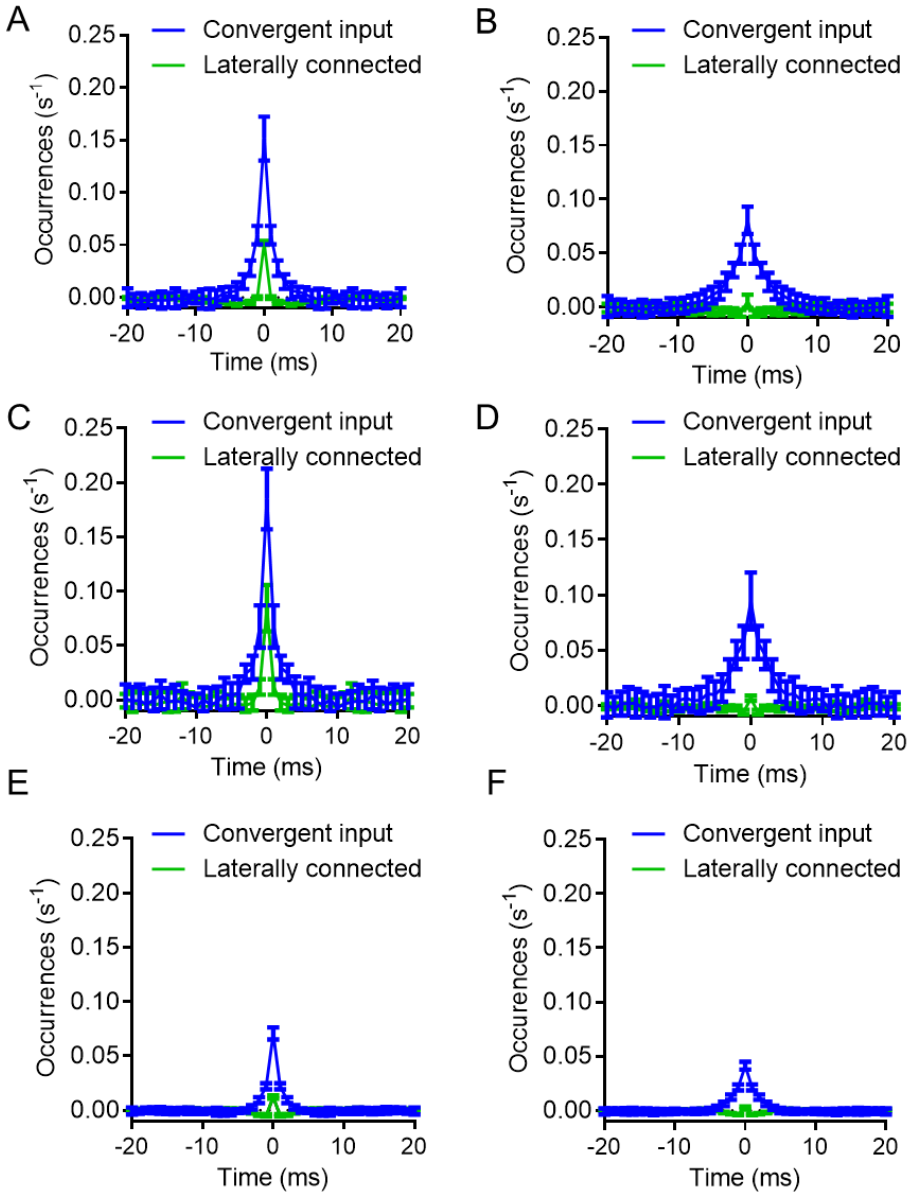

Figure 2.4: Simulations reveal that convergent cortical input induces higher levels of FSI-FSI synchrony compared to electrical synapse FSI-FSI connections. A. Convergent input shows higher FSI synchrony in the presence of synchronous input, n =10 FSIs. B. Convergent input generates synchrony among FSIs in the absence of synchronous input, n =10 FSIs. C and D. Same as A and B, but instead n = 5. E and F. Same as A and B, but instead n = 50. Each condition was simulated 20 times. Data represented as mean ± SD.

2.3.5 Parameter scans show larger synchrony in a convergent input than laterally connected.

Although the parameters used for these simulations were informed from our experimental results, we performed a series of parameter scans calculating the synchrony at the 0s lag, to explore whether or not parameter values varied the interpretation of our results (**Figure 2.5**). Across each of the parameters tested, we found no cases in which the laterally connected model had larger synchrony than the convergent model. In **figure 2.5b** and **d** as we approach 0 the synchrony appears to approach infinity, this is due to the low firing of FSIs during these conditions and MATLABs xcorr function will disproportionately weigh them as more synchronous.

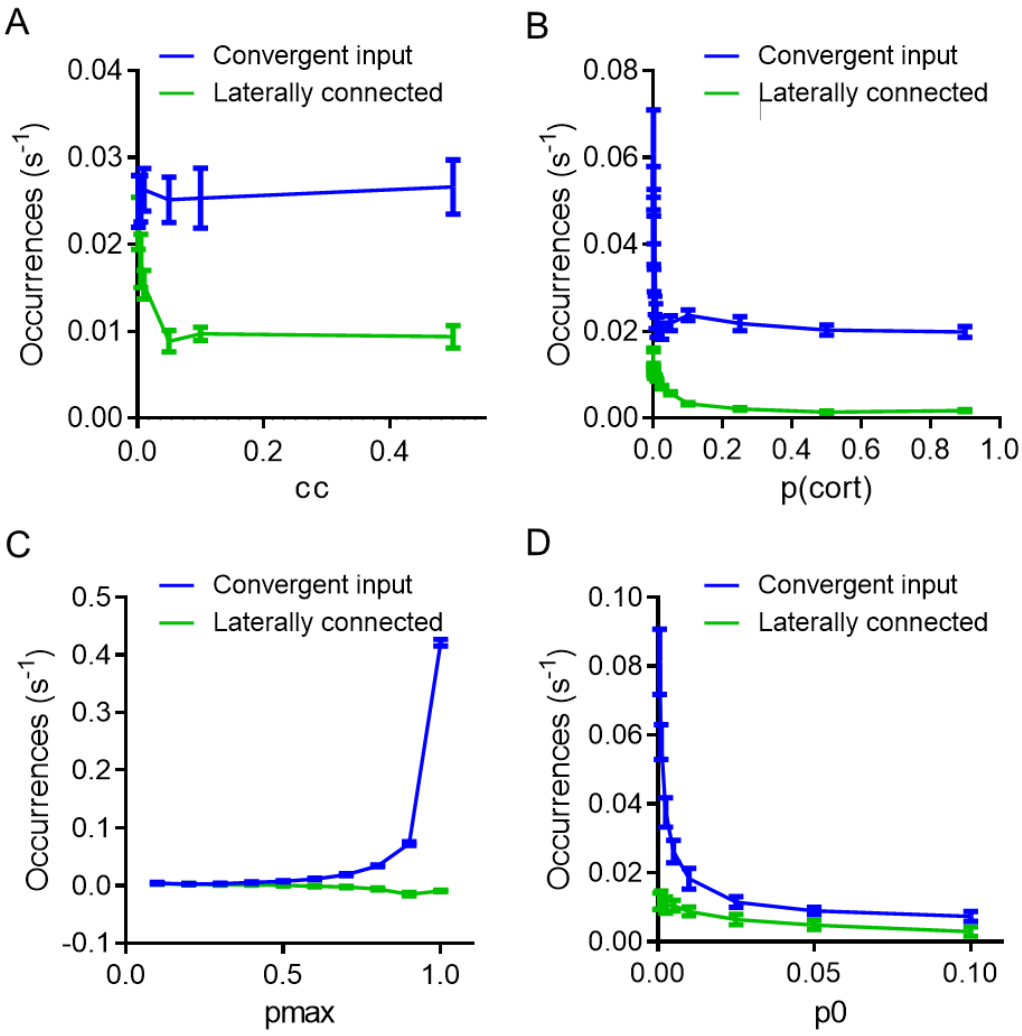

Figure 2.5: Parameter scans show larger synchrony in a convergent input than laterally connected. A) Changing the coupling coefficient (CC) results in a decline in synchrony for the laterally connected model. B) Changing the probability of cortical neurons to fire (p_cort) shows a decline in synchrony with increasing cortical firing. C) Increasing the probability to fire if all inputs have been activated (pmax), results in increasing synchrony for the convergent model but not changes to the laterally connected model. D) Increasing the baseline probability of an action potential (p0) results in decrease synchrony across the two models. In each of the simulations the variables were kept constant unless otherwise stated as cc = 0.03, pmax = 0.7, p0 = 0.005. Additionally, these simulations were done under the spontaneous input conditions with n = 10 FSIs. 20 trials were run for each condition. Data represented as mean ± SD.

2.3.6 Increasing convergent cortical input increases FSI synchrony, but increasing FSI-FSI electrical synaptic connections does not.

To further assess the role of convergent input versus FSI-FSI lateral electrical synaptic connectivity contributions to FSI synchrony (**Figure 2.3b**), we varied the percentage of convergence and lateral connections independently of one another and observed whether this affected FSI-FSI action potential firing event occurence (**Figure 2.6**). Increasing the percentage of cortical convergence in the absence of any lateral connections increased observed occurences for a network of 10 FSIs (**Figure 2.6a**). However, increasing the percentage of lateral connections between FSIs in a network that had no cortical input convergence resulted in no significant change in occurrences (**Figure 2.6b**). We repeated these simulations with n = 5 FSIs (**Figure 2.6c** and **d**) and n = 50 FSIs (**Figure 2.6e** and **f**). These modeling data - informed by empirically derived cortico-FSI synaptic properties - suggest that convergent cortical input influences FSI synchrony to a greater extent than lateral FSI-FSI connectivity.

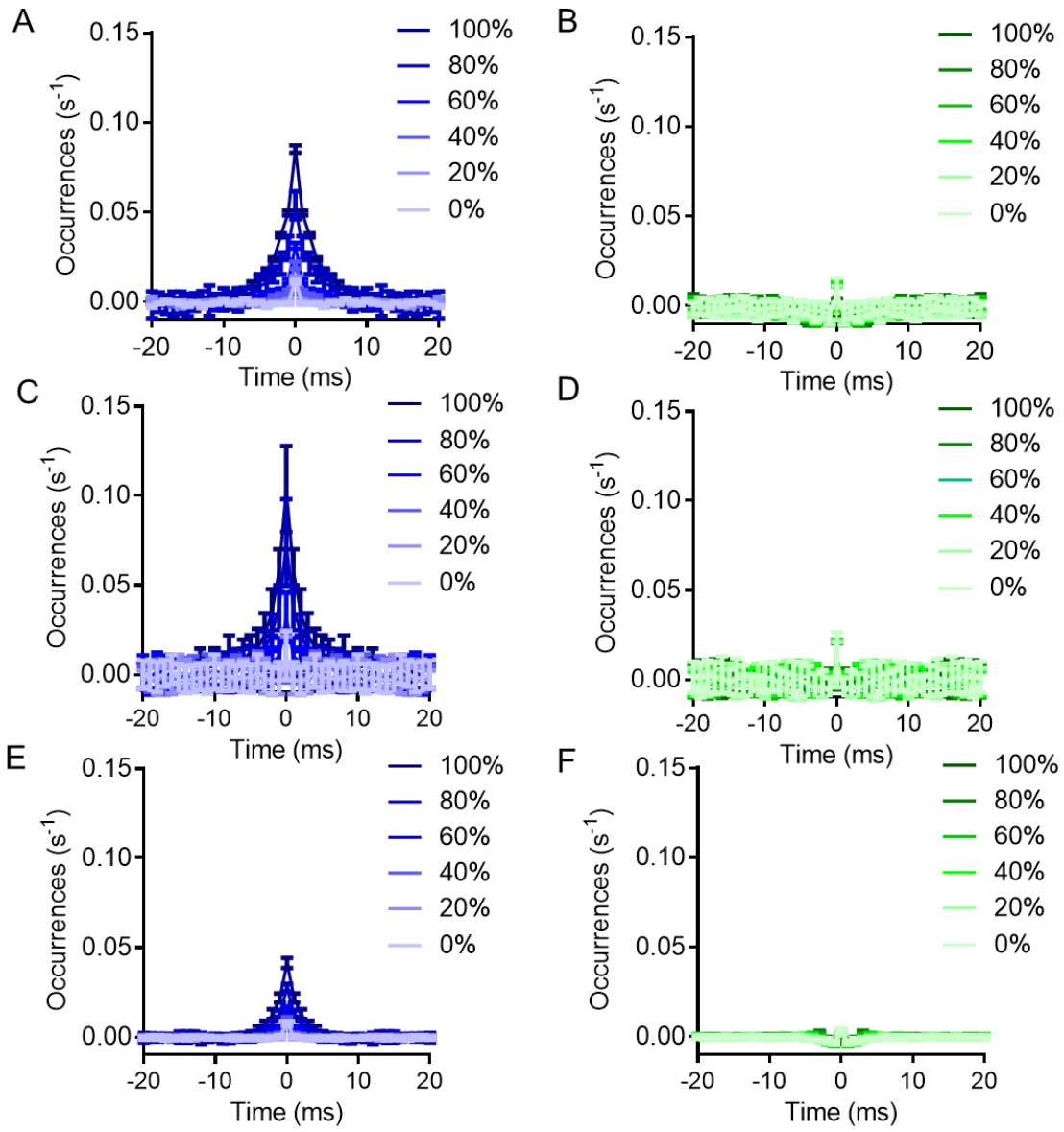

Figure 2.6. Increasing convergent cortical input increases FSI synchrony, but increasing FSI-FSI electrical synaptic connections does not. A. Increasing the percent of cortical input convergence directly increases FSI synchrony, n = 10 FSIs B. Increasing the percent of FSI-FSI electrical synaptic connections does not increase FSI-FSI synchrony, n = 10 FSIs. C and D: Same as A and B, but instead n = 5. E and F: Same as A and B, but instead n = 50. Each condition was simulated 20 times. Data represented as mean ± SD.

2.4 Discussion

We found that FSI-FSI electrical coupling in adult mice occurred at ~8% of assayed pairs and that FSIs fired with greater fidelity under cortical afferent stimulation than MSNs. Using these empirical FSI-FSI connectivity and cortico-FSI synaptic strength findings to inform our neural simulations of variant cortico-FSI networks, we showed that a major source of FSI-FSI synchrony may derive from convergent cortical input, while FSI-FSI electrical synapses may provide minor contributions to bulk FSI synchrony (**Figure 2.7)**.

Strong evidence exists for electrical synapses to promote synchronous neuronal firing in the striatum, hippocampus, cortex, neocortex, and cerebellum (Galarreta and Hestrin, 1999; Mann-Metzer and Yarom, 1999; Beierlein et al., 2000; Hormuzdi, et al., 2001; Traub et al., 2001; LeBeau et al., 2003; Pfeuty et al., 2003; Zhang et al., 2017). In cortical FSIs, however, genetic deletion of connexin-36 does not abolish synchrony among this interneuron population (Salkoff et al., 2015). This is consistent with our computational findings, which suggest that the observed sparser electrical coupling between FSIs in adulthood, as compared to adolescence, may only fine-tune synchronous FSI responses to excitatory drive from the cortex. However, in the absence of coincident cortical excitation, electrical coupling between FSIs may actually shunt current and possibly suppress FSI firing (Hjorth et al., 2009). Taken together with the findings of Hjorth et al. (2009), these data suggest that the ability of electrical synapses to promote FSI-FSI synchrony may not only diminish with age, but also may only do so when FSIs are receiving coincident glutamatergic barrage from convergent cortical inputs.

There are important caveats to consider with the present modeling data. First, because our model is based on the number of action potentials in response to cortical

afferent activation, it does not account for the possible lateral chemical synaptic inhibition from neighboring FSIs or inhibitory input from the globus pallidus (Bevan et al., 1998; Mallet et al., 2012). Also, while cortical input into striatum is the largest source of excitatory input onto FSIs, our model does not consider excitatory inputs from other areas such as thalamic nuclei (Sciamanna et al., 2015; Klug et al., 2018; Assous and Tepper, 2019a; Assous and Tepper, 2019b) and the pedunculopontine nucleus (Assous et al., 2019). Second, the model assumes homogeneity of FSI morphology and response properties. This assumption was made to simplify the model for simulations to directly target the role of electrical synapses. However, FSIs may vary in their presynaptic inputs and weight distributions (Assous and Tepper, 2019b). Introducing heterogeneity in cortico-FSI synaptic weights could shift the results toward heterogeneous populations of synchronized FSIs, potentially reflecting functional FSI ensembles (Roberts et al., 2019). Lastly, the simulations presented here range from 5-50 FSIs in a circuit, while it is unknown exactly how many FSIs form functional ensembles, the model is limited in how many FSIs can be included to generate interpretable results. This is due to the nature of increasing lateral electrical synapses in network models, which results in increased firing rates (Damadoran et al., 2014). That is, if the model exceeds 100 FSIs in a network the firing rates reach non-physiological firing rates (~1000 Hz).

Electrical synapse diminishment from development to adulthood is observed elsewhere in the mammalian central nervous system (Belluardo et al., 2000; Condorelli et al., 2000). The functional significance of this is unclear. Because development is a period in which rapid, extensive action learning occurs (Watanabe et al., 2007; DePasque and Galvan, 2017), perhaps electrical synapses between striatal FSIs aid in de novo action

acquisition. Interestingly, alcohol inhibits connexin 36-containing electrical synapses in adulthood (Mustonen et al., 2004; Wentlandt et al., 2004; Mustonen et al., 2005), yet facilitates habit learning (Corbit et al., 2012). The impact of decreased connexin-36 and electrical synapse numbers between FSIs on the consolidation of actions and habits into adulthood requires further exploration.

In conclusion, we find that FSI electrical synapses weakly contribute to the synchrony of striatal FSIs in adult mice while convergent, and coincident, cortical excitation significantly drives FSI-FSI synchrony. These empirical data-informed modeling results support extant modeling data (Hjorth et al., 2009) and provide further insight into the origins of FSI functional ensemble behavior, which ultimately shape MSN output (Damodaran et al., 2014; Owen et al., 2018). These findings advance our current understanding of how the DLS processes excitatory input to promote automatized action (Diaz-Hernandez et al., 2018; Kim et al., 2019; Klaus et al., 2019). Given that FSIs regulate different, specific action subcomponents by firing in ensembles (Roberts et al., 2019), it is possible that different areas of cortex converge onto specific FSI ensembles to modulate the speed, and therefore timing (Kim et al., 2019), of the specific action subcomponents they encode. This mechanism could also drive specific FSI ensembles to fire during reward learning in order to distinguish between cues (Bakhurin et al., 2016; Lee et al., 2017). Considering that FSIs are causally linked to habitual responding (O'Hare et al., 2017) and are necessary for the development of compulsive ethanol consumption (Patton et al., 2021), the present data also implicate the cortico-FSI synapse as a possible viable target for therapeutic intervention in compulsive drug and alcohol consumption.

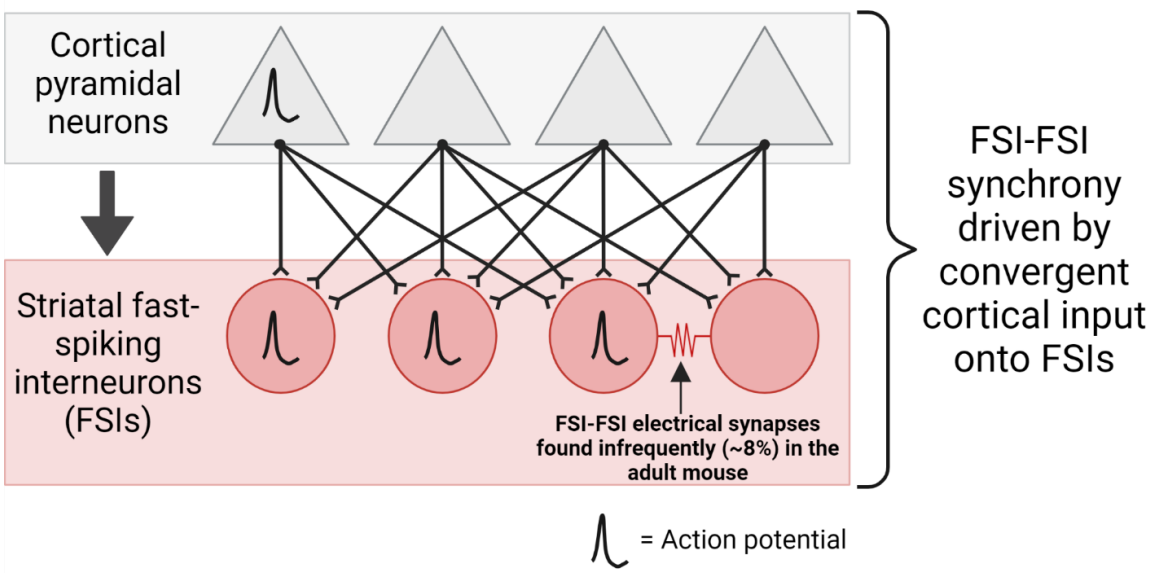

Figure 2.7. Proposed model for FSI synchrony. Convergent and coincident cortical excitation of FSIs drives them to synchronously fire. Electrical synapses between FSIs are infrequent and only subtly contribute to synchrony driven by cortex.

Chapter 3: The rewarding properties of ethanol many be mediated by BDNF signaling in the nucleus accumbens core

Abstract

The nucleus accumbens (NAc) integrates a variety of inputs to enable associations between external cues and rewards. Alcohol, a major drug of abuse, strengthens a form of inhibitory plasticity in the NAc that is mediated by brain derived neurotrophic factor (BDNF) signaling through its canonical receptor tropomyosin kinase B (TrkB). Whether this enhanced disinhibition of the NAc by alcohol drives the rewarding properties of this substance is unknown. Herein, we find that midbrain dopamine terminals in the NAc serve as a necessary and sufficient source of BDNF for induction of NAc inhibitory plasticity, that this synaptic depression is enhanced by alcohol, and that *in vivo* activation of these terminals is rewarding in a TrkB-dependent manner. Furthermore, we find that a subthreshold rewarding dose of ethanol coupled with subthreshold rewarding induction of inhibitory plasticity *in vivo* is rewarding in a TrkB-dependent manner. These findings suggest that alcohol reward may be driven, in part, by BDNF-TrkB signaling at inhibitory synapses formed between the VTA and NAc medium spiny neurons.

3.1 Introduction

Recent human studies demonstrate that sensitivity to the rewarding properties of alcohol is a robust predictor of alcohol use disorder (AUD) development and that elevated reward sensitivity persists even in those diagnosed with AUD (King et al., 2011; King et al., 2014; King et al., 2016; King et al., 2021; King et al., 2022). As such, uncovering the mechanisms mediating the rewarding properties of alcohol is critical to improving our

understanding of why individuals are driven to drink. Thus, further investigation into the mechanisms mediating the rewarding properties of alcohol is warranted.

Reward-related behaviors are mediated by nucleus accumbens (NAc) medium spiny projection neurons (MSNs), the output of which is driven by integration of excitatory, inhibitory, and modulatory synaptic inputs (Sesack and Grace, 2010; Grueter et al., 2011; Schultz, 2016; Russo and Nestler, 2013). While NAc MSN excitatory synapses are susceptible to aberrant modulation by drugs of abuse such as cocaine and ethanol (EtOH) that may mediate drug-seeking behavior (Thomas et al., 2001; Boudreau and Wolf, 2005; Martin et al., 2006; Conrad et al., 2008; Huang et al., 2009; Luscher and Malenka, 2011; Pascoli et al., 2011), investigation of inhibitory synapse strength modulation by drugs of abuse is lacking. This is despite the powerful influence of GABAergic transmission on MSNs (Nisenbaum and Berger, 1992), which arise from both extrinsic and intrinsic sources (Russo and Nestler, 2013).

MSN inhibition is modulated by long-term plasticity in the NAc that is mediated by brain-derived neurotrophic factor (BDNF) and augmented by EtOH in a manner dependent upon BDNF signaling through its canonical postsynaptic receptor tyrosine receptor kinase B (TrkB), which is termed NAc-iLTD (Patton et al., 2019). Herein, we utilize optogenetics and whole cell patch-clamp electrophysiology to discover a two sources of BDNF mediating NAc-iLTD: ventral tegmental area (VTA) dopaminergic neurons and prelimbic prefrontal cortex (plPFC) glutamatergic neurons. We find that oLFS of BDNF-releasing afferents in the NAc, which drives NAc-iLTD in slice, drives a conditioned place preference (CPP). Furthermore, we find that VTA afferents in the NAc may contribute to the rewarding properties of EtOH.

3.2 Methods

All procedures were performed in accordance with the United States Public Health Service Guide for Care and Use of Laboratory Animals and were approved by the Institutional Animal Care and Use Committee at the University of Maryland School of Medicine. Mice were housed with littermates (2-5 per cage) under a 12-hr light/dark cycle (lights on at 0700 hrs, off at 1900 hrs) with *ad libitum* access to food and water. Homozygous floxed-TrkB (Flx-TrkB) mice, heterozygous dopamine transporter cre mice (DAT-cre; Zhuang et al. 2005), and all other mice used for slice electrophysiology and behavioral experiments were on a C57Bl/6J background. Male and female mice used were over 6 wks old at the time of surgery and over 2 months old during experimentation.

3.2.1 Stereotaxic surgery and viral vectors. At the time of surgery, mice were anesthetized with isoflurane (induction 5%; maintenance 1-2%) and placed into a stereotaxic frame (David Kopf Instruments). A heating pad was used to maintain body temperature and mineral oil was applied to the eyes. Carprofen (5 mg/kg) was injected subcutaneously for analgesia. Mouse breath rate was monitored and toe pinches were delivered throughout the duration of the surgical procedure to ensure mice were properly anesthetized. To target VTA dopaminergic afferents into the NAc for optogenetic stimulation in acute slices, 300 nL of viral construct expressing channelrhodopsin and mCherry under the human synapsin 1 gene promoter (AAV5-dflox-ChR2-mCherry; UPenn) was pressure injected into the VTA (-3.08 mm AP, ±0.5 mm ML from bregma, -4.25 mm DV from brain surface) of DAT-cre mice. Prelimbic prefrontal cortices (plPFC) were targeted for optogenetic stimulation in the NAc by injecting ChR2 expressing enhanced yellow fluorescent protein (eYFP) into the plPFC of wild type mice. To

selectively delete TrkB from all cells in the NAc while allowing for optogenetic activation of VTA afferents in the NAc, bilateral stereotactic injections of AAV9-hSyn-cre-enhanced green fluorescent protein (eGFP; UPenn) were delivered into the NAc (A/P +1.5 mm from bregma, M/L ±0.8 from midline, D/V −3.5 from top of brain) of homozygous Flx-TrkB mice 4 wks following ChR2 injections (Luikart et al., 2003; Lobo et al., 2010). Following all viral injections, the scalps of the mice were sutured together with aliphatic polymers monofilament Blue nonabsorbable suture and the mice were singly housed in cages for 3 days of recovery. During the first day of recovery, lidocaine was applied to the head wound and carprofen (5 mg/kg) was administered subcutaneously.

To enable optogenetic interrogation of VTA afferents *in vivo*, all mice also received bilateral optic fiber implantations into their NAc (+1.5 mm AP, -0.8 mm ML from bregma, -3.25 from brain surface for one implant and, for the other, at a 24° angle: +1.35 mm AP, +2.13 mm ML from bregma, -3.07 from brain surface) in a second surgery 4 wks following viral injection surgeries. Subsequent to fiber implantation, TitanBond or DenBond (both from Amazon.com) were applied directly to the skull. After a 30 min wait to allow for drying, dental cement caps were then created by using a syringe to deliver a mix of cement liquid and cement powder (Amazon.com) to the skull and around the fibers. Following all surgical procedures, carprofen (5 mg/kg) was administered for another two days of recovery before mice were rehoused with their cage mates.

3.2.2 Acute slice preparation. Following >6 wks post viral transfection surgery for DAT-cre mice and >4 wks for wild type mice, mice expressing ChR2 in the NAc were deeply anesthetized with isoflurane (vaporized, 5%). Their heads were rapidly decapitated and their brains were immediately extracted and submerged in 95% oxygen, 5% carbon dioxide

(carbogen)-bubbled ice cold cutting solution (in mM: 194 sucrose, 30 NaCl, 4.5 KCl, 1 $MgCl_2$, 26 $NaHCO_3$, 1.2 NaH_2PO_4, and 10 D-glucose). Extracted brains were sliced at 250 μm with a vibratome (Leica VT 1200) and transferred to carbogen-bubbled artificial cerebrospinal fluid (aCSF; in mM: 124 NaCl, 4.5 KCl, 2 $CaCl_2$, 1 $MgCl_2$, 26 $NaHCO_3$, 1.2 NaH_2PO_4, and 10 D-glucose). Brain slices containing the NAcc were incubated at 32.4 °C for 30 min before they were removed and stored at room temperature until recordings were performed.

3.2.3 Whole-cell patch-clamp electrophysiology. To record, brain slices were hemisected and transferred to a recording bath where they were perfused throughout recording with carbogen-bubbled aCSF (29–31 °C) via gravity perfusion. MSNs targeted by ChR2-containing VTA dopaminergic or plPFC glutamatergic afferents were visualized and targeted for whole cell current clamp recordings through the epifluorescent light path illuminated by a light-emitting diode (LED) system (X-Cite series 120Q). All whole-cell experiments were recorded using borosilicate glass pipettes (resistances ranging from 2–5 MΩ) filled with a cesium chloride-based solution (in mM: 150 cesium chloride, 10 HEPES, 2 $MgCl_2$, 3 ATP-Mg, 0.3 GTP-Na, 0.2 BAPTA-4Cs, and 5 QX-314; osmolarity ranging from 290-295 mOsm; pH ~7.3). Cells were voltage clamped using a MultiClamp 700B amplifier (Molecular Devices) and Clampex 10.4.1.4 software (Molecular Devices) was used for data acquisition. All recordings were filtered at 2 kHz and digitized at 10 kHz.

In experiments with wildtype mice, inhibitory postsynaptic currents (IPSCs) were evoked every 20 s using a concentric bipolar stimulating electrode (World Precision Instruments) located ~100 μm away from the recording electrode. Electrically evoked-low-frequency stimulation (eLFS; 1 Hz, 240 pulses) was delivered while holding MSNs at

−80 mV (down state) after acquiring a stable baseline. To induce NAc-iLTD in the down state, the holding potential of the MSN was decreased from −60 mV to −80 mV by −4 mV increments every 4 s during the last 20 s before eLFS began. MSNs were returned to the up state (−60 mV) by reversing the protocol during the first 20 s of the post-eLFS file. Wildtype mice with ChR2 in their plPFC underwent the same protocols, except LFS was delivered utilizing an optical fiber (delivering pulses of blue light; 4 ms pulse width, 470 nm). The same protocols were used to evoke IPSCs and induce NAc-iLTD in experiments with DAT-cre mice expressing ChR2 in VTA dopaminergic afferents in the NAc. However, an optical fiber was used for the duration of the recording.

3.2.4 Conditioned Place Preference (CPP). Approximately 6 wks following bilateral ChR2-injection into the VTA and bilateral indwelling optical fiber implants into the NAc, DAT-cre mice were habituated to the CPP arena (overall dimensions: 70 x 30 x 25 cm; each zone: 30 x 29.3 cm, neutral zone: 11.5 x 10 cm). Both zones of the arena were labeled with distinct shapes on the walls (a combination of circles, vertical stripes, triangles, horizontal wavy lines, solid black bars, or diamonds). The animal's movements were tracked using EthoVision XT Software. At this time, mice were also habituated to intraperitoneal (i.p.) injections of saline (2 injections separated by 90 mins) and optical patch cords. Baseline or "pre-light" measurements of time spent in both zones were taken to determine the preferred zone. On day 2 of the protocol, mice were injected i.p. with either saline, brain blood barrier-penetrant cyclotraxin B (*tat*-CTX-B; 2 x 20 mg/kg mixed with 20 mg/kg *tat* peptide in saline; Cazorla et al., 2010; Constandil et al., 2010), *tat* peptide alone (non-toxic transduction domain of the *tat* protein from HIV type 1, "vehicle"; 2 x 20 mg/kg in saline; Gump and Dowdy, 2007), or flupenthixol dihydrochloride (2 x 0.5 mg/kg;

Wenzel et al., 2013) 2 hrs before and 30 mins before being restricted to the non-preferred zone (adapted from Cunningham and Noble, 1992 and Joffe et al, 2017). oLFS was delivered twice for 4 mins, separated by 11 mins without stimulation. Mice receiving 0.25 Hz stimulation also received it twice for 4 mins, separated by 11 mins. Mice receiving optogenetic stimulation of plPFC received saline injections (2 x saline, i.p., 90 min interval) prior to conditioning.

Mice receiving subthreshold rewarding light delivery received oLFS once for 4 mins followed by 11 mins without stimulation. Mice receiving subthreshold rewarding doses of EtOH during conditioning received a single 2 g/kg dose 3-5 mins prior to the conditioning session (incorporation of EtOH injection into CPP informed by Cunningham and Noble, 1992). At least 2 hrs following all variations of the conditioning session, mice were given access to the full arena again and the amount of time spent in each zone was measured during what we term the "Test" or "post-light" session.

All reagents for slice electrophysiology cutting and recording solutions as well as 95% EtOH were purchased from Sigma-Aldrich. CTX-B and flupenthixol dihydrochloride were purchased from Tocris Bioscience. TAT peptide was purchased from Anaspec.

3.2.5 Immunohistochemistry

To verify injection sites following slice physiology recordings, NAc slices incubated in 4% PFA at 4 °C for at least 3 days and a shortened Brain BLAQ immunohistochemistry procedure was performed (Kupferschmidt et al., 2015). To visualize mCherry or eYFP-expressing adeno-associated viruses following CPP experiments, chicken anti-mCherry (Novus Biologicals NBP2-25158) and AlexaFluor594 donkey-anti-chicken antibodies (Jackson ImmunoResearch 703-545-155; 1:500) were used. To visualize eGFP

fluorescence, chicken-anti-GFP (Abcam ab13970; 1:2000) and AlexaFluor594 donkey-anti-chicken antibodies were used. Sections were imaged using a Nikon Eclipse 90i.

3.2.6 Statistical analyses

For slice electrophysiology experiments, electrically-induced or optogenetically-induced IPSC amplitudes were measured on Clampfit 10.4.1.4, averaged per min, and expressed as a percent change from baseline. The final 5 min of all cells in the experiment were averaged and compared to the 5 min baseline using a two-tailed paired t-test (GraphPad Prism). To compare between experimental groups, the final 5 min of the recordings were averaged and compared using a two-tailed unpaired t-test. All data are reported as mean ± standard error of the mean (SEM).

For CPP experiments, time (ms) and distance moved (cm) in the non-preference zone during the first 15 min of baseline and test sessions were determined through tracking on EthoVision XT Software. These values were compared statistically using two-tailed paired t-tests (GraphPad Prism).

3.3 Results

3.3.1 Midbrain dopamine neurons contribute to NAc disinhibition.

BDNF mRNA expression is high in the ventral tegmental area (VTA) and co-localizes with tyrosine hydroxylase positive neurons in this region (Seroogy et al., 1994). To determine if NAc-iLTD requires dopaminergic input from the VTA, we unilaterally lesioned dopaminergic projections into the NAc using the selective dopaminergic neurotoxin 6-hydroxydopamine (6-OHDA; **Figure 3.1a** and **b**). We recorded from MSNs residing in non-lesioned and lesioned sides and found that NAc-iLTD expression was eliminated when

dopaminergic inputs into the NAc were removed (eIPSC amplitude = 112.9 ± 17.89, t=0.72, df=7 mice, p=0.5, **Figure 3.1c**), while NAc-iLTD was observed in the non-lesioned hemisphere (IPSC amplitude = 60.55 ± 7.36, t=5.36, df=5 mice, p=0.003; lesion IPSC amplitude versus control: t=2.4, df=12 mice, p=0.03, unpaired t test, **Figure 3.1c**). Because signaling cascades downstream of dopamine receptor activation are known to intersect with BDNF pathways (Hasbi et al., 2009; Morella et al., 2020) and may also separately modulate GABA receptor expression (Swant et al., 2008; Hoerbelt et al., 2015; Leggio et al., 2019), we sought to investigate whether dopamine signaling modulates NAc-iLTD *ex vivo.* We electrically induced NAc-iLTD with inclusion of the dopamine type-1 and -2 receptor antagonist flupenthixol dihydrochloride (1 uM; Chetrit et al., 2013) in the external recording solution and found that it did not alter the magnitude of NAc-iLTD (eIPSC amplitude 76.35 ± 1.61% of baseline, t=7.22, df=5, p=0.001, **Figure 3.1d**).

Phasically driving VTA dopaminergic afferents in the NAc increases BDNF levels in the NAc (Koo et al., 2016). Further, dopaminergic VTA projection neurons co-release GABA onto NAc MSNs (Tritsch et al., 2014). Therefore, we investigated whether driving dopaminergic inputs is sufficient to induce NAc-iLTD. To do this we injected a cre-sensitive ChR2-expressing virus in the VTA of DAT-cre mice to optogenetically drive VTA dopaminergic/GABAergic/BDNF-ergic projections of the NAc (**Figure 3.1e** and **f**). Optogenetically delivering LFS (oLFS) while voltage-clamping MSNs in the down state elicited NAc-iLTD (optogenetically-evoked IPSC (oIPSC) amplitude = 64.52 ± 13.36% of baseline, t=2.66, df=9, p=0.03) that was blocked by cyclotraxin B (CTX-B; oIPSC amplitude = 110.4 ± 16.81 % of baseline, t=0.62, df=6, p=0.56; control oIPSC amplitude versus oIPSC amplitude in cyclotraxin B: t=2.16, df=15, p=0.047, unpaired t test, **Figure**

3.1g). We previously found that inclusion of EtOH in the recording solution at a dose comparable to that which is on the brain during high levels of alcohol consumption (50 mM; Lovinger and Roberto, 2013) augments NAc-iLTD (Patton et al. 2019). To determine whether EtOH augments iLTD driven by VTA dopamine neuron afferent stimulation, we applied 50 mM EtOH to the external recording solution and found that it indeed augments NAc-iLTD in this circuit (control oIPSC amplitude 83.33 ± 4.54% of baseline versus EtOH oIPSC amplitude 47.89 ± 2.06% of baseline, t=2.92, df=10, p=0.02, unpaired t test, **Figure 3.1h**).

Figure 3.1. Midbrain dopamine neurons contribute to nucleus accumbens disinhibition (NAc-iLTD). Ventral tegmental area (VTA) dopaminergic input activation is necessary and sufficient for long-term depression of inhibition onto nucleus accumbens medium spiny neurons (NAc-iLTD). (A) Schematic of the experimental condition: wild type mice received unilateral 6-hydroxydopamine (6-OHDA) lesions. (B) Top: Tyrosine hydroxylase (TH) staining in intact slices (left) and 6-OHDA (right) slices. Scale bars: 250 µm. Bottom: 20x magnification demonstrating MSNs (red) were recorded in intact slices (left) and lesioned slices (right). Scale bars: 50 µm. (C) Left: Electrically-evoked inhibitory postsynaptic current (eIPSC) amplitudes recorded from cells from slices with intact dopaminergic neuron afferents in the NAc undergo iLTD following electrical low frequency stimulation (eLFS; 240 pulses at 1 Hz) while being held in their down state (-80 mV Vhold; eIPSC amplitude = 60.55 ± 7.36, t=5.36, df=5, p=0.003**). Right: Unilaterally lesioning dopaminergic projections from the VTA to NAc eliminated NAc-iLTD expression (eIPSC amplitude = 112.9 ± 17.89, t=0.72, df=7, p=0.5, paired t test; lesion IPSC amplitude versus control: t=2.4, df=12, p=0.03*, unpaired t test). Insets: representative traces before (dark) and after (light) NAc-iLTD induction. Scale bars: 200 pA, 200 ms. (D) Delivering eLFS in a wildtype mouse in the presence of dopamine type 1 and 2 receptor antagonist flupenthixol dihydrochloride (1 uM) did not alter NAc-iLTD expression (eIPSC amplitude 76.35 ± 1.611% of baseline, t=7.22, df=5, p=0.0008***). Inset: representative traces before (dark) and after (light) NAc-iLTD induction. Scale bars: 250 pA, 100 ms. (E) Schematic representing the injection site into the VTA of mice expressing cre-recombinase under control of the dopamine transporter promoter (DAT-cre). (F) Left: The injection site for adeno-associated virus (AAV) expressing channelrhodopsin (ChR2) and mCherry in the VTA. Arrowheads indicate tract marks from the injection needle. VTA is outlined in a dashed line. Right: VTA terminals expressing ChR2-mCherry in the NAc. NAc core is outlined in dashed line. Scale bars: 250 µm. (G) Optogenetic low-frequency-stimulation (oLFS), 240 pulses of blue light at 1 Hz, induced NAc-iLTD (black; optogenetically-evoked IPSC (oIPSC) amplitude = 64.52 ± 13.36% of baseline, t=2.66, df=9, p=0.03*) that was sensitive to brain-derived neurotrophic factor (BDNF) receptor tyrosine receptor kinase B (TrkB) inhibitor 2 µM cyclotraxin B (red; oIPSC amplitude = 110.4 ± 16.81% of baseline, t=0.62, df=6, p=0.56, paired t test; control oIPSC amplitude versus oIPSC amplitude in cyclotraxin B: t=2.16, df=15, p=0.047*, unpaired t test). Scale bars for representative traces inset: 200 pA, 200 ms. (G) oLFS delivery in the presence of a high dose of ethanol (EtOH; 50 mM) significantly augmented NAc-iLTD as compared to controls (control oIPSC amplitude 83.33 ± 4.54% of baseline versus EtOH oIPSC amplitude 47.89 ± 2.06% of baseline, t=2.92, df=10, p=0.015*, unpaired t test). Scale bars for representative traces inset: 200 pA, 200 ms. ac: anterior commissure. All data are represented as mean ± standard error of the mean (SEM).

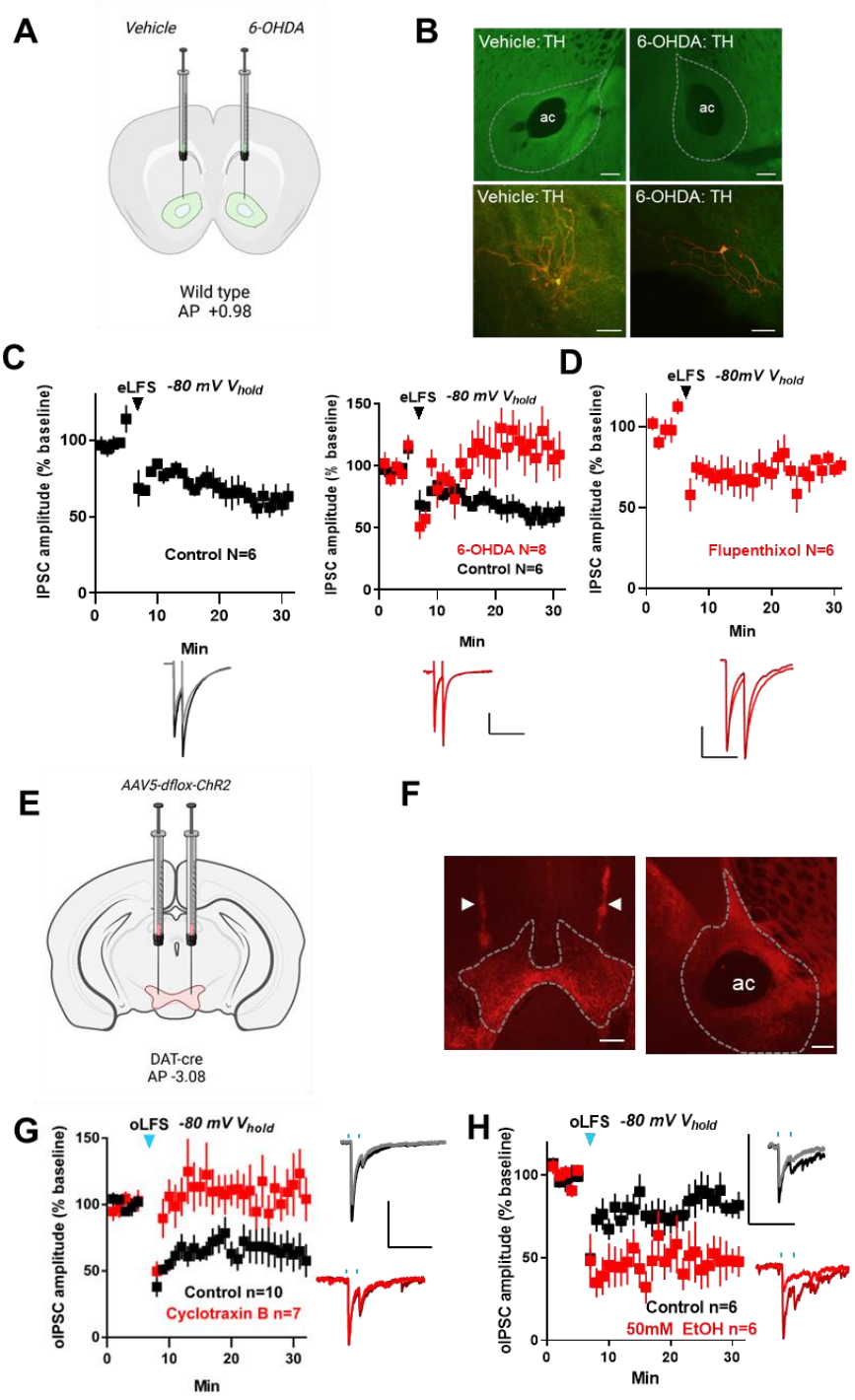
A
Vehicle
6-OHDA
Wild type
AP +0.98
B
Vehicle: TH
6-OHDA: TH
ac
Vehicle: TH
6-OHDA: TH
C
eLFS -80 mV Vhold
IPSC amplitude (% baseline)
Control N=6
Min
eLFS -80 mV Vhold
6-OHDA N=8
Control N=6
Min
D
eLFS -80mV Vhold
Flupenthixol N=6
Min
E
AAV5-dflox-ChR2
DAT-cre
AP -3.08
F
ac
G
oLFS -80 mV Vhold
oIPSC amplitude (% baseline)
Control n=10
Cyclotraxin B n=7
Min
H
oLFS -80 mV Vhold
oIPSC amplitude (% baseline)
Control n=6
50mM EtOH n=6
Min

3.3.2 oLFS delivery in vivo is rewarding.

NAc-iLTD in slice was elicited by optogenetically driving VTA dopamine terminals in the NAc. Thus, we predicted that delivering oLFS *in vivo* would support behavioral reward. To test this, we implanted optical fibers in the NAc of DAT-cre mice that were injected with a cre-sensitive AAV-ChR2-mCherry in the VTA (**Figure 3.2a**). Two rounds of oLFS (4 min) separated by 11 min were delivered on the naturally non-preferred side of a two-sided CPP chamber (**Figure 3.2b**). We found that animals injected with saline spent significantly more time on the side of the two-sided chamber in which oLFS was delivered during the conditioning phase (average time spent in the stimulation-paired chamber pre-light = 227.2 ± 48.45 s, average time spent in stimulation-paired chamber post-light delivery = 441.6 ± 63.56 s, t=5.01, df=7, p=0.002, paired t test, **Figure 3.2c**), and this CPP was not observed in mice in which oLFS was delivered in the presence of *tat*-CTX-B (non-toxic transduction domain of the *tat* protein from HIV type 1 mixed with CTX-B in saline, 20 mg/kg, i.p.; Cazorla et al., 2010; Constandil et al., 2012; average time spent in the stimulation-paired chamber pre-light = 218.1 ± 41.90 s, average time spent in stimulation-paired chamber post-light delivery = 259.9 ± 38.52 s, t=1.40, df=10, p=0.19, paired t test, **Figure 3.2d**). Mice injected with the vehicle *tat* alone (referred to as "vehicle," 20 mg/kg, i.p.) did experience an oLFS-induced CPP (average time spent in the stimulation-paired chamber pre-light = 279.6 ± 27.84 s, average time spent in stimulation-paired chamber post-light delivery = 407.7 ± 29.11 s, t=2.540, df=8, p=0.03, paired t test, **Figure 3.2d**). Further, oLFS did not produce a CPP in DAT-cre mice expressing a control fluorophore (AAV-mCherry or -eYFP) in the VTA (average time spent in the stimulation-paired chamber pre-light = 307.3 ± 30.18 s, average time spent in stimulation-paired chamber

post-light delivery = 342.7 ± 27.24 s, *t*=0.76, df=9, *p*=0.47, paired t test, **Figure 3.2c**), or in mice receiving vehicle injections or *tat*-CTX-B alone (average time spent in the stimulus-paired chamber pre-vehicle = 290.1 ± 37.71 s, average time spent in the stimulus-paired chamber post-vehicle = 379.9 ± 43.15 s, t=1.88, df=9, p=0.10; average time spent in the stimulus-paired chamber pre-*tat*-CTX-B = 311.3 ± 36.66 s, average time spent in stimulus-paired chamber post-*tat*-CTX-B = 381.5 ± 55.57 s, t=1.862, df=8, p=0.10, paired t tests for both groups, **Figure 3.2f**). To examine the role of dopamine on the observed CPP, we next injected the broad dopamine receptor antagonist flupenthixol dihydrochloride (0.5 mg/kg, i.p.) into mice prior to conditioning. We found that CPP was abolished (average time spent in the stimulation-paired chamber pre-light = 255.8 ± 36.94 s, average time spent in stimulation-paired chamber post-light delivery = 300.2 ± 46.23 s, t=0.98, df=9, p=0.35, paired t test, **Figure 3.2e**). Finally, overall distance traveled did not differ in any of the groups (light + saline group: distance moved pre-light = 2646 ± 176.7 cm, distance moved post-light = 2601 ± 395.2 cm, t=0.12, df=7, p=0.91, **Figure 3.2c**; light + *tat*-CTX-B group: distance moved pre-light = 1853 ± 305.8 cm, average distance moved post-light = 2460 ± 364.3 cm, t=1.76, df=10, p=0.11, **Figure 3.2d**; light + vehicle *tat* group: distance moved pre-light = 2113 ± 251.0 cm, distance moved post-light = 2780 ± 303.9, t=1.88, df=8, p=0.10, **Figure 3.2d**; control fluorophore group: distance moved pre-light = 3278 ± 404.6 cm, distance moved post-light = 3285 ± 363.4 cm, t=0.019, df=9, p=0.99, **Figure 3.2c**; vehicle *tat* only group: distance moved pre-vehicle = 3078 ± 518.4 cm, distance moved post-vehicle = 2668 ± 307.9 cm, t=0.80, df=8, p=0.45, **Figure 3.2f**; *tat*-CTX-B only group: distance moved pre-*tat*-CTX-B = 3512 ± 371.7 cm, distance moved post-*tat*-CTX-B 3268 ± 440.5 cm, t=0.69, df=8, p=0.51, **Figure 3.2f**; flupenthixol

dihydrochloride group: distance moved pre-light = 2359 ± 346.8 cm, distance moved post-light = 2274 ± 312.4 cm, t=0.30, df=9, p=0.77, **Figure 3.2e**; paired t test for all groups).

Figure 3.2. oLFS delivery in vivo is rewarding. (A) Left: Schematic representing the experimental condition. DAT-cre mice were injected with an AAV expressing ChR2 into the VTA and optical fibers were implanted into the NAc. Right: Example image of fiber placement in the NAc and VTA terminals expressing ChR2-mCherry. Dashed line represents the location of the NAc core. Scale bars: 250 μm. (B) Schematic representing the 2-day long CPP protocol. On day 1 of testing, mice were habituated to the CPP arena (30 min) and then 2+ hours later time spent and distance moved in both sides of the arena were recorded via Ethovision software during baseline sessions (30 min). On day 2 of testing, mice were conditioned in the side of the arena they spent least amount of time in (non-preference zone). 2+ hours following conditioning, mice were allowed to freely explore the arena again during test sessions and time spent in the non-preference zone was statistically compared to time spent in non-preference zone during baseline recordings. (C) Far left: Delivering two rounds of oLFS (4 min) separated by 11 min in vivo on one side of the chamber during the conditioning phase increased the time spent in the chamber paired with stimulation during a later test phase (average time spent in the stimulation-paired chamber pre-light = 227.2 ± 48.45 s, average time spent in stimulation-paired chamber post-light delivery = 441.6 ± 63.56 s, t=5.01, df=7, p=0.002**, paired t test). Middle left: Representative heat plots before (top) and after (bottom) oLFS delivery. Warmer colors indicate greater time spent in a given location. Middle: Distance moved was not significantly different pre- and post-light delivery (average distance moved in stimulation-paired chamber pre-light delivery = 2646 ± 176.7 cm, average distance moved in stimulation-paired chamber post-light delivery = 2601 ± 395.2 cm, t=0.12, df=7, p=0.91, paired t test). Middle right: The time spent in the chamber paired with light was not greater in control fluorophore-expressing mice (average time spent in the stimulation-paired chamber pre-light = 307.3 ± 30.18 s, average time spent in stimulation-paired chamber post-light delivery = 342.7 ± 27.24 s, t=0.76, df=9, p=0.47, paired t test). Far right: Distance moved was unchanged pre- and post-light delivery for the control fluorophore group (average distance moved in stimulation-paired chamber pre-light delivery = 3278 ± 404.6 cm, average distance moved in stimulation-paired chamber post-light delivery = 3285 ± 363.4 cm, t=0.02, df=9, p=0.99, paired t test) (D) Far left: oLFS-induced CPP was not present in mice injected intraperitoneally (i.p.) with brain penetrant *tat* peptide mixed with cyclotraxin B (*tat*-CTX-B; average time spent in the stimulation-paired chamber pre-light = 218.1 ± 41.90 s, average time spent in stimulation-paired chamber post-light delivery = 259.9 ± 38.52 s, t=1.40, df=10, p=0.19, paired t test). Middle left: Representative heat plots before (top) and after (bottom) oLFS delivery in mice injected with *tat*-CTX-B. Middle: Distance moved for mice receiving oLFS and *tat*-CTX-B injections was not different pre- and post-light delivery (average distance moved in stimulation-paired chamber pre-light delivery = 1853 ± 305.8 cm, average distance moved in stimulation-paired chamber post-light delivery = 2460 ± 364.3 cm, t=1.76, df=10, p=0.11, paired t test). Middle right: Mice spent more time in the chamber paired with light following injections of *tat*, the vehicle used to enable CTX-B blood brain barrier penetration (average time spent in the stimulation-paired chamber pre-light = 279.6 ± 27.84 s, average time spent in stimulation-paired chamber post-light delivery = 407.7 ± 29.11 s, t=2.54, df=8, p=0.03*, paired t test). Far right: Injections of vehicle with light delivery did not alter distance moved (average distance moved in stimulation-paired chamber pre-light = 2113 ± 251.0 cm, average distance moved in stimulation-paired chamber post-light delivery = 2780 ± 303.9, t=1.88,

df=8, p=0.10, paired t test). (E) Left: Mice receiving 0.5 mg/kg injections of flupenthixol dihydrochloride to block dopamine 1-like and 2-like receptors did not find oLFS during conditioning rewarding (average time spent in the stimulation-paired chamber pre-light = 255.8 ± 36.94 s, average time spent in stimulation-paired chamber post-light delivery = 300.2 ± 46.23 s, t=0.98, df=9, p=0.35, paired t test). Middle: Representative heat plots before (top) and after (bottom) oLFS delivery. Right: Light delivery and flupenthixol dihydrochloride administration did not alter distance moved (average distance moved in stimulation-paired chamber pre-light delivery = 2359 ± 346.8 cm, average distance moved in stimulation-paired chamber post-light delivery = 2274 ± 312.4 cm, t=0.30, df=9, p=0.77, paired t test). (F) Far left: Schematic representing the CPP protocol. Mice were conditioned in their non preference zone with only injections of either the vehicle *tat* or *tat*-CTX-B. Middle left: Injections of vehicle *tat* did not induce CPP (average time spent in the stimulus-paired chamber pre-vehicle = 290.1 ± 37.71 s, average time spent in stimulus-paired chamber post-vehicle = 379.9 ± 43.15 s, t=1.88, df=9, p=0.10, paired t test). Middle: Distance moved was unchanged following vehicle injections (average distance moved in pre-vehicle injection = 3078 ± 518.4 cm, average distance moved post-vehicle = 2668 ± 307.9 cm, t=0.80, df=8, p=0.45, paired t test). Middle right: Injections of *tat*-CTX-B did not induce CPP (average time spent in the stimulus-paired chamber pre-*tat*-CTX-B = 311.3 ± 36.66 s, average time spent in stimulation-paired chamber post-light delivery = 381.5 ± 55.57 s, t=1.86, df=8, p=0.10, paired t test). Far right: Distance moved was unchanged pre- and post-*tat*-CTX-B injections (average distance moved in stimulus-paired chamber pre-tat-CTX-B = 3512 ± 371.7 cm, average distance moved post-tat-CTX-B = 3268 ± 440.5 cm, t=0.69, df=8, p=0.51, paired t test). i.p. = intraperitoneal. n.s. = not significant. All data are represented as mean ± SEM.

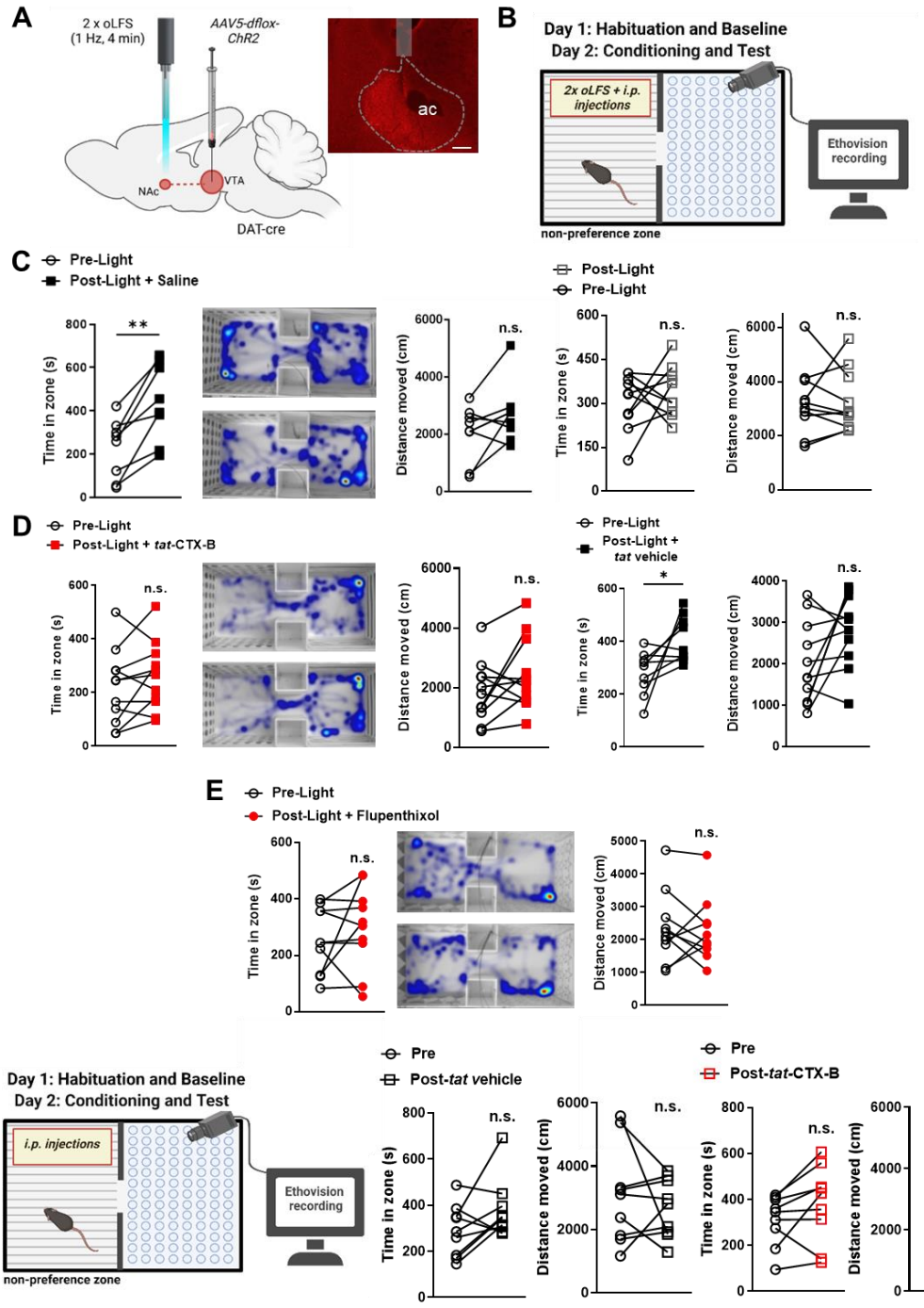
A
2 x oLFS
(1 Hz, 4 min)
AAV5-dflox-ChR2
ac
NAc
VTA
DAT-cre
B
Day 1: Habituation and Baseline
Day 2: Conditioning and Test
2x oLFS + i.p. injections
Ethovision recording
non-preference zone
C
Pre-Light
Post-Light + Saline
Post-Light
Pre-Light
Time in zone (s)
Distance moved (cm)
**
n.s.
D
Pre-Light
Post-Light + tat-CTX-B
Post-Light + tat vehicle
*
E
Pre-Light
Post-Light + Flupenthixol
F
Day 1: Habituation and Baseline
Day 2: Conditioning and Test
i.p. injections
Ethovision recording
non-preference zone
Pre
Post-tat vehicle
Post-tat-CTX-B

3.3.3 Genetic ablation of TrkB receptors in the NAc abolishes CPP.

To validate our pharmacological findings demonstrating that BDNF signaling through TrkB is required for oLFS-induced CPP, we injected AAV-ChR2 into the VTA and a virus expressing cre-recombinase into the NAc of mice in which the TrkB gene is flanked by loxP sites (Flx-TrkB), to locally ablate TrkB receptors in the NAc while enabling optogenetic stimulation of VTA afferents in the NAc (**Figure 3.3a**). Two rounds of oLFS (4 min) separated by 11 min delivered on the naturally non-preferred side of the CPP chamber (**Figure 3.3b)** did not condition the mice in this experimental group (average time spent in the stimulation-paired chamber pre-light = 294.1 ± 42.46 s, average time spent in stimulation-paired chamber post-light delivery = 386.7 ± 78.19 s, t=1.33, df=7, p=0.22, paired t test, **Figure 3.3c**). Control mice with control fluorophore viral injections into either their VTA or NAc were also not conditioned during CPP (average time spent in the stimulation-paired chamber pre-light for NAc control = 263.7 ± 31.32 s, average time spent in stimulation-paired chamber post-light delivery = 436.8 ± 93.51 s, t=2.04, df=5, p=0.09, note to readers: this is meant to be a positive control and will be updated with more animals; average time spent in the stimulation-paired chamber pre-light for VTA control = 264.0 ± 30.52 s, average time spent in stimulation-paired chamber post-light delivery = 284.4 ± 88.58 s, t=0.28, df=4, p=0.79, paired t test for both groups, **Figure 3.3d**). Distance moved pre- and post-light delivery was unchanged for all Flx-TrkB groups (distance moved in stimulation-paired chamber pre-light delivery for Flx-TrkB experimental group = 2574 ± 528.8 cm, distance moved in stimulation-paired chamber post-light delivery = 2326 ± 220.7 cm, t=0.5487, df=7, p=0.60; average distance moved in the stimulation-paired chamber pre-light for NAc control = 2938 ± 241.7 cm, average distance moved in stimulation-paired

chamber post-light delivery = 3431 ± 541.7 cm, t=0.78, df=5, p=0.47; average distance moved in the stimulation-paired chamber pre-light for VTA control = 2145 ± 212.0 cm, average distance moved in stimulation-paired chamber post-light delivery = 1813 ± 124.5 cm, t=1.51, df=4, p=0.21; paired t test for all groups, **Figure 3.3c** and **d**).

Figure 3.3. Genetic ablation of TrkB receptors in the NAc abolishes CPP. (A) Left: Schematic representing the experimental condition. Floxxed-TrkB (Flx-TrkB) mice were injected with an AAV expressing ChR2 into the VTA. They were also injected with a virus expressing cre recombinase (cre)-enhanced green fluorescent protein (eGFP) into the NAc to locally ablate TrkB receptors and received optical fiber implantations into the NAc for optogenetic stimulation of VTA afferents in vivo. Right: Example image of fiber placement in the NAc and expression of eGFP wherever there is cre present in NAc. Dashed line represents the location of the NAc core. Scale bars: 250 μm. (B) Schematic of behavioral paradigm, mice were conditioned in their non-preference zones with two rounds of oLFS spaced 11 min apart and received saline injections as previously described. (C) Left: Flx-TrkB mice with cre-eGFP in their NAc and ChR2 in their VTA did not find oLFS delivery rewarding (average time spent in the stimulation-paired chamber pre-light = 294.1 ± 42.46 s, average time spent in stimulation-paired chamber post-light delivery = 386.7 ± 78.19 s, t=1.33, df=7, p=0.22, paired t test). Middle: Representative heat plots before (top) and after (bottom) oLFS delivery. Right: Distance moved for Flx-TrkB mice was unchanged throughout the duration of CPP (distance moved in stimulation-paired chamber pre-light delivery for Flx-TrkB experimental group = 2574 ± 528.8 cm, distance moved in stimulation-paired chamber post-light delivery = 2326 ± 220.7 cm, t=0.55, df=7, p=0.60, paired t test). (D) Control fluorophore injection groups (far left: ChR2 injection into VTA, mCherry injection into NAc; middle right: eYFP injection into VTA, cre-eGFP injection into NAc) did not result in CPP (average time spent in the stimulation-paired chamber pre-light for NAc control = 263.7 ± 31.32 s, average time spent in stimulation-paired chamber post-light delivery = 436.8 ± 93.51 s, t=2.04, df=5, p=0.09, paired t test; average time spent in the stimulation-paired chamber pre-light for VTA control = 264.0 ± 30.52 s, average time spent in stimulation-paired chamber post-light delivery = 284.4 ± 88.58 s, t=0.28, df=4, p=0.79, paired t test). Distance moved was unchanged during CPP for these controls (middle left: average distance moved in the stimulation-paired chamber pre-light for NAc control = 2938 ± 241.7 cm, average distance moved in stimulation-paired chamber post-light delivery = 3431 ± 541.7 cm, t=0.78, df=5, p=0.47; far right: average distance moved in the stimulation-paired chamber pre-light for VTA control = 2145 ± 212.0 cm, average distance moved in stimulation-paired chamber post-light delivery = 1813 ± 124.5 cm, t=1.51, df=4, p=0.21; paired t test for both groups). ac = anterior commissure. i.p. = intraperitoneal. n.s. = not significant. All data are represented as mean ± SEM.

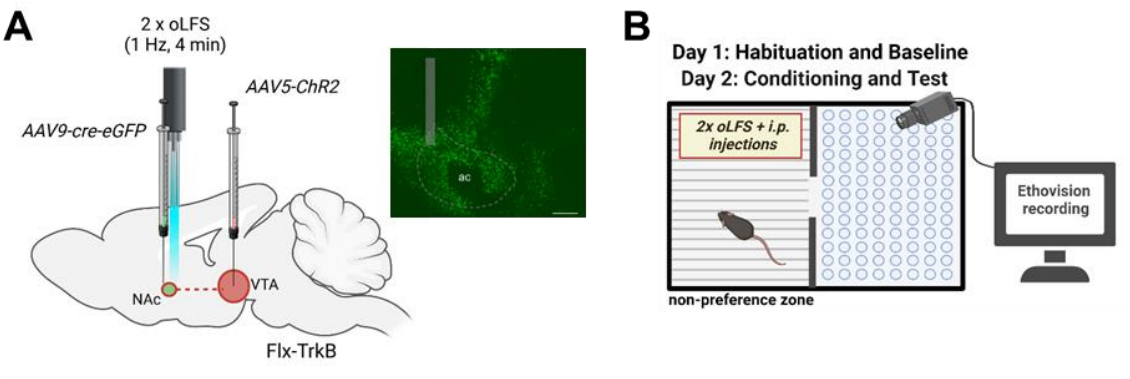
A
2 x oLFS
(1 Hz, 4 min)
AAV5-ChR2
AAV9-cre-eGFP
ac
NAc
VTA
Flx-TrkB
B
Day 1: Habituation and Baseline
Day 2: Conditioning and Test
2x oLFS + i.p. injections
Ethovision recording
non-preference zone

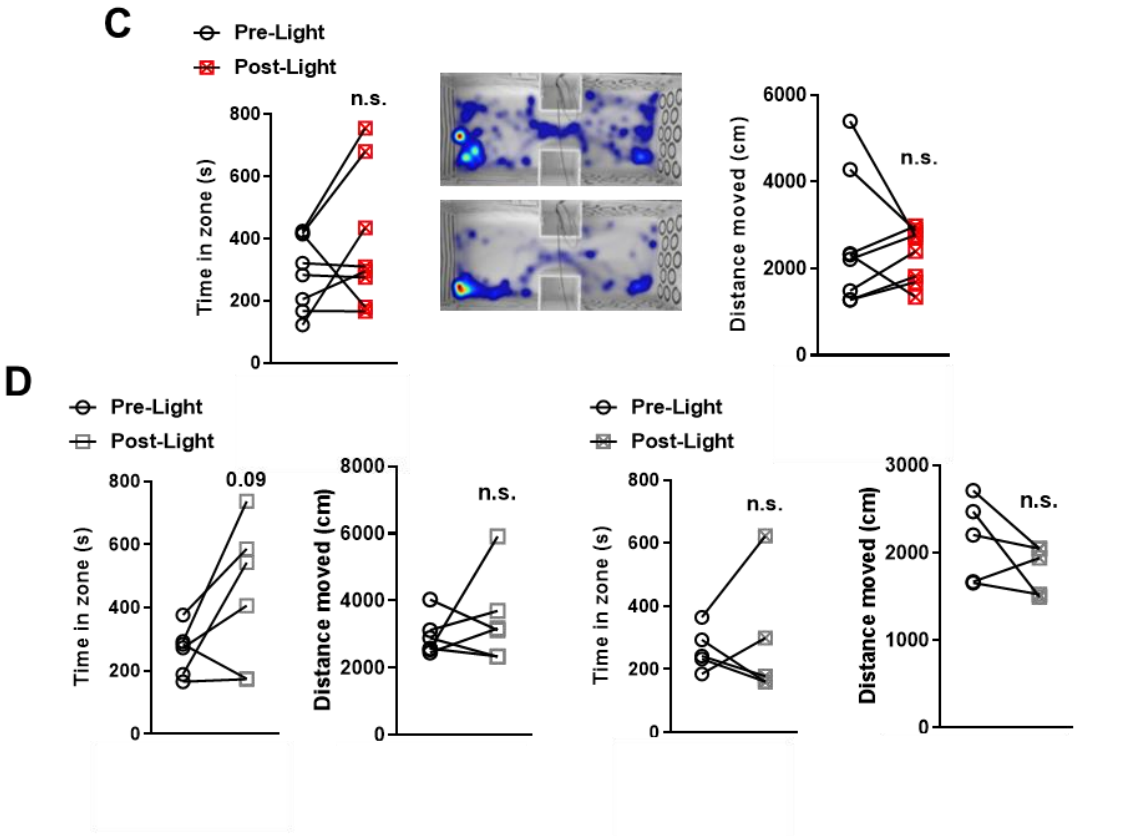
C
Pre-Light
Post-Light
n.s.
Time in zone (s)
800
600
400
200
0
Distance moved (cm)
6000
4000
2000
0
n.s.
D
Pre-Light
Post-Light
0.09
n.s.
Time in zone (s)
Distance moved (cm)
8000
6000
4000
2000
0
3000
1000

3.3.4 Changing the frequency of LFS abolishes NAc-iLTD *ex vivo* and CPP *in vivo*.

We next investigated whether the frequency of stimulation *ex vivo* impacts induction of NAc-iLTD. While holding MSNs at -80 mV, we electrically stimulated the slice at 0.25 Hz as opposed to 1 Hz and found that it was not sufficient to produce NAc-iLTD (eIPSC amplitude 87.19 ± 4.98% of baseline, t=1.83, df=9, p=0.10, paired t test, **Figure 3.4a)**. We utilized this group as a control for our *in vivo* CPP experiments; following the same viral injection and fiber placement strategy as depicted in Figure 2a (**Figure 3.4b**), we conditioned mice with two rounds of 0.25 Hz stimulation (4 mins) spaced 11 mins apart in their non-preference chamber (**Figure 3.4c**) and found that it did not drive a CPP (average time spent in the stimulation-paired chamber pre-light = 308.8 ± 28.36 s, average time spent in stimulation-paired chamber post-light delivery = 368.7 ± 38.23 s, *t*=1.67, df=10, *p*=.13, paired t test, **Figure 3.4d**). Distance moved for this group was unaltered (average distance moved in the stimulation-paired chamber pre-light = 3072 ± 416.5 cm, average distance moved in the stimulation-paired chamber post-light delivery = 3289 ± 415.7 cm, t=0.62, df=10, p=0.55, paired t test, **Figure 3.4d**).

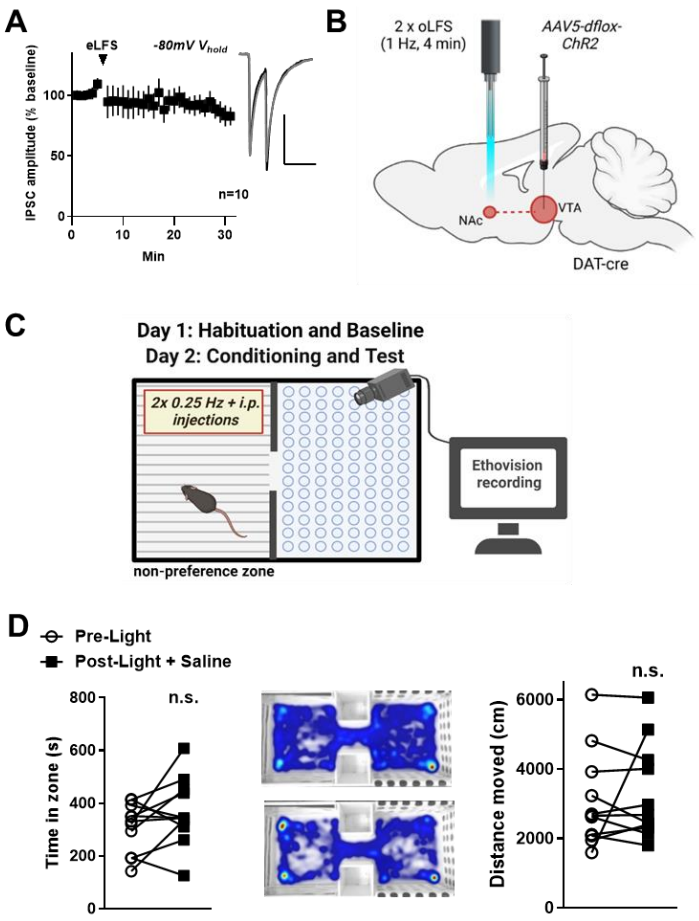

Figure 3.4. Changing the frequency of LFS abolishes NAc-iLTD *ex vivo* and CPP *in vivo*. (A) Electrically stimulating the slice at a 0.25 as opposed to 1 Hz frequency while voltage-clamping the cell at -80 mV does not sufficiently induce NAc-iLTD (eIPSC amplitude 87.19 ± 4.98% of baseline, t=1.83, df=9, p=0.10, paired t test). Scalebars represent 300 pA and 125 ms. (B) Experimental conditions depicted: AAV expressing ChR2 was stereotaxically injected into the VTA and this was followed by another surgery implanting optical fibers into the NAc for *in vivo* experiments 6 wks later. (C) Schematic of behavioral procedure, mice were conditioned in their non-preference zones with two rounds of 0.25 Hz optogenetic stimulation in their NAc (duration per round 4 min, spaced 11 min apart) and received saline injections prior to entry into arena. (D) Left: Conditioning the mice with 2 rounds of 0.25 Hz stimulation did not drive a CPP (average time spent in the stimulation-paired chamber pre-light = 308.8 ± 28.36 s, average time spent in stimulation-paired chamber post-light delivery = 368.7 ± 38.23 s, t=1.67, df=10, p=.13, paired t test). Middle: Heatmaps depicted of pre- and post-light sessions. Right: Distance moved during this experimental condition was unchanged across the cohort (average distance moved in the stimulation-paired chamber pre-light = 3072 ± 416.5 cm, average distance moved in the stimulation-paired chamber post-light delivery = 3289 ± 415.7 cm, t=0.62, df=10, p=0.55, paired t test). i.p. = intraperitoneal. n.s. = not significant. All data are represented as mean ± SEM.

3.3.5 BDNF release from the prelimbic prefrontal cortex (plPFC) drives NAc-iLTD and CPP. BDNF is also released onto NAc MSNs from the prefrontal cortex (Altar et al., 1997). We investigated whether BDNF provided from this source is sufficient to drive NAc-iLTD by injecting ChR2 into the plPFC of wildtype mice (**Figure 3.5a**). We found that oLFS of plPFC afferents in the NAc induces NAc-iLTD (eIPSC amplitude 68.95 ± 7.29% of baseline, t=4.26, df=7, p=0.004, **Figure 3.5b**). Inclusion of TrkB inhibitor CTX-B in the internal recording solution abolished NAc-iLTD driven by plPFC, demonstrating this NAc-iLTD is attributable to BDNF release (oIPSC amplitude 103.6 ± 11.32% of baseline, t=0.32, df=5, p=0.76, paired t test; control IPSC amplitude versus CTX-B amplitude: t=2.80, df=12, p=0.02, unpaired t test, **Figure 3.5b**).

We determined whether oLFS of NAc plPFC inputs drives a CPP by implanting fibers into the NAc following the ChR2 injection into plPFC (**Figure 3.5c**). We found that two rounds of oLFS (4 mins) spaced 1l mins apart conditions mice to their non-preference side of the CPP chamber (**Figure 3.5d** for schematic; average time spent in the stimulation-paired chamber pre-light = 198.6 ± 26.50 s, average time spent in stimulation-paired chamber post-light delivery = 388.7 ± 73.96 s, *t*=2.57, df=9, *p*=0.03, paired t test, **Figure 3.5e**). Movement was not altered in these mice (distance moved in the stimulation-paired chamber pre-light = 2115 ± 189.40 cm distance moved in the stimulation-paired chamber post-light delivery = 2354 ± 278.6 cm, t=0.96, df=9, p=0.36, paired t test, **Figure 3.5e**).

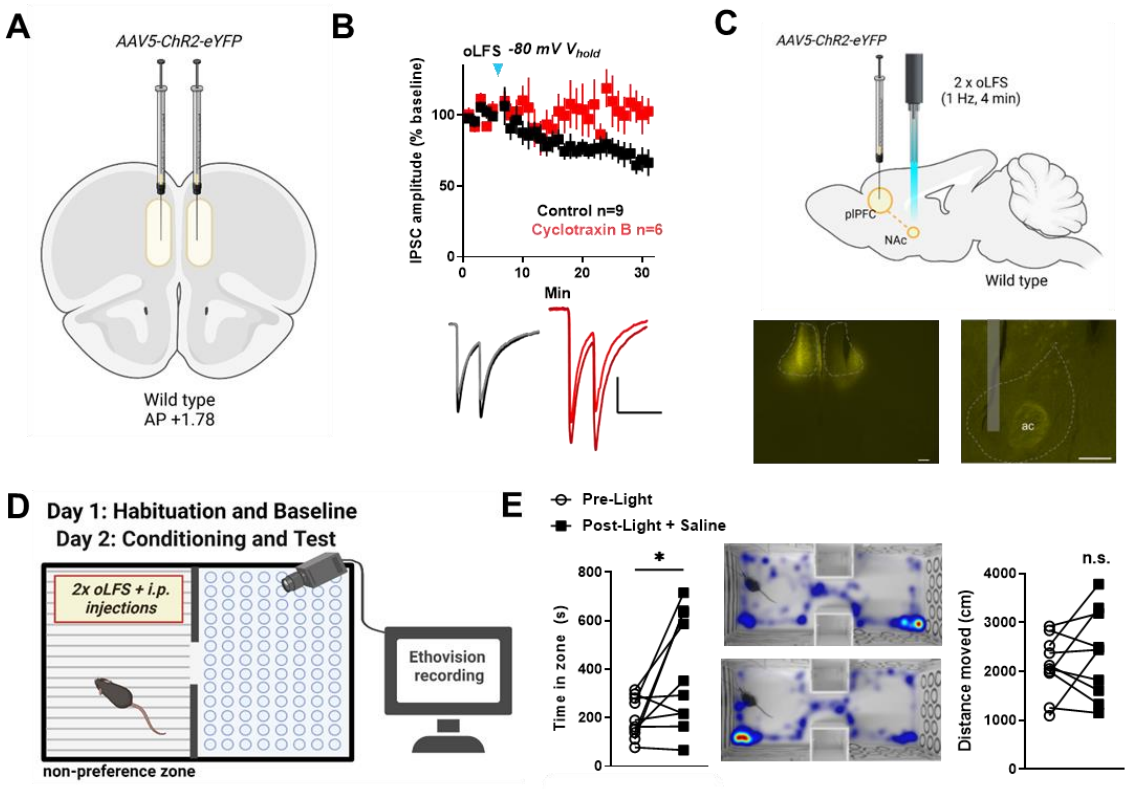

Figure 3.5. BDNF release from the prelimbic prefrontal cortex (plPFC) drives NAc-iLTD and CPP. (A) Schematic of viral injection strategy. AAV-ChR2 was bilaterally injected into the plPFC of wildtype mice. (B) Optogenetically stimulating the ChR2-expressing plPFC afferents at 1 Hz frequency while voltage-clamping the cell at -80 mV does sufficiently induce NAc-iLTD (oIPSC amplitude 68.95 ± 7.29% of baseline, t=4.26, df=7, p=0.004**). In the presence of CTX-B, NAc-iLTD is abolished (oIPSC amplitude 103.6 ± 11.32% of baseline, t=0.32, df=5, p=0.76, paired t test; control IPSC amplitude versus CTX-B amplitude: t=2.80, df=12, p=0.02*, unpaired t test). Scalebars for traces: 250 pA and 100 ms. (C) Top: Schematic of viral injection and fiber placement strategy. Bottom left: Example image of ChR2-eYFP injection into the plPFC. Dotted line encompasses plPFC. Bottom right: Example image of ChR2-eYFP-expressing plPFC afferents in the NAc with fiber placement depicted. (D) Schematic depicting the CPP paradigm. Mice were conditioned with two rounds of 1 Hz stimulation spaced 11 min apart and received saline injections prior to entry into their non-preference zones. (E) Left: Mice spent more time in their non-preference zones following conditioning (average time spent in the stimulation-paired chamber pre-light = 198.6 ± 26.50 s, average time spent in stimulation-paired chamber post-light delivery = 388.7 ± 73.96 s, t=2.57, df=9, p=0.03*, paired t test). Middle: Heatmaps depict pre-light and post-light sessions. Right: Distance moved was unchanged across the cohort (distance moved in the stimulation-paired chamber pre-light = 2115 ± 189.4 cm distance moved in the stimulation-paired chamber post-light delivery = 2354 ± 278.6 cm, t=0.96, df=9, p=0.36, paired t test). i.p. = intraperitoneal. n.s. = not significant. All data are represented as mean ± SEM.

3.3.6 Subthreshold rewarding dose of EtOH coupled with subthreshold rewarding oLFS of midbrain neurons together drive a CPP.

Induction of NAc-iLTD *ex vivo* with inclusion of low and high doses of EtOH in the external recording solution augments its magnitude (10 and 50 mM, respectively; Patton et al., 2019). We sought to determine whether this interaction occurs *in vivo* to underlie alcohol reward. We predicted that a subthreshold rewarding induction of oLFS together with a subthreshold rewarding dose of EtOH during conditioning would drive a CPP in mice. We found that eliciting one round of oLFS as opposed to two was not rewarding to the mice (average time spent in the stimulation-paired chamber pre-light = 320.7 ± 21.80 s, average time spent in stimulation-paired chamber post-light delivery = 384.2 ± 46.44 s, t=1.31, df=9, p=0.22, paired t test, **Figure 3.6b**). Likewise, a single 2 g/kg i.p. injection of EtOH 3-5 mins prior to conditioning was not rewarding to the mice (average time spent in the stimulus-paired chamber pre-EtOH = 281.6 ± 36.45 s, average time spent in stimulus-paired chamber post-EtOH = 343.2 ± 47.56 s, t=2.01, df=8, p=0.08, paired t test, **Figure 3.6c**). Administering both of these stimuli during conditioning induced a CPP (average time spent in the stimulation-paired chamber pre-light and EtOH = 278.2 ± 26.32 s, average time spent in stimulation-paired chamber post-light and EtOH delivery = 410.7 ± 47.25 s, t=3.68, df=10, p=0.004, paired t test, **Figure 3.6d**). Distances moved for these three groups were unchanged pre- and post-stimulus pairing with the non-preference chamber (average distance moved in stimulation-paired chamber pre-light delivery for saline group = 3412 ± 317.5 cm, average distance moved in stimulation-paired chamber post-light delivery = 2505 ± 334.8 cm, t=0.34, df=9, p=0.75; average distance moved in stimulation-paired chamber pre-EtOH = 1894 ± 436.1 cm, average distance moved in stimulation-paired

chamber post-EtOH delivery = 1950 ± 404.5 cm, t=0.29, df=8, p=0.78; average distance moved in the stimulation-paired chamber pre-light and EtOH = 3064 ± 186.7 cm, average distance moved in stimulation-paired chamber post-light and EtOH delivery = 2877 ± 274.8 cm, t=1.27, df=10, p=0.23; paired t test for all groups, **Figure 3.6b, c,** and **d**). Mice with viral fluorophore injections in their NAc receiving one round of oLFS in conjunction with the 2 g/kg EtOH injection did not exhibit a CPP, nor did they exhibit altered distance movement (average time spent in the stimulation-paired chamber pre-light and EtOH = 320.3 ± 26.60 s, average time spent in stimulation-paired chamber post-light and EtOH delivery = 387.5 ± 52.79 s, t=0.98, df=8, p=0.36; average distance moved in the stimulation-paired chamber pre-light and EtOH = 2450 ± 239.3 cm, average distance moved in stimulation-paired chamber post-light and EtOH delivery = 1906 ± 136.8 cm, t=1.95, df=8, p=0.09; paired t test for both analyses, **Figure 3.6d**).

We predicted that the interaction between EtOH and oLFS would be dependent upon BDNF signaling through TrkB receptors on NAc MSNs, as seen in the acute slice preparation (Patton et al., 2019). We first tested this pharmacologically by injecting mice twice with *tat*-CTX-B spaced 90 min apart as well as 2 g/kg EtOH prior to conditioning with one round of oLFS, and found that the mice were not conditioned to find their non-preference chambers rewarding (average time spent in the stimulation-paired chamber pre-light + EtOH + CTX-B = 281.1 ± 38.10 s, average time spent in stimulation-paired chamber post-light + EtOH + CTX-B = 398.0 ± 61.39 s, t=2.18, df=8, p=0.06, paired t test, **Figure 3.6e**). Injections of the vehicle (2 x 20 mg/kg *tat* in saline, i.p.) in parallel to the 2 g/kg EtOH injection prior to delivery of a single round of oLFS did result in a CPP(average time spent in the stimulation-paired chamber pre-light + EtOH + tat vehicle = 198.3 ± 28.30 s,

average time spent in stimulation-paired chamber post-light + EtOH + Vehicle = 375.9 ± 54.94 s, t=3.67, df=11, p=0.005, paired t test, **Figure 3.6e**). We validated this finding genetically using the previously defined Flx-TrkB line of mice with ablated TrkB receptors in the NAc and ChR2 injections in the VTA (**Figure 3.6f)**. Delivery of one round of oLFS combined with a 2 g/kg dose of EtOH did not induce CPP in these mice (average time spent in the stimulation-paired chamber pre-light + EtOH = 317.8 ± 19.00 s, average time spent in stimulation-paired chamber post-light + EtOH = 373.8 ± 34.86 s, t=1.82, df=6, p=0.12, paired t test, **Figure 3.6f**). Distances moved for all groups were unaffected (average distance moved in the stimulation-paired chamber pre-light + EtOH + *tat*-CTX-B = 1553 ± 220.0 cm, average distance moved in stimulation-paired chamber post-light + EtOH + *tat*-CTX-B = 1718 ± 251.0 cm, t=0.89, df=8, p=0.40; average distance moved in the stimulation-paired chamber pre-light + EtOH + Vehicle = 1976 ± 258.9 cm, average distance moved in stimulation-paired chamber post-light + EtOH + Vehicle delivery = 1958 ± 169.5 cm, t=0.06, df=11, p=0.96; average distance moved in the stimulation-paired chamber pre-light and EtOH = 2607 ± 294.6 cm, average distance moved in stimulation-paired chamber post-light and EtOH delivery = 2753 ± 291.3 cm, t=2.02, df=8, p=0.10; paired t test for all groups, **Figure 3.6e** and **f**).

Figure 3.6. A subthreshold rewarding dose of EtOH coupled with subthreshold rewarding oLFS together drive a BDNF-dependent CPP. (A) Schematic representing the experimental condition. DAT-cre mice were injected with a virus expressing ChR2 into the VTA and optical fibers were implanted into the NAc. (B) Left: Schematic depicting the behavioral paradigm. Mice were conditioned in their non-preference zone with one round of oLFS (4 min long, 11 min following that to explore freely). Middle: Delivering one round of oLFS during conditioning did not increase the time spent in the chamber paired with stimulation during a later test phase (average time spent in the stimulation-paired chamber pre-light = 320.7 ± 21.80 s, average time spent in stimulation-paired chamber post-light delivery = 384.2 ± 46.44 s, t=1.31, df=9, p=0.22, paired t test). Right: Distance moved pre- and post- light delivery in non-preference zone was not different (average distance moved in stimulation-paired chamber pre-light delivery for saline group = 3412 ± 317.5 cm, average distance moved in stimulation-paired chamber post-light delivery = 2505 ± 334.8 cm, t=0.34, df=9, p=0.75, paired t test). (C) Left: Schematic depicting behavioral paradigm. Mice were conditioned in their non-preference zones with a single 2 g/kg EtOH injection several min prior to the 15 min conditioning session. Middle: A single i.p. injection of 2 g/kg EtOH did not increase time spent in chamber paired with the injection (average time spent in the stimulus-paired chamber pre-EtOH = 281.6 ± 36.45 s, average time spent in stimulus-paired chamber post-EtOH = 343.2 ± 47.56 s, t=2.01, df=8, p=0.08, paired t test). Right: Distances moved pre- and post-EtOH administration were unchanged (average distance moved in stimulation-paired chamber pre-EtOH = 1894 ± 436.1 cm, average distance moved in stimulation-paired chamber post-EtOH delivery = 1950 ± 404.5 cm, t=0.29, df=8, p=0.78, paired t test). (D) Far left: Schematic depicting behavioral paradigm. Mice were conditioned in their non-preference zones with a single 2 g/kg EtOH injection 3-5 min prior to one round of oLFS. Middle left: one round of oLFS together with a single injection of 2 g/kg EtOH was rewarding to the mice (average time spent in the stimulation-paired chamber pre-light and EtOH = 278.2 ± 26.32 s, average time spent in stimulation-paired chamber post-light and EtOH delivery = 410.7 ± 47.25 s, t=3.68, df=10, p=0.004**, paired t test). Middle: Representative heat plots before (top) and after (bottom) oLFS delivery. Warmer colors indicate greater time spent in a given location. Middle right: Distances moved pre- and post-light and EtOH delivery were unchanged (average distance moved in the stimulation-paired chamber pre-light and EtOH = 3064 ± 186.7 cm, average distance moved in stimulation-paired chamber post-light and EtOH delivery = 2877 ± 274.8 cm, t=1.27, df=10, p=0.23; paired t test for all groups). Far right: Mice with a control fluorophore injected into their VTA as opposed to ChR2 were not conditioned following one round of oLFS and a single EtOH injection (average time spent in the stimulation-paired chamber pre-light and EtOH = 320.3 ± 26.60 s, average time spent in stimulation-paired chamber post-light and EtOH delivery = 387.5 ± 52.79 s, t=0.98, df=8, p=0.36, paired t test) nor did they experience any differences in distance moved (average distance moved in the stimulation-paired chamber pre-light and EtOH = 2450 ± 239.3 cm, average distance moved in stimulation-paired chamber post-light and EtOH delivery = 1906 ± 136.8 cm, t=1.95, df=8, p=0.09, paired t test). (E) Far left: Schematic depicting behavioral paradigm. Mice were conditioned with i.p. injections and a single round of oLFS in their non-preference zones. Middle left: Delivering one round of oLFS in vivo on one side of the chamber during the conditioning phase while administering a single 2 g/kg injection of EtOH as well as injections of *tat*-CTX-B did not alter time spent

in the chamber paired with these stimuli during a later test phase (average time spent in the stimulation-paired chamber pre-light + EtOH + *tat*-CTX-B = 281.1 ± 38.10 s, average time spent in stimulation-paired chamber post-light = 398.0 ± 61.39 s, t=2.18, df=8, p=0.061, paired t test). Middle: Representative heat plots before (top) and after (bottom) oLFS delivery. Warmer colors indicate greater time spent in a given location. Far right: Delivering one round of oLFS in vivo on one side of the chamber during the conditioning phase while administering a single 2 g/kg injection of EtOH as well as injections of the brain penetrant vehicle *tat* was rewarding to mice, as they spent more time in the chamber paired with these stimuli during a later test phase (average time spent in the stimulation-paired chamber pre-light + EtOH + *tat* vehicle = 198.3 ± 28.30 s, average time spent in stimulation-paired chamber post-light = 375.9 ± 54.94 s, t=3.67, df=11, p=0.005**, paired t test). Distances moved for these two groups were unchanged pre- and post-conditioning (middle right: average distance moved in the stimulation-paired chamber pre-light + EtOH + *tat*-CTX-B = 1553 ± 220.0 cm, average distance moved in stimulation-paired chamber post-light = 1718 ± 251.0 cm, t=0.89, df=8, p=0.40; far right: average distance moved in the stimulation-paired chamber pre-light + EtOH + *tat* vehicle = 1976 ± 258.9 cm, average distance moved in stimulation-paired chamber post-light = 1958 ± 169.5 cm, t=0.06, df=11, p=0.96; paired t tests for both groups). (F) Far left: Schematic representing the experimental condition. Flx-TrkB mice were injected with a virus expressing ChR2-mCherry into the VTA. They were also injected with an AAV expressing cre-eGFP into the NAc and received optical fiber implantations into the NAc. Middle left: Flx-TrkB with ChR2-mCherry in their VTA and cre-eGFP in their NAc for genetic TrkB ablation were not conditionined by one round of oLFS paired with one injection of 2 g/kg EtOH (average time spent in the stimulation-paired chamber pre-light + EtOH = 317.8 ± 19.00 s, average time spent in stimulation-paired chamber post-light = 373,8 ± 34.86 s, t=1.82, df=6, p=0.12, paired t test). Middle right: Representative heat plots before (top) and after (bottom) oLFS delivery. Warmer colors indicate greater time spent in a given location. Far right: Distance moved pre- and post-light and EtOH pairing was unchanged (average distance moved in the stimulation-paired chamber pre-light + EtOH = 2607 ± 294.6 cm, average distance moved in stimulation-paired chamber post-light delivery = 2753 ± 291.3 cm, t=2.02, df=8, p=0.10, paired t test). n.s. = not significant. Data represented as mean ± SEM.

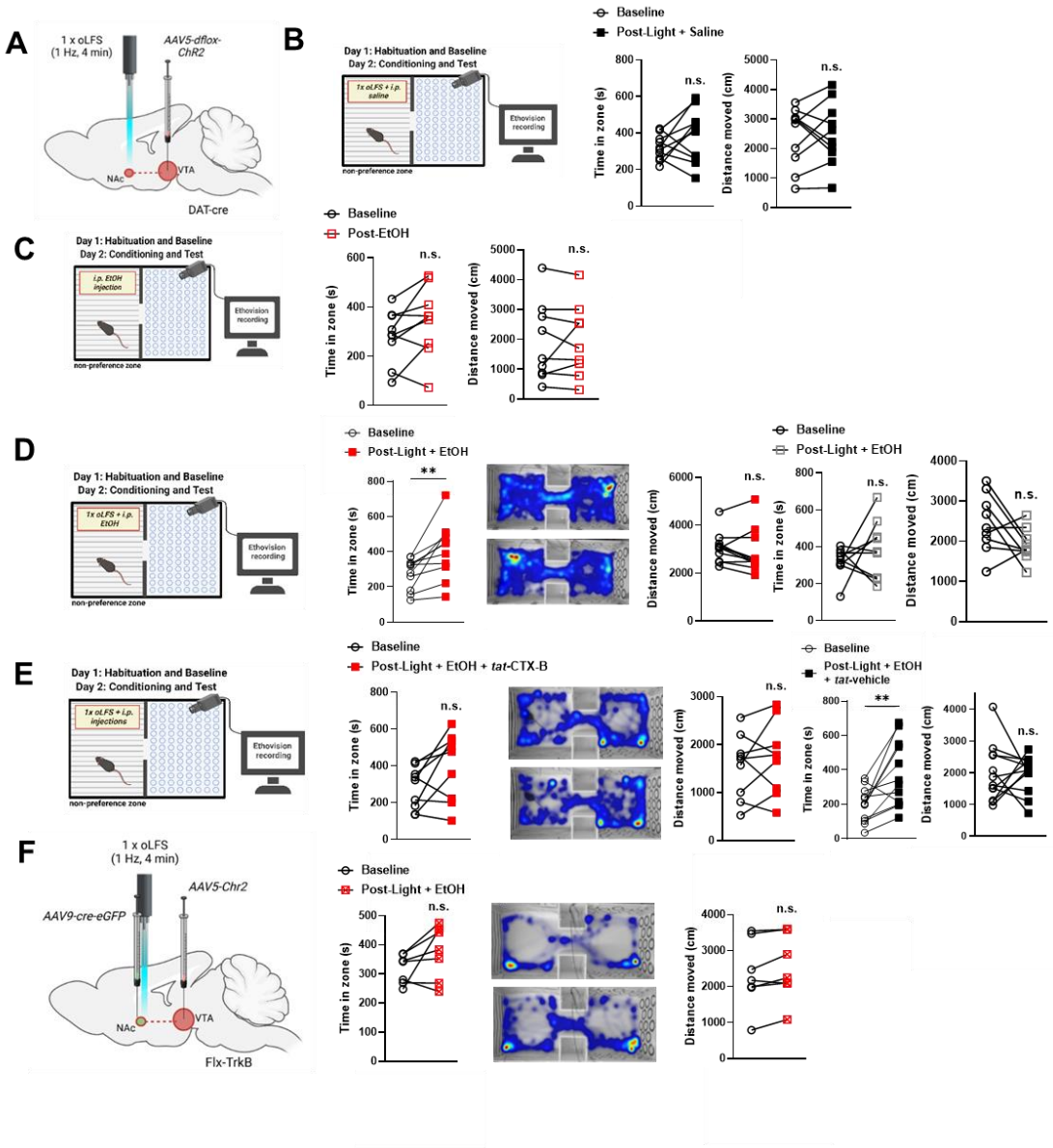
A
1 x oLFS
(1 Hz, 4 min)
AAV5-dflox-ChR2
NAc
VTA
DAT-cre
B
Day 1: Habituation and Baseline
Day 2: Conditioning and Test
1x oLFS + i.p. saline
Ethovision recording
non-preference zone
Baseline
Post-Light + Saline
Time in zone (s)
Distance moved (cm)
n.s.
C
Day 1: Habituation and Baseline
Day 2: Conditioning and Test
i.p. EtOH injection
Ethovision recording
non-preference zone
Baseline
Post-EtOH
Time in zone (s)
Distance moved (cm)
n.s.
D
Day 1: Habituation and Baseline
Day 2: Conditioning and Test
1x oLFS + i.p. EtOH
Ethovision recording
non-preference zone
Baseline
Post-Light + EtOH
**
n.s.
Time in zone (s)
Distance moved (cm)
E
Day 1: Habituation and Baseline
Day 2: Conditioning and Test
1x oLFS + i.p. injections
Ethovision recording
non-preference zone
Baseline
Post-Light + EtOH + tat-CTX-B
Post-Light + EtOH + tat-vehicle
**
n.s.
Time in zone (s)
Distance moved (cm)
F
1 x oLFS
(1 Hz, 4 min)
AAV5-Chr2
AAV9-cre-eGFP
NAc
VTA
Flx-TrkB
Baseline
Post-Light + EtOH
n.s.
Time in zone (s)
Distance moved (cm)

3.4 Discussion

We discover that BDNF release from the VTA diminishes inhibition onto NAc MSNs and that EtOH augments this disinhibition. We also find that plPFC release of BDNF may also sufficiently diminish the strength of inhibition onto MSNs. Furthermore, conditioning mice *in vivo* by optogenetically interrogating VTA or plPFC afferents with oLFS is sufficient to drive a CPP. We discover that the diminishment of inhibition onto NAc MSNs *ex vivo* is frequency dependent, and we also find that when oLFS is delivered at a different frequency *in vivo*, mice no longer are conditioned by VTA afferent stimulation. Finally, we determine that subthreshold rewarding induction of oLFS together with a subthreshold rewarding dose of EtOH conditions mice during CPP.

Our lab previously reported that eLFS *ex vivo* induces NAc-iLTD of equal magnitude onto MSNs expressing either dopamine 1- or 2-like receptors (Patton et al., 2019) and here we find that oLFS *in vivo* is rewarding to mice. Canonically, the expression of dopamine 1- or 2- like receptors on MSNs dictates whether they go on to activate direct or indirect output pathways to mediate reward or aversion, respectively. This has informed large bodies of research (Hikida et al., 2010; Sesack and Grace, 2010; Xia et al., 2011; Tai et al., 2012; Hikida et al., 2013; Yamaguchi et al., 2015; Nguyen et al., 2018; Sandoval-Rodriguez et al., 2023; Nakanishi et al., 2014; Volkow and Morales, 2015). However, our findings could potentially expand upon previous studies suggesting that direct and indirect pathway output is not mediated by dopamine receptor-type expression on MSNs (Kupchik et al., 2015; Kupchik and Kalivas, 2017). Notably, however, we have not validated whether we have indeed induced inhibitory plasticity in the NAc *in vivo* under our experimental conditions. Two rounds of VTA or plPFC oLFS delivery *in vivo* may not sufficiently

induce LFS-driven NAc-iLTD as we see *ex vivo*. Furthermore, it is possible that the MSN subtype non-specificity of NAc-iLTD *ex vivo* (Patton et al., 2019) is not paralleled *in vivo*. TrkB receptor expression is higher on MSNs expressing dopamine 2-like receptors (Lobo et al., 2010; Baydyuk et al., 2011), suggesting this subpopulation may be preferentially targeted by afferents releasing BDNF. This supports work demonstrating that BDNF mediates social stress-induced depressive behaviors (Koo et al., 2016). Moreover, others have found that BDNF release from the VTA strengthens inhibition onto dopamine 1-like receptor expressing MSNs to reduce morphine reward (Koo et al., 2012) and enable resilience to social stress (Pagliusi et al., 2022). But the role of BDNF in reward has been highly disputed, as others find that BDNF can support reward. For instance, BDNF expression in the lateral-medial forebrain bundle of rats is critical for regulating reward reinforcement (Sagarkar et al., 2021). Furthermore, alcohol interacts with BDNF/TrkB activation (McGough et al., 2004; Logrip et al., 2009; Jeanblanc et al., 2013; Logrip et al., 2015) and acute administration of alcohol not only dose-dependently elevates BDNF mRNA levels in the VTA (Raivio et al., 2014), but also sufficiently enhances the reinforcing properties of ethanol when administered exogenously in the NAc prior to drug exposure (Waeiss et al., 2010). The disparity between these conceptualizations for the role of BDNF in reward suggests that the system is highly context dependent. It is apparent that the contexts in which BDNF is released and in which the BDNF signaling system is manipulated drastically impact its role in behavior and internal states and further investigations looking at its roles in these different contexts is the only way to further elucidate why this is the case.

We herein demonstrate that NAc-iLTD is not modulated by dopamine signaling *ex vivo*, yet utilizing the same induction protocol *in vivo* to drive a CPP while administering a broad dopamine receptor antagonist effectively abolished CPP. This suggests that dopamine-dependent reward mechanisms are also being induced *in vivo*, and more experiments are needed to confirm if this is the case. Because we administered flupenthixol dihydrochloride i.p., it is likely that its interruption of dopamine signaling in other areas of the brain and circuits impacted the ability of mice to experience reward. But we also did not differentiate between dopamine 1-like and 2-like receptor expressing MSNs when inducing NAc-iLTD *ex vivo* in the presence of flupenthixol. It is possible that dopamine signaling modulates inhibitory plasticity differentially on MSN subpopulations and we were not able to detect this with our slice experiment setup.

We did not explore whether *ex vivo* EtOH augmentation of NAc-iLTD and the *in vivo* interaction of these two stimuli require dopamine signaling to be intact. Acute EtOH can increase dopamine transmission in the NAc and this mechanism is largely accepted as being the predominant mediator of the rewarding properties of EtOH (Chiara, 1997; Soderpalm and Ericson, 2009; Bassareo et al., 2017; Dahchour and Ward, 2022), so it is possible that EtOH modulation of inhibitory synaptic strength in the NAc is not entirely dopamine-independent. This is further supported by lines of evidence linking dopamine signaling with GABAergic signaling in the NAc (Lof et al., 2007) and even specifically BDNF interplay with dopaminergic modulation of GABA receptor expression (Jeanblanc et al., 2006; Leggio et al., 2019). However, these findings suggest that dopamine and BDNF postsynaptic signaling cascades converge to strengthen GABA inhibition in the NAc and control EtOH consumption, which theoretically opposes what we find herein.

Determination of whether dopamine modulates EtOH augmentation of NAc-iLTD is critical for furthering our understanding of BDNF and dopamine interplay as it relates to inhibitory plasticity and EtOH reward.

Despite our findings suggesting that VTA BDNF contributes to NAc-iLTD, we also find that plPFC BDNF can sufficiently drive NAc-iLTD and that stimulation of these afferents *in vivo* drives a CPP. Because we did not inhibit BDNF signaling during this CPP, it remains unclear whether the CPP driven by plPFC afferent stimulation is mediated by BDNF signaling. We also did not test whether excitation of plPFC inputs alters the strength of glutamatergic neurotransmission in the NAc. As such, it is possible that we observed a CPP mediated by altered glutamate synaptic strength driven by plPFC terminal activation in the NAc, as others have found that elevated plPFC glutamate is associated with initiation, learning, and remembrance of reward-associated behaviors (Kalivas and Volkow, 2005; Alasmari et al., 2018; Pena-Bravo et al., 2019). Recording excitatory postsynaptic currents (EPSCs) *ex vivo* before and after oLFS of plPFC afferents would elucidate whether excitatory projections are altered following plPFC afferent stimulation in the NAc. Alternatively, PFC afferents in the NAc can activate dopaminergic terminals (Mateo et al., 2017) and it is possible that oLFS of plPFC activates VTA dopaminergic terminals to indirectly drive a CPP.

We herein support previous studies demonstrating that VTA dopaminergic projections non-canonically release BDNF (Seroogy et al., 1994, Koo et al., 2016) and GABA (Tritsch et al., 2014) and provide evidence that this release of BDNF is involved in mediating NAc inhibitory synaptic plasticity in the slice preparation and may influence behavior. Furthermore, we provide data suggesting that this mechanism is susceptible to

modulation by EtOH. Human studies reveal that sensitivity to alcohol reward predicts whether individuals go on to develop AUD (King et al., 2011; King et al., 2014; King et al., 2016; King et al., 2021; King et al., 2022). Thus, investigating mechanisms mediating the rewarding properties of alcohol, which may drive binge consumption, are critical towards developing a better understanding of how alcohol reconstructs the strength of circuits mediating reward over time. Furthermore, inhibitory neurotransmission in the NAc and its relevance towards reward as it relates to drug misuse and addiction is highly unexplored and it is critically important that it continues to be investigated to enhance our understanding of reward circuitry. Exploring the role of BDNF signaling as a mediator of inhibitory plasticity onto NAc MSNs will help fill many gaps in knowledge about NAc MSN output, the relationship between BDNF and reward, and how alcohol hijacks midbrain circuitry.

Chapter 4: Discussion

4.1 Alcohol and DLS FSI network activity

We here discover that the FSI-FSI electrical coupling in adult mice rarely occurs (**Figure 2.1**) and that FSIs are more sensitive to cortical afferent stimulation, firing with greater fidelity than MSNs (**Figure 2.2**). These empirical data informed our neural simulations of variant cortico-FSI networks, which enabled us to find that FSI electrical synapses weakly contribute to the synchrony of striatal FSIs in adult mice while convergent, and coincident, cortical excitation significantly drives FSI-FSI synchrony (**Figure 2.4-6**).

It is important to first note caveats with the present modeling data. First, because our model is based on the number of action potentials in response to cortical afferent activation, it does not account for the possible lateral chemical synaptic inhibition from neighboring FSIs or inhibitory input from the globus pallidus (Bevan et al., 1998; Mallet et al., 2012). Also, while cortical input into striatum is the largest source of excitatory input onto FSIs, our model does not consider excitatory inputs from other areas such as subthalamic and thalamic nuclei (Sciamanna et al., 2015; Klug et al., 2018; Assous and Tepper, 2019a; Assous and Tepper, 2019b) as well as the pedunculopontine nucleus (Assous et al., 2019). Understanding how FSIs integrate these inputs in parallel or discretely from corticostriatal inputs, especially as compared to MSNs, could enable a stronger understanding of how the dorsal striatum is able to efficiently integrate so many inputs to quickly drive discrete action sequences. Furthermore, if it is true that alcohol modulates FSI synchrony to enable the development of quicker, more efficient action

sequences, elucidating how other synapses contribute to FSI synchrony may point to other potential synaptic targets for alcohol.

The model also assumes homogeneity of FSI morphology and response properties. This assumption was made to simplify the model for simulations to directly target the role of electrical synapses. However, FSIs may vary in their presynaptic inputs and weight distributions (Assous and Tepper, 2019b). Introducing heterogeneity in cortico-FSI synaptic weights could shift the results toward heterogeneous populations of synchronized FSIs, potentially reflecting functional FSI ensembles (Roberts et al., 2019). But contradictory optogenetic studies (Qi et al., 2016 versus Chen et al., 2019, for example) point to the fact that FSIs, which are typically uncoordinated during novel reward-seeking tasks (Berke, 2008), may be difficult to examine experimentally without artificially using broad network activation or inhibition (Covey and Yocky, 2021). Given that broad network activation or inhibition of FSIs rarely happens *in vivo*, findings from this experimental strategy may be misleading. It may be more informative to use methods such as *in vivo* electrophysiology or calcium imaging for visualization of heterogeneity in firing amongst FSI groups that may occur as a result of convergent excitatory input excitation.

The high sensitivity of the brain to acute alcohol exposure and binge alcohol consumption makes it unsurprising that as repeated binge drinking sessions for alcohol occur, brain circuits quickly adapt in ways that are hard to reverse. Alcohol facilitates habit formation by targeting DLS circuitry (Everitt et al., 2001; Graybiel, 2005). The influence of chronic alcohol use over the formation of automatized actions is so strong that it accelerates not only continual habitual consumption of ethanol, but also habitual responding for natural rewards such as sucrose (Lesscher et al., 2010; Sjoerds et al., 2013;

Corbit et al., 2012). Interestingly, the extent of habitual decision making can even predict relapse in alcohol-dependent individuals (Sebold et al., 2014; Duka et al., 2017; Sebold et al., 2017).

On a cellular level, FSIs are causally linked to habit formation (O'Hare et al., 2017) and compulsive consumption of alcohol, but not natural substances such as sucrose or water (Patton et al., 2021). This suggests that alcohol targets FSIs. Furthermore, in the absence of FSIs, the microstructure of licks for alcohol in mice are drastically changed; mice lick less frequently but for longer periods of time when they do attempt to drink (Patton et al., 2021). This suggests that the lack of inhibition onto MSNs from FSIs hinders their ability to constrain selected actions. In an intact system, MSNs organize into neuronal ensembles as actions are learned (Jin and Costa, 2010; Bakhurin et al., 2016; Martiros et al., 2018; Gritton et al., 2019). This promotes goal-directed, task-oriented actions while inhibiting unwanted ones. Repeating actions in pursuit of a reward facilitates this process, enabling refined, automatized motor sequences (Aldridge and Berridge, 1998; Jin and Costa, 2010; Martiros et al., 2018). This refined ensemble activity is associated with the transition of flexible towards more inflexible circuitry and cognition associated with habits (Graybiel, 2008; Lipton et al., 2019).

MSN ensemble formation is shaped and organized by FSI ensemble network activity (Owen et al., 2018, Duhne et al., 2020). Separate FSI ensembles encode the speed of specific, discrete action sub-components such as ambulation and head movements (Roberts et al., 2019). Disruption of FSI ensembles reduces MSN co-activation and significantly alters the balanced, controlled output of MSN subpopulation (Damodaran et al., 2014). Because FSIs are so outnumbered by MSNs, making up only 1% of the striatal

cell population (Luk and Sadicot, 2001), their ensemble formation is critical for their control over MSN output (Damodaran et al., 2014; Owen et al., 2018; Duhne et al., 2020). This is supported by FSIs preferentially targeting D1R MSNs over D2R MSNs (Gittis et al., 2010; Bahuguna et al., 2015), which may enable stronger refinement of DLS output and reduce unwanted movements. While it is clear that FSI network activity enables refinement of MSN ensemble activity and output, it is widely unknown how these networks are targeted by alcohol to facilitate refinement and action sub-component formation, especially in the pursuit and consumption of alcohol.

For decades, FSI ensemble formation has been attributed to FSI-FSI electrical coupling (Koos and Tepper, 1999; Lau et al., 2010; Zhang et al., 2014). This is supported by dual electrophysiological patch-clamp recordings of FSIs in juvenile mouse brain slices demonstrating that the electrical synapse rate between FSIs is nearly a third of their population (Koos and Tepper, 1999). But electrical coupling, or gap junction formation, is mediated by connexin-36 (Cummings et al., 2008). Expression of this protein declines throughout development and into adulthood (Bruzzone et al., 1996; Belluardo et al., 2000). We herein provide dual-patch electrophysiological evidence in support of this finding, demonstrating that only ~8% of FSIs (from a total of 78 pairs) display electrical coupling (**Figure 2.1**). The theoretical implication of this is that FSI ensemble formation then must also decline, which is supported by our finding that FSI-FSI gap junctions on their own do not contribute to FSI synchrony (**Figure 2.4**). But shifting between goal-directed and habitual behavior is essential throughout human life, suggesting there must be another mechanism involved in FSI ensemble formation. Thus, we herein identify a gap in

knowledge in the literature: that the canonically accepted mechanism for FSI synchrony does not suitably drive synchrony in adults.

Our finding that FSIs display higher responsivity to cortical convergence as compared to MSNs supports the idea that FSIs act as a refining filter or break for excitatory inputs into the dorsal striatum (**Figure 2.2)**. This finding also supports anatomical findings that demonstrate broad areas of cortex converge onto FSIs as compared to MSNs (Ramanathan et al., 2002; **Figure 2.2**). Given that FSIs regulate different, specific action subcomponents by firing in ensembles (Roberts et al., 2019), it is possible that different areas of cortex converge onto specific FSI ensembles to regulate the speed, and therefore timing (Kim et al., 2019), of the specific action subcomponents they encode. Furthermore, our findings may point to a novel mechanism for the formation of discrete FSI ensembles mediating reward learning in order to distinguish between cues (Bakhurin et al., 2016; Lee et al., 2017).

We herein provide the first evidence of the integration of demonstrably high levels of convergent cortical input onto FSIs (Ramanathan et al., 2002) serving a functional physiological role as a mediator of FSI synchronous firing (**Figure 2.4**). This stands in support of findings about other inhibitory cell networks in the brain demonstrating convergent excitation onto an inhibitory neuron population may mediate synchrony and feedforward inhibition networks (Wang et al., 2019) and opens doors to further investigation of how this mechanism may be targeted in contexts where habits are formed or facilitated.

4.2 Midbrain BDNF and alcohol reward

We find *ex vivo* that the VTA and plPFC both release BDNF into the NAc, which diminishes inhibition onto NAc MSNs (**Figure 3.1** and **3.5**). We also find that ethanol augments this disinhibition at least at VTA → NAc MSN synapses (**Figure 3.1**). Furthermore, stimulating both these projections with oLFS separately *in vivo* drives a CPP (**Figure 3.2** and **3.5**). NAc-iLTD induction *ex vivo* is frequency-dependent, as well as VTA-induced CPP (**Figure 3.4**). Additionally, CPP driven by oLFS of VTA is dependent upon BDNF signaling but may also require dopamine signaling (**Figure 3.2**). Lastly, subthreshold rewarding stimulation of VTA afferents coupled with a subthreshold rewarding dose of ethanol together drive CPP in a BDNF-dependent manner (**Figure 3.6**).

NAc disinhibition is equally expressed on MSNs expressing either D1R or D2R (Patton et al., 2019). Here we find that optogenetically stimulating plPFC or VTA afferents in the NAc utilizing our *ex vivo* NAc-iLTD induction protocol (LFS) drives a CPP *in vivo* (**Figures 3.2** and **3.5**), suggesting it is rewarding to the mice. While much work remains to be done in determining whether the disinhibition of NAc MSNs we see in slice that is dependent upon BDNF signaling is mediating the CPP we observe, our work has the potential to stand in support of mounting evidence that MSN output pathways are not dependent upon whether the MSNs activated express D1R or D2R (Kupchik et al., 2015; Kupchik and Kalivas, 2017). It is impossible to conclude from our findings that the effects we see *in vivo* are directly attributable to the mechanism we have detected *ex vivo*. But even in the case that they are, the MSN subtype non-specificity of NAc disinhibition *ex vivo* (Patton et al., 2019) may very well not be paralleled *in vivo*. TrkB receptor expression is higher on MSNs expressing D2R (Lobo et al., 2010; Baydyuk et al., 2011), suggesting

this subpopulation may be preferentially targeted by afferents releasing BDNF. Viral tracing techniques enable visualization of afferents targeting the dendrites and somas of postsynaptic targets, and that would an efficient way to broaden our understanding of how the VTA and plPFC target D1R and D2R MSNs in the NAc.

We demonstrate that NAc disinhibition is not modulated by dopamine signaling *ex vivo* (**Figure 3.1**) and our *in vivo* data suggest that BDNF release in the NAc supports motivated behaviors (**Figures 3.2, 3.3,** and **3.6)**. This stands in support of many studies demonstrating that BDNF positively modulates reward learning and reinstatement: activation of TrkB via exogenous intrastriatal infusion of BDNF minimizes response preservation to an initial strategy for obtaining a reward, thereby facilitating faster strategy shifting for receipt of a reward (D'Amore et al., 2013). Moreover, increases in BDNF driven expression by the enzyme LSD1 is critical for rats to be successfully conditioned to press for rewarding self-stimulation (Sagarkar et al., 2021). However, the CPP we observe is abolished following administration of a broad dopamine receptor antagonist (**Figure 3.2**). This suggests that dopamine-dependent reward mechanisms are being induced *in vivo*, and more experiments are needed to confirm if this is the case. It is possible that *in vivo*, dopamine and BDNF interact to drive reward. In a molecular investigation on dopamine signaling in NAc D1R MSNs and its regulation of reward-related behavior via downstream signaling activation of mitogen-activated protein kinase (MAPK), investigators discovered that MAPK phosphorylates Neuronal Per Arnt Sim domain protein 4 (Npas4) to increase its interaction with CREB-binding protein (CBP), thereby increasing the transcriptional activity of Npas4 at the BDNF promoter to enhance reward-related learning and memory (Funahashi et al., 2019). Because we administered flupenthixol dihydrochloride

intraperitoneally, it is also possible that its interruption of dopamine signaling in other areas of the brain impacted the ability of mice to experience reward. A more localized administration of the drug via cannulation prior to conditioning could address this. We also did not differentiate between D1R and D2R MSNs when inducing NAc-iLTD *ex vivo* in the presence of flupenthixol, thus it is possible that dopamine signaling modulates inhibitory plasticity differentially on MSN subpopulations and we were not able to detect this with our slice experiment setup. Recording from MSN subpopulations in the presence of dopamine receptor antagonists could help confirm this.

We provide data suggesting that this BDNF-mediated mechanism is susceptible to modulation by ethanol (**Figure 3.1g and 3.6**). This supports previous findings suggesting that systemic delivery or self-administration of alcohol leads to activation of NAc H-Ras, a protein downstream of TrkB receptors, which is required for alcohol seeking and elevated consumption (Hamida et al., 2012). Further validation that the two indeed interact during CPP *in vivo* is critical to conclude that this mechanism mediates any aspect of alcohol reward; recording inhibitory postsynaptic currents in NAc MSNs following subthreshold oLFS and subthreshold ethanol CPP and determining whether NAc-iLTD is occluded would enable a better understanding of whether NAc MSNs experienced disinhibition. Repeating this experiment with inclusion of CTX-B or with the Flx-TrkB line of mice would provide more clues about whether this interaction truly requires BDNF signaling.

Moreover, we did not explore whether *ex vivo* ethanol augmentation of NAc-iLTD (Patton et al., 2019 and **Figure 3.1**) and the *in vivo* interaction of these two stimuli (**Figure 3.6**) require dopamine signaling to be intact. Acute ethanol can increase dopamine transmission in the NAc and this mechanism is largely accepted as being the predominant

mediator of the rewarding properties of ethanol (Di Chiara, 1997; Soderpalm and Ericson, 2009; Bassareo et al., 2017; Dahchour and Ward, 2022). Thus, it is possible that ethanol modulation of inhibitory synaptic strength in the NAc is not entirely dopamine-independent. This is further supported by lines of evidence linking dopamine signaling with GABAergic signaling in the NAc (Lof et al., 2007) and even specifically BDNF interplay with dopaminergic modulation of GABA receptor expression (Jeanblanc et al., 2006; Leggio et al., 2019). However, these findings suggest that dopamine and BDNF postsynaptic signaling cascades converge to strengthen GABA inhibition in the NAc and control ethanol consumption, which theoretically opposes what we observe herein. Determination of whether dopamine modulates ethanol augmentation of NAc disinhibition is essential for furthering our understanding of BDNF and dopamine interplay as it relates to inhibitory plasticity and ethanol reward. Utilizing flupenthixol dihydrochloride while eliciting subthreshold oLFS in combination with a subthreshold rewarding dose of ethanol during conditioning *in vivo* may provide some clues.

Despite our findings suggesting that VTA BDNF contributes to NAc-iLTD (**Figure 3.1**), we also find that plPFC BDNF is sufficient to drive NAc-iLTD and that stimulation of these afferents *in vivo* drives a CPP (**Figure 3.5**). Because we did not inhibit BDNF signaling during this CPP, it remains unclear whether the CPP driven by plPFC afferent stimulation is mediated by BDNF signaling. We also did not test whether excitation of plPFC inputs alters the strength of glutamatergic neurotransmission in the NAc. As such, it is possible that we observed a CPP mediated by altered glutamate synaptic strength driven by plPFC terminal activation in the NAc, as others have found that elevated plPFC glutamate is associated with initiation, learning, and remembrance of reward-associated

behaviors (Kalivas and Volkow, 2005; Alasmari et al., 2018; Pena-Bravo et al., 2019). Recording excitatory postsynaptic currents (EPSCs) *ex vivo* before and after oLFS of plPFC afferents would elucidate whether excitatory projections are altered following plPFC afferent stimulation in the NAc. Alternatively, PFC afferents in the NAc can activate dopaminergic terminals (Mateo et al., 2017). Perhaps optogenetically stimulating plPFC afferents twice over the span of 30 mins activates VTA dopaminergic terminals to indirectly drive a CPP. Administration of flupenthixol dihydrochloride prior to conditioning could enable determination of whether plPFC-induced CPP is dopamine-dependent.

We herein support previous studies demonstrating that VTA dopaminergic projections non-canonically release BDNF (Seroogy et al., 1994, Koo et al., 2016) and GABA (Tritsch et al., 2014) and provide evidence that this release of BDNF is involved in mediating NAc inhibitory synaptic plasticity in the slice preparation and may influence behavior. Confirmation of whether we actually induced NAc disinhibition *in vivo* with oLFS is needed; recording inhibitory postsynaptic currents following CPP and investigating if NAc-iLTD is occluded could address this. Alternatively, recording NAc MSN activity with *in vivo* electrophysiology or calcium imaging and determining whether cells are more active following oLFS in the presence of CTX-B or flupenthixol dihydrochloride would help broaden our understanding of whether NAc disinhibition mediated by BDNF occurs following oLFS. Intracranially administering BDNF into the NAc and recording NAc MSN output *in vivo* may further elucidate the behavioral relevance of our *ex vivo* findings, which have also revealed that exogenous BDNF administration is sufficient to disinhibit the NAc (Patton et al., 2019). *In vivo* electrophysiology experiments

could also be used to further confirm if the dopamine-dependent CPP we observe is attributable to disinhibition of NAc MSNs, by stimulating VTA afferents with oLFS in the presence of flupenthixol dihyrochloride and measuring resultant MSN activity. Inhibitory neurotransmission in the NAc and its relevance towards reward as it relates to drug misuse and addiction is highly unexplored and it is critically important it continues to be investigated in order to enable a broader understanding of reward circuitry. Continuing to unravel the role of BDNF signaling in mediating inhibitory plasticity onto NAc MSNs will help fill in many gaps in knowledge about NAc MSN output, the relationship between BDNF and reward, and how alcohol hijacks midbrain circuitry.

4.3 Future Directions

FSI ensembles and alcohol

We find that increasing the level of cortical convergence onto FSIs increases their synchrony (**Figure 2.6**). It is possible that alcohol strengthens the cortico-FSI synapse itself to strengthen cue-reward associations for the development of compulsive alcohol consumption and habitual responding for alcohol. But the fact that the basal strength of inhibition in the DLS is twice that of the DMS (Wilcox et al., 2014) points to alcohol modulation of GABAergic strength as a likely indirect mechanism through which alcohol may alter FSI integration of corticostriatal inputs. Acute alcohol exposure diminishes the strength of inhibition from FSIs and other MSNs onto MSNs (Patton et al., 2016) and repeated alcohol exposure causes differential changes in sensitivity to GABAergic transmission in the DLS and DMS, whereby it enhances inhibitory tone in the DMS and diminishes it in the DLS (Wilcox et al., 2014). These findings coupled with our model

suggest that diminished inhibition onto FSIs by alcohol may increase their sensitivity to cortical innervation, thus increasing their efficiency as modulators of MSN output to support compulsive action sequences, such as that of the pursuit and consumption of alcohol.

To determine whether this is the case, we first need to know whether alterations in corticostriatal strength impact FSI ensembles *in vivo* and whether this impacts the encoding of action sub-components. Our lab has previously utilized *in vivo* calcium imaging for the discovery of FSI ensemble activity encoding action sub-components (Bradley et al., 2019). I propose utilizing this method for detection of discrete FSI ensembles while inhibiting cortico-FSI strength with the prediction that weakened corticostriatal strength will significantly impact action kinematic encoding and may lead to more uncoordinated movement. To weaken the cortico-FSI projection, I would use various concentrations of IEM-1460, a blocker of AMPA receptors lacking the GluA2 subunit that are expressed only on FSIs (Magazanik et al., 1997; Oran and Bar-Gad, 2018). Use of this inhibitor in other studies results in abnormal movements that is associated with diminished firing rate of FSIs (Bronfield and Bar-Gad, 2011; Oran and Bar-Gad, 2018), but no one has looked at the consequences of this inhibitor on FSI synchrony. Should I find that IEM-1460 indeed results in diminished FSI ensemble synchrony, it would be worthwhile to utilize this drug as a tool to determine whether alcohol relies on FSI ensembles regulated by cortical activity to facilitate habitual consumption of alcohol. Thus, I would subject mice to a chronic intermittent voluntary ethanol consumption paradigm (Drinking in the Dark or DID; Rhodes et al., 2005) while treating them with IEM-1460 and measure the extent (if any) mice elevate their consumption over time as well as compulsivity (measured by whether

mice continue to consume ethanol despite addition of the bitterant quinine to their bottles) as compared to control groups. If alcohol indeed targets FSI ensembles and relies on the strength of their synchrony to regulate habit formation, I predict that these mice would drink less than controls and not compulsively consume it. If alcohol acts through other means to enhance the synchrony of FSIs (such as inhibitory inputs or via FSI → MSN synapses), I would expect little differences between these groups.

BDNF, NAc disinhibition, and context-dependence

The role of BDNF in alcohol reward is highly disputed. Investigations on GABA, dopamine, and BDNF as they relate to alcohol consumption are contradictory, but also highly informative. Genetic deletion or pharmacologically blocking D3R (a D2-like receptor) increases expression of $GABA_A$ receptors (Leggio et al., 2015), which inhibits voluntary alcohol consumption due to the resultant elevated strength of inhibitory neurotransmission in the NAc (Leggio et al., 2014; Leggio et al., 2019). Pharmacologically inhibiting D3R diminishes consumption of ethanol in mice with intact D3R receptors (Leggio et al., 2014). This may be due to a mechanism involving BDNF, as blocking BDNF signaling with an antagonist diminishes ethanol intake and lowers D3R expression in wildtypes (Leggio et al., 2014). These findings suggest that D3R together with increased RACK1/BDNF expression reinforces ethanol consumption (Leggio et al., 2014), which is supported by other work finding that acute systemic administration of alcohol activates NAc H-Ras, a protein activated downstream of TrkB that alcohol directly targets as does operant self-administration of alcohol (Hamida et al., 2012). Genetic knockdown or pharmacological inhibition of NAc H-Ras reduces ethanol consumption alone as compared to other solutions and attenuates goal-directed seeking for alcohol (Hamida et al., 2012).

However, others examining this exact mechanism and its relationship to alcohol completely contradict this understanding. Diminishing BDNF levels in the dorsal striatum increases behavioral responding for alcohol (McGough et al., 2004). Conversely, following acute ethanol administration or ethanol consumption, RACK1 translocates to the nucleus of neurons to increase BDNF expression, which resultantly elevates D3R expression in the striatum to suppress consumption of ethanol (McGough et al., 2004; Jeanblanc et al., 2006). This suggests that perhaps alcohol triggers a homeostatic, protective mechanism to reduce further consumption. Although these studies contradict in their understanding of the exact role of BDNF in alcohol intake, they agree that BDNF is targeted by alcohol in a behaviorally impactful way.

Human studies reveal that sensitivity to alcohol reward predicts whether individuals go on to develop AUD (King et al., 2011; King et al., 2014; King et al., 2016; King et al., 2021; King et al., 2022). Thus, investigating mechanisms mediating the rewarding properties of alcohol, which drive binge consumption and goal-directed pursuit of alcohol, are critical towards developing a better understanding of how alcohol reconstructs the strength of circuits mediating reward over time. Elevation of $GABA_A$ due to D3R receptor deletion inhibits voluntary ethanol consumption (Leggio et al., 2015) and H-Ras activation downstream of TrkB promotes consumption of ethanol (Hamida et al., 2012), suggesting that BDNF-mediated weakening of GABAergic neurotransmission in the NAc would support consumption of ethanol. However, VTA BDNF is also associated with enhanced sensitivity to social defeat stress (Berton et al., 2006; Krishnan et al., 2007; Koo et al., 2016), which can also lead to elevated drug consumption (Graham et al., 2007; Grimm et al., 2003; Narita et al., 2003; Nikulina et al., 2008; Wang et al., 2016; Wang et al., 2017).

The disparity between these investigations into the role of BDNF in reward suggests that the system is highly context dependent. It is apparent that the contexts in which BDNF is released and in which the BDNF signaling system is manipulated drastically impact whether it supports reward or stress. Continuing to investigate its roles in these different contexts is the only way to discover why this is the case. But what all of these investigations do agree on is that BDNF signaling increases sensitivity to the environment, cues, and internal states whether they be reward- or stress-related.

We find that optogenetically interrogating BDNF-releasing terminals in the NAc results in a CPP. But we have a long way to go in determining the implications of this. What does NAc-iLTD encode? What are the implications of its interaction with alcohol? I first propose determining whether NAc MSNs are disinhibited following LFS with *in vivo* electrophysiology. Following that, I would utilize the same experimental setup to confirm that this mechanism is primarily BDNF-mediated through the use of dopamine antagonists, CTX-B, and Flx-TrkB mice with TrkB ablated in the NAc.

I then would propose investigating whether BDNF-mediated NAc disinhibition promotes reward-related consumption of ethanol and/or chronic stress-induced susceptibility to depressive behaviors. I hypothesize that BDNF enhances the sensitivity of the NAc and that in circumstances where its expression or release is elevated, whether they be rewarding or aversive, the triggers and cues in those environments become more salient. I would test this by investigating whether oLFS of VTA afferents in the NAc contributes to voluntary ethanol consumption (DID) and chronic social defeat stress (Koo et al., 2016). For all groups in experiments, I would compare controls to groups of mice undergoing the same procedures with altered BDNF signaling (via targeting of H Ras or TrkB). For the

DID condition, I would oLFS VTA afferents as mice undergo the voluntary ethanol paradigm (once every 30 minutes for the 4 sessions over the course of the 4 week protocol) and measure their consumption over time. We know that mice can be trained to escalate their ethanol consumption in the DID paradigm and that by the end of the 4 weeks, they compulsively consume ethanol. But I predict that mice with BDNF signaling intact will escalate their drinking faster and drink larger volumes than mice with blocked BDNF signaling. Moreover, I predict that those with BDNF signaling intact also receiving VTA oLFS will escalate their consumption the fastest and drink the most. For the chronic social defeat stress condition, I would oLFS VTA afferents in the NAc before or during the daily defeat stress sessions and measure their social interaction ratios following defeat sessions for susceptibility or resilience to stress. I predict that mice receiving VTA oLFS in the NAc with BDNF signaling intact will be significantly more susceptible to stress-induced depressive behaviors than the other groups. These findings would support that BDNF modulates the VTA → NAc circuit so that it is more sensitive to environmental cues and internal states. Should this be the case, BDNF may theoretically be a promising target for AUD; heightened sensitivity to stress and heightened sensitivity to reward are the primary proposed reasonings for alcohol misuse and abuse.

However, others have reported that BDNF release from the VTA reduces morphine reward (Koo et al., 2012) and enables resilience to social stress via its targeting of D1R MSNs (Pagliusi et al., 2022). Additionally, recall that NAc-iLTD is expressed on both D1R and D2R MSNs (Patton et al., 2019). An alternative hypothesis is that oLFS of VTA afferents *in vivo* preferentially targets D1R MSNs, or that D1R MSN disinhibition is more salient to mice; if this is the case, I would expect to see increased resilience to stress.

Revisiting the contradictory findings on the interplay between BDNF, dopamine, and ethanol, lack of D3R (a D2R-like receptor) increases $GABA_A$ expression to inhibit consumption (Leggio et al., 2015), yet increased BDNF from ethanol consumption increases D3R expression to also suppress ethanol consumption (McGough et al., 2004; Jeanblanc et al., 2006). Using the 4 week long voluntary ethanol consumption paradigm of DID while stimulating VTA afferents and manipulating the BDNF system may enable a better understanding of these discrepancies as it is possible that the role of BDNF in consumption of ethanol changes over time; perhaps different mechanisms are engaged depending on the stage in which mice are engaging in consumption of ethanol.

In the dorsal striatum, the effect of ethanol over time is that it shifts brain circuitry from being flexible during learning processes to being inflexible for the regulation of habits. Under that same logic for the ventral striatum, BDNF may support flexibility in NAc circuitry during earlier stages of alcohol consumption. Over time, as alcohol use progresses, the NAc may become more inflexible to rewarding cues, including alcohol, but the memory of alcohol reward remains and thus a habitual pursuit for this reward in response to external triggers or cues continues.

4.4 Rethinking AUD treatment strategies

There are currently few treatment options available for AUD. The Food and Drug Administration has approved three medications: disulfiram, naltrexone, and acamprosate (Ross and Peselow, 2009). Disulfiram (Antabuse) targets the metabolism of alcohol, causing unpleasant symptoms upon consumption of the drug (Hughes and Cook, 1997). Because it does not target withdrawal symptoms of AUD, those treated with disulfiram

tend to stop taking it so that they can continue to consume alcohol to alleviate withdrawal symptoms (Fuller and Gordis, 2004). Naltrexone (an opioid receptor antagonist) and acamprosate (an inhibitor of glutamate signaling via NMDA receptors; al Qatari et al., 1998) are a bit more effective than disulfiram, but this is largely due to the fact that you have to already be abstinent from alcohol prior to taking them as their purpose is to diminish relapse following abstinence (Snyder and Bowers, 2008). How does an individual become abstinent prior to pharmaceutical intervention? This typically requires cognitive or behavioral therapeutic intervention or admittance into mutual-support groups such as Alcoholic's Anonymous (AA; Smart and Mann, 2000; Kelly and Yeterian, 2011). There are more homeopathic treatment options available for AUD as well, including acupuncture, which even demonstrably inhibits VTA GABAergic and dopaminergic neuronal activity to reduce ethanol self-administration in rats (Yang et al., 2010; Bills et al., 2022). While these options are effective for some recovering patient populations, they do not work for everyone. Furthermore, the process of seeking treatment often ironically increases stress, which in and of itself worsens relapse; alcohol users report high rates of relapse when they are under great stress and cycles of alcohol consumption and abstinence activate stress systems (Koob and Le Moal, 2008; Koob, 2013).

Development of treatment options beyond these is difficult. For decades, the focus for preclinical drug development has been on targeting symptomology of later stages of AUD, such as withdrawal. But these efforts are not met with much success in patient populations. Furthermore, symptomology that arises early in the onset of AUD such as heightened sensitivity to reward and compulsivity may reliably predict populations of individuals susceptible to AUD development. As previously described, those that binge

drink or misuse alcohol frequently consume alcohol in that manner; quickly identifying these populations of individuals and treating their sensitivity to alcohol reward or their compulsive consumption of alcohol following exposure to salient, triggering cues could potentially bring down the adverse health comorbidities that arise as alcohol misuse continues and chronic alcohol exposure wreaks havoc on the brain and body (as reported by the World Health Organization, also see reviews: Gunnar et al., 1971; Segel e tal., 1984; Dunne, 1989; Spies et al., 2001; Reidy et al., 2011; Gao and Bataller, 2011; Kim et al., 2012; de Menezes et al., 2013; Surtel et al., 2014; Rocco et al., 2014; Pasala et al., 2015; Simet and Sisson, 2015; Szabo and Saha, 2015; Dunn and Shah, 2016; McHugh and Weiss, 2019; Kourkoumpetis and Sood, 2019; Helle et al., 2020; Geoffroy et al., 2020; McGinn et al., 2021; Wang et al., 2021; Wigger et al., 2022; Martinez-Costillo et al., 2023).

BDNF is likely not a realistic treatment target due to its widespread expression across the brain and body, which raises the likelihood of adverse side effects. While proteins downstream of TrkB activation show promise as potential targets preclinically (such as HRas: Hamida et al., 2012), there is little evidence to support that these targets primarily enable alcohol-related pursuit and that disrupting their signaling would not impede upon other motivated behaviors. BDNF supports a wide variety of behavioral phenotypes in a highly context-dependent manner. With regards to reward-related behaviors, it even drives oppositional region-specific effects (hippocampus vs. VTA → NAc BDNF), demonstrating the high risk in targeting the BDNF system to treat diseases such as AUD (Nestler and Carlezon, 2006). However, it is possible that BDNF and proBDNF could be used as biomarkers for AUD. Biomarkers are critical tools when treating a disease that develops over long periods of time, such as AUD, not only because

they enable more accurate diagnostics but also because they serve as a measurable way of discerning whether a treatment is working – sometimes even before those being treated feel any different. For AUD and other addictions, biomarkers may be especially useful as a tool because the onset and severity of addictions are so context specific. Investigations of BDNF as a biomarker for a variety of diseases and conditions relating to altered motivation and reward-related behavior show promise. For instance, lower BDNF serum and plasma levels are seen in those with eating disorders (Shobeiri et al., 2022; Phillips et al., 2014). BDNF blood levels have been broadly explored with regards to alcohol use and context of alcohol intake. Even the age in which individuals start drinking impacts proBDNF and BDNF blood levels. While BDNF concentration increases over time throughout adolescence in non-drinking individuals, those who drink prior to 15 years of age exhibit lower proBDNF and BDNF levels (Miguez et al., 2020). Interestingly, those who use alcohol after the age of 15 also have altered BDNF levels as compared to non-drinkers, with higher levels of BDNF despite unchanged proBDNF levels (Miguez et al., 2020). It is well established that during the progression of AUD, the brain and body adapt to the alterations alcohol makes and thus chronic alcohol exposure is known to have drastically different effects as compared to "acute" alcohol exposure. As such, it falls to reason that those with alcohol dependence may have altered BDNF blood levels as compared to those drinking heavily over a shorter period of time. Joe et al. (2007) found that there is decreased plasma BDNF in alcohol-dependent individuals. However, as previously mentioned, many suffering from AUD also endure psychiatric comorbidities. BDNF blood levels in these populations provide insight not only about BDNF as a biomarker but also about transdiagnostic aspects involved with AUD and psychiatric

disorders. For instance, those experiencing anhedonia in AUD and depression have reduced peripheral levels of BDNF (Levchuk et al., 2020). As many of those being treated from AUD are abstinent from alcohol, researchers have also investigated BDNF blood levels in patients undergoing detoxification. Similarly to those still consuming alcohol, decreased BDNF plasma concentrations can be seen (Garcia-Marchena et al., 2017). While more investigations are needed, BDNF serum and plasma levels seem to be incredibly sensitive to alcohol use over time as well as the context in which it is consumed, suggesting that BDNF may serve as an effective biomarker for alcohol use, AUD severity, and detoxification.

Comorbidity of psychiatric illnesses with AUD is an important variable to consider in the development of treatment options. Additional illness(es) may affect the course of AUD as well as response to treatment. Interestingly, investigations into treatment options for comorbidities of AUD that impair the experience of reward have revealed that many of these therapeutics work, in part, through their targeting of the BDNF system. For instance, escitalopram oxalate (Lexapro) is an approved drug in the treatment of depression and researchers have found that it targets intracellular pathways linked to BDNF cascades while increasing pro-BDNF levels in rat prefrontal cortex (Alboni et al., 2010). Additionally, inhibiting BDNF signaling in the hippocampus is preventative against the beneficial impact of exercise on mood and cognitive function, including learning and recall abilities (Vaynman et al., 2004). Buspirone has begun to be explored as a novel therapeutic for AUD (Collins et al., 1987; see also review: Malec et al., 1996). Buspirone targets the interplay between BDNF and dopamine signaling systems to diminish ethanol intake (Leggio et al., 2014). Ethanol consumption is substantially higher in wildtype mice as

compared to D3R knockout mice, and, while it effectively increases RACK1 and BDNF expression in both wildtype and D3R knockout mice, it increases D3R expression only in wildtypes (Leggio et al., 2014). Blocking BDNF signaling with an antagonist diminishes ethanol intake and lowers D3R expression in wildtypes and blocking signaling via D3R with buspirone also diminishes ethanol consumption culminating in the understanding that increased D3R associated with RACK1/BDNF expression may reinforce ethanol consumption (Leggio et al., 2014). But others find that D3R and BDNF/RACK1 signaling drive a homeostatic mechanism that attenuates alcohol consumption (Logrip et al., 2009). And notably, the efficacy of buspirone is not as strong in AUD populations that do not also suffer from anxiety disorders (Malec et al., 1996; Kranzler et al., 1994). This supports the theory that different patient populations have different needs; more discrete treatment strategies must be developed, whereby the health of individuals beyond their AUD is considered before moving forward with treatment.

Since the 1980s, researchers have attempted to categorize those suffering from AUD, as mounting evidence suggests that AUD is a heterogeneous disease (Clonginger et al., 1981; Cohen et al., 2019; Duko et al., 2019; Schmid et al., 2020; Maurage et al., 2021; Kovacs et al., 2022; Maisto et al., 2022; Pickard, 2022; Puddlephatt et al., 2022). The success of cognitive and behavioral therapies and group therapies such as AA over pharmaceutical treatment in reducing relapse (Smart and Mann, 2000; Kelly and Yeterian, 2011) may be due to the fact that these options are more specific to the distinct needs of individuals with AUD. Furthermore, they provide patients with individuals and environments that support them as they learn to identify the cues that trigger them to use alcohol while developing healthier coping strategies.

Beyond neurobiological heterogeneity in AUD, it is important to acknowledge that there are also economic and social differences amongst those suffering from addiction (Pickard, 2022). Many barriers exist for therapeutic intervention such as personal family issues, lack of insurance or "hassles" with Medicaid, suspicion, aversion to treatment due to methadone maintenance, limited slots available in treatment programs, homelessness, child-care issues, and the lack of personal identification (Appel et al., 2004). Even if these barriers are overcome, tensions between treatment personnel and patient populations can make communication and meeting needs appropriately difficult. This is worsened by agency manager reports of inadequate funding and lack of appropriate programs, as well as the social stigmatization of addicts (Appel et al., 2004). Since the 1990s, there has been an awareness that alcohol addiction and drug abuse recovery services with programs for women, adolescents, and the mentally ill may be critical for treatment of many homeless populations suffering from addiction (Drake et al., 1991; McCarty et al., 1991; Robertson, 1991). Easing up on insurance and identification requirements as well as increasing resources and funding even if just by a little year after year are a couple proposed remedies for these issues (Appel et al., 2004), but unfortunately, most proposed solutions are ignored and these problems have largely persisted over the years. Hopefully, educating the public, scientists, and clinicians about the many disparities in ease of access to treatment can help enable better communication with patient populations so that the voices of AUD populations who are not able to speak for themselves are strengthened.

Bibliography

1. Abrahao, K. P., Salinas, A. G., & Lovinger, D. M. (2017). Alcohol and the Brain: Neuronal Molecular Targets, Synapses, and Circuits. Neuron, 96(6), 1223–1238.

2. Abudukeyoumu N., Hernandez-Flores T., Garcia-Munoz M., Arbuthnott G. W. (2019). Cholinergic modulation of striatal microcircuits. Eur. J. Neurosci. 49 604–622.

3. al Qatari, M., Bouchenafa, O., & Littleton, J. (1998). Mechanism of action of acamprosate. Part II. Ethanol dependence modifies effects of acamprosate on NMDA receptor binding in membranes from rat cerebral cortex. Alcoholism, clinical and experimental research, 22(4), 810–814.

4. Alasmari, F., Goodwani, S., McCullumsmith, R. E., & Sari, Y. (2018). Role of glutamatergic system and mesocorticolimbic circuits in alcohol dependence. Progress in neurobiology, 171, 32–49.

5. Alboni, S., Benatti, C., Capone, G., Corsini, D., Caggia, F., Tascedda, F., Mendlewicz, J., & Brunello, N. (2010). Time-dependent effects of escitalopram on brain derived neurotrophic factor (BDNF) and neuroplasticity related targets in the central nervous system of rats. European journal of pharmacology, 643(2-3), 180–187.

6. Aldridge, J. W., & Berridge, K. C. (1998). Coding of serial order by neostriatal neurons: a "natural action" approach to movement sequence. The Journal of neuroscience : the official journal of the Society for Neuroscience, 18(7), 2777–2787

7. Alexander, G. E., DeLong, M. R., & Strick, P. L. (1986). Parallel organization of functionally segregated circuits linking basal ganglia and cortex. Annual review of neuroscience, 9, 357–381.

8. Al-Hasani, R., Gowrishankar, R., Schmitz, G. P., Pedersen, C. E., Marcus, D. J., Shirley, S. E., Hobbs, T. E., Elerding, A. J., Renaud, S. J., Jing, M., Li, Y., Alvarez, V. A., Lemos, J. C., & Bruchas, M. R. (2021). Ventral tegmental area GABAergic inhibition of cholinergic interneurons in the ventral nucleus accumbens shell promotes reward reinforcement. Nature neuroscience, 24(10), 1414–1428.

9. Allen, H.C., Weafer, J., Wesley, M.J., and Fillmore, M.T. (2021). Acute Rewarding and Disinhibiting Effects of Alcohol as Indicators of Drinking Habits. Psychopharmacology (Berl). 238, 181-191.

10. Altar CA, Cai N, Bliven T, Juhasz M, Conner JM, Acheson AL, et al. (1997). Anterograde transport of brain-derived neurotrophic factor and its role in the brain. Nature, 389, 856–60.

11. Aoki S, Liu AW, Zucca A, Zucca S, Wickens JR. (2015). Role of striatal cholinergic interneurons in set-shifting in the rat. J Neurosci. 35(25), 9424–9431.

12. Appel, P. W., Ellison, A. A., Jansky, H. K., & Oldak, R. (2004). Barriers to enrollment in drug abuse treatment and suggestions for reducing them: opinions of drug injecting street outreach clients and other system stakeholders. The American journal of drug and alcohol abuse, 30(1), 129–153.

13. Arienzo, D., Happer, J. P., Molnar, S. M., Alderson-Myers, A., & Marinkovic, K. (2020). Binge drinking is associated with altered resting state functional connectivity of reward-salience and top down control networks. Brain imaging and behavior, 14(5), 1731–1746.

14. Assous M, Dautan D, Tepper JM & Mena-Segovia J. (2019) Pedunculopontine glutamatergic neurons provide a novel source of feedforward inhibition in the striatum by selectively targeting interneurons. The Journal of Neuroscience 39, 4727–4737.

15. Assous, M. and Tepper, J.M. (2019a) Cortical and thalamic inputs exert cell type-specific feedforward inhibition on striatal GABAergic interneurons. J. Neurosci. Res. 97, 1491-1502.

16. Assous, M. and Tepper, J.M. (2019b) Excitatory extrinsic afferents to striatal interneurons and interactions with striatal microcircuitry. Eur. J. Neurosci. 49, 593-603.

17. Augier, E., Barbier, E., Dulman, R.S., Licheri, V., Augier, G., Domi, E., Barchiesi, R., Farris, S., Natt, D., Mayfield, R.D., Adermark, L., and Heilig, M. (2018). A molecular mechanism for choosing alcohol over an alternative reward. Science, 360, 1321-1326.

18. Avshalumov M. V., Patel J. C., Rice M. E. (2008). AMPA receptor-dependent H2O2 generation in striatal medium spiny neurons but not dopamine axons: one source of a retrograde signal that can inhibit dopamine release. J. Neurophysiol. 100 1590–1601.

19. Bahuguna, J., Aertsen, A., & Kumar, A. (2015). Existence and control of Go/No-Go decision transition threshold in the striatum. PLoS computational biology, 11(4), e1004233.

20. Bakhurin, K. I., Mac, V., Golshani, P., & Masmanidis, S. C. (2016). Temporal correlations among functionally specialized striatal neural ensembles in reward-conditioned mice. Journal of neurophysiology, 115(3), 1521–1532

21. Bakusic, J., Vrieze, E., Ghosh, M., Pizzagalli, D. A., Bekaert, B., Claes, S., & Godderis, L. (2021). Interplay of Val66Met and BDNF methylation: effect on reward learning and cognitive performance in major depression. Clinical epigenetics, 13(1), 149.

22. Barker, J. M., & Taylor, J. R. (2014). Habitual alcohol seeking: modeling the transition from casual drinking to addiction. Neuroscience and biobehavioral reviews, 47, 281–294.

23. Barnett, W. H., Kuznetsov, A., & Lapish, C. C. (2023). Distinct cortico-striatal compartments drive competition between adaptive and automatized behavior. PloS one, 18(3), e0279841.

24. Barry, P. H. (1994) JPCalc, a software package for calculating liquid junction potential corrections in patch-clamp, intracellular, epithelial and bilayer measurements and for correcting junction potential measurements. J. Neurosci. Methods 51, 107–116.

25. Bassareo, V., Cucca, F., Frau, R., & Di Chiara, G. (2017). Changes in Dopamine Transmission in the Nucleus Accumbens Shell and Core during Ethanol and Sucrose Self-Administration. Frontiers in behavioral neuroscience, 11, 71.

26. Baydyuk M, Russell T, Liao G-Y, Zang K, An JJ, Reichardt LF, et al. (2011). TrkB receptor controls striatal formation by regulating the number of newborn striatal neurons. Proc Natl Acad Sci U S A. 108, 1669–74.

27. Baydyuk M, Russell T, Liao G-Y, Zang K, An JJ, Reichardt LF, et al. (2011). TrkB receptor controls striatal formation by regulating the number of newborn striatal neurons. Proc Natl Acad Sci U S A. 108, 1669–74.

28. Beierlein, M., Gibson, J.R., and Connors, B.W. (2000) A network of electrically coupled interneurons drives synchronized inhibition in neocortex. Nat. Neurosci. 3, 904-910.

29. Belin-Rauscent A, Everitt BJ, Belin D. (2012). Intrastriatal shifts mediate the transition from drug-seeking actions to habits. Biol Psychiatry. 72(5), 343–345.

30. Belluardo, N. et al. (2000) Expression of connexin36 in the adult and developing rat brain. Brain Res. 865, 121–38.

31. Ben Hamida, S., Neasta, J., Lasek, A. W., Kharazia, V., Zou, M., Carnicella, S., Janak, P. H., & Ron, D. (2012). The small G protein H-Ras in the mesolimbic system is a molecular gateway to alcohol-seeking and excessive drinking behaviors. The Journal of neuroscience : the official journal of the Society for Neuroscience, 32(45), 15849–15858.

32. Bennett BD, Bolam JP. (1994). Synaptic input and output of parvalbumin-immunoreactive neurones in the neostriatum of the rat. Neuroscience. 62:707–719.

33. Berke J. D. (2008). Uncoordinated firing rate changes of striatal fast-spiking interneurons during behavioral task performance. The Journal of neuroscience : the official journal of the Society for Neuroscience, 28(40), 10075–10080.

34. Berton O, McClung CA, Dileone RJ, Krishnan V, Renthal W, Russo SJ, Graham D, Tsankova NM, Bolanos CA, Rios M, Monteggia LM, Self DW, Nestler EJ. (2006). Essential role of BDNF in the mesolimbic dopamine pathway in social defeat stress. Science. 311, 864–868.

35. Bertran-Gonzalez J, Herve D, Girault JA, Valjent E. (2004). What is the Degree of Segregation between Striatonigral and Striatopallidal Projections? Front Neuroanat. 4.

36. Bevan, M.D., Booth, P.A.C., Eaton, S.A., and Bolam, J.P. (1998) Selective Innervation of Neostriatal Interneurons by a Subclass of Neuron in the Globus Pallidus of the Rat. J. Neurosci. 18, 9438-9452.

37. Bills, K. B., Otteson, D. Z., Jones, G. C., Brundage, J. N., Baldwin, E. K., Small, C. A., Kim, H. Y., Yorgason, J. T., Blotter, J. D., & Steffensen, S. C. (2022). Mechanical Stimulation Alters Chronic Ethanol-Induced Changes to VTA GABA Neurons, NAc DA Release and Measures of Withdrawal. International journal of molecular sciences, 23(20), 12630.

38. Blomeley, C. P., Cains, S., Smith, R. and Bracci, E. (2011) Ethanol affects striatal interneurons directly and projection neurons through a reduction in cholinergic tone. Neuropsychopharmacology 36, 1033–46.

39. Bolam JP, Hanley JJ, Booth PA, Bevan MD. (2000). Synaptic organisation of the basal ganglia. J Anat. 196 (Pt 4), 527–542.

40. Boudreau, A., and Wolf, M. (2005). Behavioral Sensitization to Cocaine Is Associated with Increased AMPA Receptor Surface Expression in the Nucleus Accumbens. J Neurosci, 25, 9144–9151.

41. Bradfield LA, Bertran-Gonzalez J, Chieng B, Balleine BW. (2013). The thalamostriatal pathway and cholinergic control of goal-directed action: interlacing new with existing learning in the striatum. Neuron. 79(1), 153–166.

42. Brenner, E., Tiwari, G. R., Kapoor, M., Liu, Y., Brock, A., & Mayfield, R. D. (2020). Single cell transcriptome profiling of the human alcohol-dependent brain. Human molecular genetics, 29(7), 1144–1153.

43. Britt JP, Benaliouad F, McDevitt RA, Stuber GD, Wise RA, Bonci A. (2012). Synaptic and behavioral profile of multiple glutamatergic inputs to the nucleus accumbens. Neuron. 76(4), 790-803.

44. Bronfeld M, Bar-Gad I (2011) Loss of specificity in basal ganglia related movement disorders. Front Syst Neurosci 5:38.

45. Brown HD, McCutcheon JE, Cone JJ, Ragozzino ME, Roitman MF. (2011). Primary food reward and reward-predictive stimuli evoke different patterns of phasic dopamine signaling throughout the striatum. Eur J Neurosci. 34:1997–2006.

46. Brown LL, Smith DM, Goldbloom LM. (1998). Organizing principles of cortical integration in the rat neostriatum: corticostriate map of the body surface is an ordered lattice of curved laminae and radial points. J Comp Neurol. 392, 468–488

47. Bruzzone R., White T.W., and Paul D.L. (1996) Connections with connexins: the molecular basis of direct intracellular signaling. Eur. J. Biochem. 238, 1-27.

48. Cachope, R., Mateo, Y., Mathur, B. N., Irving, J., Wang, H. L., Morales, M., Lovinger, D. M., & Cheer, J. F. (2012). Selective activation of cholinergic interneurons enhances accumbal phasic dopamine release: setting the tone for reward processing. Cell reports, 2(1), 33–41.

49. Cai, Y., & Ford, C. P. (2018). Dopamine Cells Differentially Regulate Striatal Cholinergic Transmission across Regions through Corelease of Dopamine and Glutamate. Cell reports, 25(11), 3148–3157

50. Cardoso JM, Barbosa A, Ismail F, Pombo S. (2006) NETER alcoholic typology (NAT) Alcohol Alcohol. 41, 133–139.

51. Carpenter, R. W., Treloar Padovano, H., Emery, N. N., & Miranda, R., Jr. (2019). Rate of alcohol consumption in the daily life of adolescents and emerging adults. Psychopharmacology, 236(11), 3111–3124.

52. Cash, R., Udupa, K., Gunraj, C. A., Mazzella, F., Daskalakis, Z. J., Wong, A., Kennedy, J. L., & Chen, R. (2021). Influence of BDNF Val66Met polymorphism on excitatory-inhibitory balance and plasticity in human motor cortex. Clinical neurophysiology : official journal of the International Federation of Clinical Neurophysiology, 132(11), 2827–2839.

53. Castrén, E., & Antila, H. (2017). Neuronal plasticity and neurotrophic factors in drug responses. Molecular psychiatry, 22(8), 1085–1095.

54. Cazorla, M., Jouvenceau, A., Rose, C., Guilloux, J.-P., Pilon, C., Dranovsky, A., and Prémont, J. (2010). Cyclotraxin-B, the First Highly Potent and Selective TrkB Inhibitor, Has Anxiolytic Properties in Mice. Plos One, 5, e9777.

55. Charara, A., & Grace, A. A. (2003). Dopamine receptor subtypes selectively modulate excitatory afferents from the hippocampus and amygdala to rat nucleus accumbens neurons. Neuropsychopharmacology : official publication of the American College of Neuropsychopharmacology, 28(8), 1412–1421.

56. Chen X., Liu Z., Ma C., Ma L., Liu X. (2019). Parvalbumin interneurons determine emotional valence through modulating accumbal output pathways. Front. Behav. Neurosci. 13:110.

57. Chen, G., Cuzon Carlson, V. C., Wang, J., Beck, A., Heinz, A., Ron, D., Lovinger, D. M., & Buck, K. J. (2011). Striatal involvement in human alcoholism and alcohol consumption, and withdrawal in animal models. Alcoholism, clinical and experimental research, 35(10), 1739–1748.

58. Chen, S. Y., Lu, K. M., Ko, H. A., Huang, T. H., Hao, J. H., Yan, Y. T., Chang, S. L., Evans, S. M., & Liu, F. C. (2020). Parcellation of the striatal complex into dorsal and ventral districts. Proceedings of the National Academy of Sciences of the United States of America, 117(13), 7418–7429.

59. Cheng Y, Huang CCY, Ma T, Wei X, Wang X, Lu J, Wang J (2017). Distinct synaptic strengthening of the striatal direct and indirect pathways drives alcohol consumption. Biological psychiatry 81, 918–929.

60. Cheng Y, Wang J (2019). The use of chemogenetic approaches in alcohol use disorder research and treatment. Alcohol 74, 39–45.

61. Chetrit, J., Taupignon, A., Froux, L., Morin, S., Bouali-Benazzouz, R., Naudet, F., Kadiri, N., Gross, C. E., Bioulac, B., & Benazzouz, A. (2013). Inhibiting subthalamic D5 receptor constitutive activity alleviates abnormal electrical activity and reverses motor impairment in a rat model of Parkinson's disease. The Journal of neuroscience : the official journal of the Society for Neuroscience, 33(37), 14840–14849.

62. Chouhan, D., Uniyal, A., Gadepalli, A., Akhilesh, Tiwari, V., Agrawal, S., Roy, T. K., Shaw, S., Purohit, N., & Tiwari, V. (2020). Probing the Manipulated Neurochemical Drive in Alcohol Addiction and Novel Therapeutic Advancements. ACS chemical neuroscience, 11(9), 1210–1217.

63. Christoffel, D. J., Walsh, J. J., Hoerbelt, P., Heifets, B. D., Llorach, P., Lopez, R. C., Ramakrishnan, C., Deisseroth, K., & Malenka, R. C. (2021). Selective filtering of excitatory inputs to nucleus accumbens by dopamine and serotonin. Proceedings of the National Academy of Sciences of the United States of America, 118(24), e2106648118.

64. Chuhma N, Tanaka KF, Hen R, Rayport S. (2011). Functional connectome of the striatal medium spiny neuron. J Neurosci. 31, 1183–1192.

65. Cloninger, C. R., Bohman, M., & Sigvardsson, S. (1981). Inheritance of alcohol abuse. Cross-fostering analysis of adopted men. Archives of general psychiatry, 38(8), 861–868.

66. Cohen, R. A., Gullett, J. M., Porges, E. C., Woods, A. J., Lamb, D. G., Bryant, V. E., McAdams, M., Tashima, K., Cook, R., Bryant, K., Monnig, M., Kahler, C. W., & Monti, P. M. (2019). Heavy Alcohol Use and Age Effects on HIV-Associated Neurocognitive Function. Alcoholism, clinical and experimental research, 43(1), 147–157.

67. Collins A. L., Aitken T. J., Greenfield V. Y., Ostlund S. B., Wassum K. M. (2016). Nucleus accumbens acetylcholine receptors modulate dopamine and motivation. Neuropsychopharmacology 41 2830–2838.

68. Collins A. L., Aitken T. J., I, Huang W., Shieh C., Greenfield V. Y., Monbouquette H. G., et al. (2019). Nucleus accumbens cholinergic interneurons oppose Cue-motivated behavior. Biol. Psychiatry 86 388–396.

69. Collins, D. M., & Myers, R. D. (1987). Buspirone attenuates volitional alcohol intake in the chronically drinking monkey. Alcohol (Fayetteville, N.Y.), 4(1), 49–56.

70. Comings DE, Blum K. (2000). Reward deficiency syndrome: genetic aspects of behavioral disorders. Progress in Brain Research. 126:325–41.

71. Condorelli, D.F., Belluardo, N., Trovato-Salinaro, A., and Mudo, G. (2000) Expression of Cx36 in mammalian neurons. Brain Research Reviews. 32, 72-85.

72. Conrad, K., Tseng, K., Uejima, J., Reimers, J., Heng, L., Shaham, Y., Marinelli, M., and Wolf, M. (2008). Formation of accumbens GluR2-lacking AMPA receptors mediates incubation of cocaine craving. Nature, 454, 118-121.

73. Constandil, L., Goich, M., Hernández, A., Bourgeais, L., Cazorla, M., Hamon, M., Villanueva, L., and Pelissier, T. (2012). Cyclotraxin-B, a new TrkB antagonist, and glial blockade by propentofylline, equally prevent and reverse cold allodynia induced by BDNF or partial infraorbital nerve constriction in mice. J Pain, 13, 579–89.

74. Corbit LH, Nie H, Janak PH. (2012). Habitual alcohol seeking: time course and the contribution of subregions of the dorsal striatum. Biol Psychiatry. 72, 389–95.

75. Corbit, L. H., Nie, H., & Janak, P. H. (2012). Habitual alcohol seeking: time course and the contribution of subregions of the dorsal striatum. Biological psychiatry, 72(5), 389–395.

76. Covey, D. P., & Yocky, A. G. (2021). Endocannabinoid Modulation of Nucleus Accumbens Microcircuitry and Terminal Dopamine Release. Frontiers in synaptic neuroscience, 13, 734975.

77. Crane, N. A., Gorka, S. M., Weafer, J., Langenecker, S. A., de Wit, H., & Phan, K. L. (2017). Preliminary Evidence for Disrupted Nucleus Accumbens Reactivity and Connectivity to Reward in Binge Drinkers. Alcohol and alcoholism (Oxford, Oxfordshire), 52(6), 647–654.

78. Crews, F. T., Robinson, D. L., Chandler, L. J., Ehlers, C. L., Mulholland, P. J., Pandey, S. C., Rodd, Z. A., Spear, L. P., Swartzwelder, H. S., & Vetreno, R. P. (2019). Mechanisms of Persistent Neurobiological Changes Following Adolescent Alcohol Exposure: NADIA Consortium Findings. Alcoholism, clinical and experimental research, 43(9), 1806–1822.

79. Cui, S-z., Wang, S-j., Li, J., Xie G-q., Zhou, R., Chen, L., and Yuan, X-r. (2011) Alteration of Synaptic Plasticity in Rat Dorsal Striatum Induced by Chronic Ethanol Intake and Withdrawal via ERK Pathway. Acta. Pharmacol. Sin. 32, 175-181.

80. Cummings DM, Yamazaki I, Cepeda C, Paul DL, and Levine MS. (2008) Neuronal coupling via connexin36 contributes to spontaneous synaptic currents of striatal medium-sized spiny neurons. J Neurosci Res. 86: 2147-58.

81. Cunningham, C. L., & Noble, D. (1992). Conditioned activation induced by ethanol: role in sensitization and conditioned place preference. Pharmacology, biochemistry, and behavior, 43(1), 307–313.

82. Cunningham, C. L., Howard, M. A., Gill, S. J., Rubinstein, M., Low, M. J., & Grandy, D. K. (2000). Ethanol-conditioned place preference is reduced in dopamine D2 receptor-deficient mice. Pharmacology, biochemistry, and behavior, 67(4), 693–699.

83. Da Cunha, C., Gomez-A, A., & Blaha, C. D. (2012). The role of the basal ganglia in motivated behavior. Reviews in the neurosciences, 23(5-6), 747–767.

84. Dahchour, A., & Ward, R. J. (2022). Changes in Brain Dopamine Extracellular Concentration after Ethanol Administration; Rat Microdialysis Studies. Alcohol and alcoholism (Oxford, Oxfordshire), 57(2), 165–175.

85. Damodaran, S., Evans, R. C., & Blackwell, K. T. (2014). Synchronized firing of fast-spiking interneurons is critical to maintain balanced firing between direct and

indirect pathway neurons of the striatum. Journal of neurophysiology, 111(4), 836–848.

86. D'Amore, D. E., Tracy, B. A., & Parikh, V. (2013). Exogenous BDNF facilitates strategy set-shifting by modulating glutamate dynamics in the dorsal striatum. Neuropharmacology, 75, 312–323.

87. Darcq, E., Morisot, N., Phamluong, K., Warnault, V., Jeanblanc, J., Longo, F. M., Massa, S. M., & Ron, D. (2016). The Neurotrophic Factor Receptor p75 in the Rat Dorsolateral Striatum Drives Excessive Alcohol Drinking. The Journal of neuroscience : the official journal of the Society for Neuroscience, 36(39), 10116–10127.

88. Day JJ, Roitman MF, Wightman RM, Carelli RM. (2007). Associative learning mediates dynamic shifts in dopamine signaling in the nucleus accumbens. Nat Neurosci. 10, 1020–1028.

89. de Menezes, R. F., Bergmann, A., & Thuler, L. C. (2013). Alcohol consumption and risk of cancer: a systematic literature review. Asian Pacific journal of cancer prevention : APJCP, 14(9), 4965–4972.

90. Depasque, S., and Galvan, A. (2017) Frontostriatal development and probabilistic reinforcement learning during adolescence. Neurobiology of Learning and Memory. 143, 1-7.

91. Depoy, L., Daut, R., Brigman, J.L., MacPherson, K., Crowley, N., Gunduz-Cinar, O., Pickens, C.L., Cinar, R., Saksida, L.M., Kunos, G., Lovinger, D.M., Bussey, T.J., Camp, M.C., and Holmes, A. (2013) Chronic alcohol produes neuroadaptations to prime dorsal striatal learning. Proc Natl Acad Sci U S A. 110, 14783-8.

92. Di Chiara G. (1997). Alcohol and dopamine. Alcohol health and research world, 21(2), 108–114.

93. Diaz-Hernandez, E., Contreras-Lopez, R., Sanchez-Fuentes, A., Rodriguez-Sibrian, L., O Ramirez-Jarquin, J., and Tecuapetla, F. (2018) The Thalamostriatal Projections Contribute to the Initiation and Execution of a Sequence of Movements. Neuron. 100, 739-752.

94. Drake, R. E., Osher, F. C., & Wallach, M. A. (1991). Homelessness and dual diagnosis. The American psychologist, 46(11), 1149–1158.

95. Dubé L, Smith AD, Bolam JP. (1988). Identification of synaptic terminals of thalamic or cortical origin in contact with distinct medium size spiny neurons in the rat neostriatum. J Comp Neurol. 267:455–471.

96. Duhne, M., Lara-González, E., Laville, A., Padilla-Orozco, M., Ávila-Cascajares, F., Arias-García, M., Galarraga, E., & Bargas, J. (2021). Activation of parvalbumin-expressing neurons reconfigures neuronal ensembles in murine striatal microcircuits. The European journal of neuroscience, 53(7), 2149–2164.

97. Duka T (2017). Decision Making in Alcoholic Patients and Its Contribution to Relapse. Biological Psychiatry. 82, 779–780.

98. Duko, B., Toma, A., & Abraham, Y. (2019). Alcohol use disorder and associated factors among individuals living with HIV in Hawassa City, Ethiopia: a facility based cross- sectional study. Substance abuse treatment, prevention, and policy, 14(1), 22.

99. Dunn, W., & Shah, V. H. (2016). Pathogenesis of Alcoholic Liver Disease. Clinics in liver disease, 20(3), 445–456.

100. Dunne F. J. (1989). Alcohol and the immune system. BMJ (Clinical research ed.), 298(6673), 543–544.

101. Egervari, G., Siciliano, C. A., Whiteley, E. L., & Ron, D. (2021). Alcohol and the brain: from genes to circuits. Trends in neurosciences, 44(12), 1004–1015.

102. Ehlers, C.L., Wills, D., Karriker-Jaffe, K.J., and Gilder, D.A. (2022) Extreme Binge Drinking During Adolescence: Associations With Subsequent Substance Use Disorders in American Indian and Mexican American Young Adults. Journal of Addiction Medicine, 16(1), 33-40.

103. Eisch, AJ, Bolanos, CA, Wit, JD, Simonak, RD, Pudiak, CM, Barrot, M, et al. (2003). BDNF in the ventral midbrain-nucleus accumbens pathway: a role in depression. Bio Psychiatry, 54, 994-1005.

104. Enoch MA. (2011). The role of early life stress as a predictor for alcohol and drug dependence. Psychopharmacology. 214(1), 17–31.

105. Everitt B. J., Wolf M. E. (2002). Psychomotor stimulant addiction: a neural systems perspective. J. Neurosci. 22, 3312–3320.

106. Everitt, B. J., Dickinson, A., & Robbins, T. W. (2001). The neuropsychological basis of addictive behaviour. Brain research. Brain research reviews, 36(2-3), 129–138.

107. Exley R., Cragg S. J. (2008). Presynaptic nicotinic receptors: a dynamic and diverse cholinergic filter of striatal dopamine neurotransmission. Br. J. Pharmacol. 153 Suppl 1 S283–S297

108. Falk D. E., Yi H. Y. and Hiller-Sturmhöfel S. (2006) An epidemiologic analysis of co-occurring alcohol and tobacco use and disorders: findings from the National

Epidemiologic Survey on Alcohol and Related Conditions. Alcohol. Res. Health 29, 162–71.

109. Favier, M., Janickova, H., Justo, D., Kljakic, O., Runtz, L., Natsheh, J. Y., Pascoal, T. A., Germann, J., Gallino, D., Kang, J. I., Meng, X. Q., Antinora, C., Raulic, S., Jacobsen, J. P., Moquin, L., Vigneault, E., Gratton, A., Caron, M. G., Duriez, P., Brandon, M. P., … El Mestikawy, S. (2020). Cholinergic dysfunction in the dorsal striatum promotes habit formation and maladaptive eating. The Journal of clinical investigation, 130(12), 6616–6630.

110. Fisher, S. D., Ferguson, L. A., Bertran-Gonzalez, J., & Balleine, B. W. (2020). Amygdala-Cortical Control of Striatal Plasticity Drives the Acquisition of Goal-Directed Action. Current biology : CB, 30(22), 4541–4546.e5.

111. Flagel SB, Clark JJ, Robinson TE, Mayo L, Czuj A, Willuhn I, Akers CA, Clinton SM, Phillips PE, Akil H. (2011). A selective role for dopamine in stimulus-reward learning. Nature. 469, 53–57.

112. Flaherty AW, Graybiel AM. (1991). Corticostriatal transformations in the primate somatosensory system. Projections from physiologically mapped body-part representations. J Neurophysiol. 66, 1249–1263.

113. Ford C. P. (2014). The role of D2-autoreceptors in regulating dopamine neuron activity and transmission. Neuroscience 282 13–22.

114. Foster D. J., Gentry P. R., Lizardi-Ortiz J. E., Bridges T. M., Wood M. R., Niswender C. M., et al. (2014). M5 receptor activation produces opposing physiological outcomes in dopamine neurons depending on the receptor's location. J. Neurosci. 34 3253–3262.

115. Frank MJ. (2005). Dynamic dopamine modulation in the basal ganglia: a neurocomputational account of cognitive deficits in medicated and nonmedicated Parkinsonism. J Cogn Neurosci. 17: 51–72.

116. Friedman DP, Aggleton JP, Saunders RC. (2002). Comparison of hippocampal, amygdala, and perirhinal projections to the nucleus accumbens: combined anterograde and retrograde tracing study in the Macaque brain. J Comp Neurol. 450, 345–365.

117. Frotscher M, Rinne U, Hassler R, Wagner A. (1981). Termination of cortical afferents on identified neurons in the caudate nucleus of the cat. A combined Golgi-EM degeneration study. Exp Brain Res. 41:329–337

118. Funahashi, Y., Ariza, A., Emi, R., Xu, Y., Shan, W., Suzuki, K., Kozawa, S., Ahammad, R. U., Wu, M., Takano, T., Yura, Y., Kuroda, K., Nagai, T., Amano, M., Yamada, K., & Kaibuchi, K. (2019). Phosphorylation of Npas4 by MAPK Regulates

Reward-Related Gene Expression and Behaviors. Cell reports, 29(10), 3235–3252.e9.

119. Gagnon D., Petryszyn S., Sanchez M. G., Bories C., Beaulieu J. M., De Koninck Y., et al. (2017). Striatal neurons expressing D1 and D2 receptors are morphologically distinct and differently affected by dopamine denervation in mice. Sci. Rep. 7:41432.

120. Galarreta, M. and Hestrin. S. (1999) A network of fast-spiking cells in the neocortex connected by electrical synapses. Nature 402, 72-75.

121. Galvin, C., Lee, F. S., & Ninan, I. (2015). Alteration of the Centromedial Amygdala Glutamatergic Synapses by the BDNF Val66Met Polymorphism. Neuropsychopharmacology : official publication of the American College of Neuropsychopharmacology, 40(9), 2269–2277.

122. Gao, B., & Bataller, R. (2011). Alcoholic liver disease: pathogenesis and new therapeutic targets. Gastroenterology, 141(5), 1572–1585.

123. García-Marchena, N., Marcos, A., Flores-López, M., Moreno-Fernández, M., Requena-Ocaña, N., Porras-Perales, O., Torres-Galván, S., Araos, P., Serrano, A., Muga, R., Ruiz-Ruiz, J. J., Rodríguez de Fonseca, F., Ambrosio, E., & Pavón-Morón, F. J. (2022). Plasma Amino Acid Concentrations in Patients with Alcohol and/or Cocaine Use Disorders and Their Association with Psychiatric Comorbidity and Sex. Biomedicines, 10(5), 1137.

124. Geoffroy, P. A., Lejoyeux, M., & Rolland, B. (2020). Management of insomnia in alcohol use disorder. Expert opinion on pharmacotherapy, 21(3), 297–306.

125. Gerfen CR, Surmeier DJ. (2011). Modulation of striatal projection systems by dopamine. Annu Rev Neurosci. 34, 441–66.

126. Gerfen CR, Wilson CJ. (1996). The Basal Ganglia. In: Hokfelt T, Swanson LW, editors. Handbook of Chemical Neuroanatomy. Elsevier; pp. 365–462.

127. Gerfen CR. (1989). The neostriatal mosaic: striatal patch-matrix organization is related to cortical lamination. Science. 246, 385–388.

128. Gerfen CR. (1992). The neostriatal mosaic: multiple levels of compartmental organization in the basal ganglia. Annu Rev Neurosci. 15, 285-320.

129. Gertler TS, Chan CS, Surmeier DJ. (2008). Dichotomous anatomical properties of adult striatal medium spiny neurons. J Neurosci. 28, 10814–10824.

130. Ghasemzadeh M. B., Kalivas P. W. (1998). Expression of D1 receptor, D2 receptor, substance P and enkephalin messenger RNAs in the neurons projecting from the nucleus accumbens. Neuroscience 82 767–780.

131. Gittis AH, Nelson AB, Thwin MT, Palop JJ, Kreitzer AC. (2010). Distinct roles of GABAergic interneurons in the regulation of striatal output pathways. J Neurosci. 30, 2223–34.

132. Golden, SA, Covington III, HE, Berton, O., Russo, SJ. (2011). A standardized protocol for repeated social defeat stress in mice. Nature Protocols, 6, 1183-1191.

133. Goldstein, B.I., Diamantouros, A., Schaffer, A., & Naranjo, C.A. (2006) Pharmacotherapy of alcoholism in patients with co-morbid psychiatric disorders. Drugs, 66(9), 1229-1237.

134. Gonzales K. K., Smith Y. (2015). Cholinergic interneurons in the dorsal and ventral striatum: anatomical and functional considerations in normal and diseased conditions. Ann. N. Y. Acad. Sci. 1349 1–45.

135. Graham DL, Edwards S, Bachtell RK, DiLeone RJ, Rios M, Self DW. (2007). Dynamic BDNF activity in nucleus accumbens with cocaine use increases self-administration and relapse. Nat Neurosci. 10:1029–1037.

136. Graham DL, Krishnan V, Larson EB, Graham A, Edwards S, Bachtell RK, Simmons D, Gent LM, Berton O, Bolanos CA, DiLeone RJ, Parada LF, Nestler EJ, Self DW. Tropomyosin-related kinase B in the mesolimbic dopamine system: region-specific effects on cocaine reward. Biol Psychiatry. 2009 Apr 15;65(8):696-701.

137. Grant B. F., Goldstein R. B., Saha T. D. et al. (2015) Epidemiology of DSM-5 alcohol use disorder: results from the national epidemiologic survey on alcohol and related conditions III. JAMA Psychiatry 72, 757–66.

138. Graybiel A. M. (2005). The basal ganglia: learning new tricks and loving it. Current opinion in neurobiology, 15(6), 638–644.

139. Graybiel A. M. (2008). Habits, rituals, and the evaluative brain. Annual review of neuroscience, 31, 359–387.

140. Gremel, C. M., & Costa, R. M. (2013). Orbitofrontal and striatal circuits dynamically encode the shift between goal-directed and habitual actions. Nature communications, 4, 2264.

141. Griffin, W. C., 3rd, Haun, H. L., Hazelbaker, C. L., Ramachandra, V. S., & Becker, H. C. (2014). Increased extracellular glutamate in the nucleus accumbens promotes excessive ethanol drinking in ethanol dependent mice. Neuropsychopharmacology

: official publication of the American College of Neuropsychopharmacology, 39(3), 707–717.

142. Grimm JW, Lu L, Hayashi T, Hope BT, Su TP, Shaham Y. (2003). Time-dependent increases in brain-derived neurotrophic factor protein levels within the mesolimbic dopamine system after withdrawal from cocaine: implications for incubation of cocaine craving. J Neurosci. 23:742–747.

143. Gritton, H. J., Howe, W. M., Romano, M. F., DiFeliceantonio, A. G., Kramer, M. A., Saligrama, V., Bucklin, M. E., Zemel, D., & Han, X. (2019). Unique contributions of parvalbumin and cholinergic interneurons in organizing striatal networks during movement. Nature neuroscience, 22(4), 586–597.

144. Groenewegen H. J., Wright C. I., Beijer A. V., Voorn P. (1999). Convergence and segregation of ventral striatal inputs and outputs. Ann. N. Y. Acad. Sci. 877, 49–63.

145. Grospe, G. M., Baker, P. M., & Ragozzino, M. E. (2018). Cognitive Flexibility Deficits Following 6-OHDA Lesions of the Rat Dorsomedial Striatum. Neuroscience, 374, 80–90.

146. Grueter B. A., Rothwell P. E., Malenka R. C. (2012). Integrating synaptic plasticity and striatal circuit function in addiction. Curr. Opin. Neurobiol. 22, 545–551.

147. Gump JM, Dowdy SF. (2007). TAT transduction: the molecular mechanism and therapeutic prospects. Trends Mol Med. 13, 443–448.

148. Gunnar, R. M., Sutton, G. C., Pietras, R. J., & Tobin, J. R., Jr (1971). Alcoholic cardiomyopathy. Disease-a-month : DM, 1–30.

149. Guo Q., Wang D., He X., Feng Q., Lin R., Xu F., et al. (2015). Whole-brain mapping of inputs to projection neurons and cholinergic interneurons in the dorsal striatum. PLoS One 10:e0123381.

150. Haber S. N. (2016). Corticostriatal circuitry. Dialogues in clinical neuroscience, 18(1), 7–21.

151. Haber SN, Fudge JL, and McFarland NR (2000). Striatonigrostriatal pathways in primates form an ascending spiral from the shell to the dorsolateral striatum. J Neurosci 20, 2369–2382.

152. Hallett PJ, Spoelgen R, Hyman BT, Standaert DG, Dunah AW. (2006). Dopamine D1 activation potentiates striatal NMDA receptors by tyrosine phosphorylation-dependent subunit trafficking. J Neurosci. 26, 4690–4700.

153. Han, J., Keedy, S., Murray, C. H., Foxley, S., & de Wit, H. (2021). Acute effects of alcohol on resting-state functional connectivity in healthy young men. Addictive behaviors, 115, 106786.

154. Hao, R., Qi, Y., Hou, D. N., Ji, Y. Y., Zheng, C. Y., Li, C. Y., Yung, W. H., Lu, B., & Huang, Y. (2017). BDNF val66met Polymorphism Impairs Hippocampal Long-Term Depression by Down-Regulation of 5-HT3 Receptors. Frontiers in cellular neuroscience, 11, 306.

155. Hasbi, A., Fan, T., Alijaniaram, M., Nguyen, T., Perreault, M. L., O'Dowd, B. F., & George, S. R. (2009). Calcium signaling cascade links dopamine D1-D2 receptor heteromer to striatal BDNF production and neuronal growth. Proceedings of the National Academy of Sciences of the United States of America, 106(50), 21377–21382.

156. Haun, H. L., Griffin, W. C., Lopez, M. F., Solomon, M. G., Mulholland, P. J., Woodward, J. J., McGinty, J. F., Ron, D., & Becker, H. C. (2018). Increasing Brain-Derived Neurotrophic Factor (BDNF) in medial prefrontal cortex selectively reduces excessive drinking in ethanol dependent mice. Neuropharmacology, 140, 35–42.

157. Hedreen JC, Holm GC. (1981). Retrograde and anterograde axonal transport demonstrated by intracerebral injection of a labeled protein-acylating agent. Brain Res Bull. 7, 665–670.

158. Heilbronner SR, Rodriguez-Romaguera J, Quirk GJ, Groenewegen HJ, and Haber SN (2016). Circuit-Based Corticostriatal Homologies Between Rat and Primate. Biol Psychiatry 80, 509–521.

159. Helle, A. C., Trull, T. J., Watts, A. L., McDowell, Y., & Sher, K. J. (2020). Psychiatric Comorbidity as a Function of Severity: DSM-5 Alcohol Use Disorder and HiTOP Classification of Mental Disorders. Alcoholism, clinical and experimental research, 44(3), 632–644.

160. Hikida T, Kimura K, Wada N, Funabiki K, Nakanishi S. (2010). Distinct roles of synaptic transmission in direct and indirect striatal pathways to reward and aversivebehavior. Neuron. 66, 896–907.

161. Hikida, T., Yawata, S., Yamaguchi, T., Danjo, T., Sasaoka, T., Wang, Y., & Nakanishi, S. (2013). Pathway-specific modulation of nucleus accumbens in reward and aversive behavior via selective transmitter receptors. Proceedings of the National Academy of Sciences of the United States of America, 110(1), 342–347.

162. Hjorth, J., Blackwell, K. T., and Kotaleski, J. H. (2009) Gap junctions between striatal fast-spiking interneurons regulate spiking activity and synchronization as a function of cortical activity. J. Neurosci. 29, 5276–86.

163. Hoerbelt, P., Lindsley, T. A., & Fleck, M. W. (2015). Dopamine directly modulates GABAA receptors. The Journal of neuroscience : the official journal of the Society for Neuroscience, 35(8), 3525–3536.

164. Hoffer ZS, Alloway KD. (2001). Organization of the corticostriatal projections from the vibrissal representations in the primary motor and somatosensory cortical areas of rodents. J Comp Neurol. 439, 87–103.

165. Holly, E. N., Davatolhagh, M. F., España, R. A., & Fuccillo, M. V. (2021). Striatal low-threshold spiking interneurons locally gate dopamine. Current biology : CB, 31(18), 4139–4147

166. Hopf F.W., Chang S.J., Sparta, D.R., Bowers, S.M., and Bonci, A. (2010) Motivation for alcohol becomes resistant to quinine adulteration after 3 - 4 months of intermittent alcohol self-administration. Alcohol Clin. Exp. Res. 34, 1565-1573.

167. Hormuzdi, S.G., Pais, I., LeBeau, F.E., Towers, S.K., Rozov, A., Buhl, E.H., Whittington, M.A., Monyer, H. (2001) Impaired electrical signaling disrupts gamma frequency oscillations in connexin 36-deficient mice. Neuron 31, 487-95.

168. Huang, Y., Lin, Y., Mu, P., Lee, B., Brown, T., Wayman, G., Marie, H., Liu, W., Yan, Z., Sorg, B., et al. (2009). In Vivo Cocaine Experience Generates Silent Synapses. Neuron, 63, 40–47.

169. Hughes, J. C., & Cook, C. C. (1997). The efficacy of disulfiram: a review of outcome studies. Addiction (Abingdon, England), 92(4), 381–395.

170. Hunnicutt, B. J., Jongbloets, B. C., Birdsong, W. T., Gertz, K. J., Zhong, H., & Mao, T. (2016). A comprehensive excitatory input map of the striatum reveals novel functional organization. eLife, 5, e19103.

171. Jeanblanc J, He DY, McGough NN, Logrip ML, Phamluong K, Janak PH, Ron D. (2006). The dopamine D3 receptor is part of a homeostatic pathway regulating ethanol consumption. J Neurosci. 26, 1457–1464.

172. Jeanblanc, J., Logrip, M. L., Janak, P. H., & Ron, D. (2013). BDNF-mediated regulation of ethanol consumption requires the activation of the MAP kinase pathway and protein synthesis. The European journal of neuroscience, 37(4), 607–612.

173. Jin, X., & Costa, R. M. (2010). Start/stop signals emerge in nigrostriatal circuits during sequence learning. Nature, 466(7305), 457–462.

174. Jing, D., Lee, F. S., & Ninan, I. (2017). The BDNF Val66Met polymorphism enhances glutamatergic transmission but diminishes activity-dependent synaptic plasticity in the dorsolateral striatum. Neuropharmacology, 112(Pt A), 84–93.

175. Joe, K. H., Kim, Y. K., Kim, T. S., Roh, S. W., Choi, S. W., Kim, Y. B., Lee, H. J., & Kim, D. J. (2007). Decreased plasma brain-derived neurotrophic factor levels in patients with alcohol dependence. Alcoholism, clinical and experimental research, 31(11), 1833–1838.

176. Joffe, M., Vitter, S., and Grueter, B. (2017). GluN1 deletions in D1- and A2A-expressing cell types reveal distinct modes of behavioral regulation. Neuropharmacology, 112, 172–180.

177. Julian M. D., Martin A. B., Cuellar B., Rodriguez De Fonseca F., Navarro M., Moratalla R., et al. (2003). Neuroanatomical relationship between type 1 cannabinoid receptors and dopaminergic systems in the rat basal ganglia. Neuroscience 119 309–318.

178. Jünger, E., Javadi, A. H., Wiers, C. E., Sommer, C., Garbusow, M., Bernhardt, N., Kuitunen-Paul, S., Smolka, M. N., & Zimmermann, U. S. (2017). Acute alcohol effects on explicit and implicit motivation to drink alcohol in socially drinking adolescents. Journal of psychopharmacology (Oxford, England), 31(7), 893–905.

179. Kalivas, P. W., & Volkow, N. D. (2005). The neural basis of addiction: a pathology of motivation and choice. The American journal of psychiatry, 162(8), 1403–1413.

180. Kapasova, Z., & Szumlinski, K. K. (2008). Strain differences in alcohol-induced neurochemical plasticity: a role for accumbens glutamate in alcohol intake. Alcoholism, clinical and experimental research, 32(4), 617–631.

181. Kawaguchi Y. (1993). Physiological, morphological, and histochemical characterization of three classes of interneurons in the rat neostriatum. J Neurosci. 13, 4908–23.

182. Kelley, AE. (2004). Ventral striatal control of appetitive motivation: role in ingestive behavior and reward-related learning. Neurosci Biobehav Rev. 8, 765-76.

183. Kelly, J. F., & Yeterian, J. D. (2011). The role of mutual-help groups in extending the framework of treatment. Alcohol research & health : the journal of the National Institute on Alcohol Abuse and Alcoholism, 33(4), 350–355.

184. Kelm MK, Criswell HE, Breese GR. (2011). Ethanol-enhanced GABA release: a focus on G protein-coupled receptors. Brain Res Rev. 65, 113–123.

185. Kemp JM, Powell TPS. (1971b). The termination of fibres from the cerebral cortex and thalamus upon dendritic spines in the caudate nucleus: a study with the Golgi method. Philos Trans R Soc Lond B Biol Sci. 262:429–439.

186. Kheirbek MA, Britt JP, Beeler JA, Ishikawa Y, McGehee DS, Zhuang X. (2009). Adenylyl cyclase type 5 contributes to corticostriatal plasticity and striatum-dependent learning. J Neurosci. 29, 12115–12124.

187. Kim, A. C., Epstein, M. E., Gautam-Goyal, P., & Doan, T. L. (2012). Infections in alcoholic liver disease. Clinics in liver disease, 16(4), 783–803.

188. Kim, N., Li, H.E., Hughes, R.N., Watson, G.D.R., Gallegos, D., West, A.E., Kim, I.H., and Yin, H.H. (2019) A striatal interneuron circuit for continuous target pursuit. Nat. Commun. 10.

189. Kimbrough, A., Kim, S., Cole, M., Brennan, M., & George, O. (2017). Intermittent Access to Ethanol Drinking Facilitates the Transition to Excessive Drinking After Chronic Intermittent Ethanol Vapor Exposure. Alcoholism, clinical and experimental research, 41(8), 1502–1509.

190. King, A. C., de Wit, H., McNamara, P. J., & Cao, D. (2011). Rewarding, stimulant, and sedative alcohol responses and relationship to future binge drinking. Archives of general psychiatry, 68(4), 389–399.

191. King, A. C., Hasin, D., O'Connor, S. J., McNamara, P. J., & Cao, D. (2016). A Prospective 5-Year Re-examination of Alcohol Response in Heavy Drinkers Progressing in Alcohol Use Disorder. Biological psychiatry, 79(6), 489–498.

192. King, A. C., McNamara, P. J., Hasin, D. S., & Cao, D. (2014). Alcohol challenge responses predict future alcohol use disorder symptoms: a 6-year prospective study. Biological psychiatry, 75(10), 798–806.

193. King, A. C., Vena, A., Howe, M. M., Feather, A., & Cao, D. (2022). Haven't lost the positive feeling: a dose-response, oral alcohol challenge study in drinkers with alcohol use disorder. Neuropsychopharmacology : official publication of the American College of Neuropsychopharmacology, 47(11), 1892–1900.

194. King, A., Vena, A., Hasin, D. S., deWit, H., O'Connor, S. J., & Cao, D. (2021). Subjective Responses to Alcohol in the Development and Maintenance of Alcohol Use Disorder. The American journal of psychiatry, 178(6), 560–571.

195. Kircher, D. M., Aziz, H. C., Mangieri, R. A., & Morrisett, R. A. (2019). Ethanol Experience Enhances Glutamatergic Ventral Hippocampal Inputs to D1 Receptor-Expressing Medium Spiny Neurons in the Nucleus Accumbens Shell. The Journal of neuroscience : the official journal of the Society for Neuroscience, 39(13), 2459–2469.

196. Kita H, Kosaka T, and Heizmann CW (1990). Parvalbumin-immunoreactive neurons in the rat neostriatum: a light and electron microscopic study. Brain Res. 536, 1–15.

197. Klaus, A., Alves da Silva, J., and Costa, R.M. (2019) What, If, and When to Move: Basal Ganglia Circuits and Self-Paced Action Initiation. Annu. Rev. Neurosci. 42, 459-483.

198. Klawonn A. M., Malenka R. C. (2018). Nucleus accumbens modulation in reward and aversion. Cold Spring Harb. Symp. Quant. Biol. 83 119–129.

199. Klug, J.R., Engelhardt, M.D., Cadman, C.N., Li, H., Smith J.B., Ayala, S., Williams, E.W., Hoffman, H., and Jin, X. (2018) Differential inputs to striatal cholinergic and parvalbumin interneurons imply functional distinctions. eLife, 7, e35657.

200. Kolpakova, J., van der Vinne, V., Giménez-Gómez, P., Le, T., You, I. J., Zhao-Shea, R., Velazquez-Marrero, C., Tapper, A. R., & Martin, G. E. (2021). Binge Alcohol Drinking Alters Synaptic Processing of Executive and Emotional Information in Core Nucleus Accumbens Medium Spiny Neurons. Frontiers in cellular neuroscience, 15, 742207.

201. Koo, J. W., Lobo, M. K., Chaudhury, D., Labonté, B., Friedman, A., Heller, E., Peña, C. J., Han, M. H., & Nestler, E. J. (2014). Loss of BDNF signaling in D1R-expressing NAc neurons enhances morphine reward by reducing GABA inhibition. Neuropsychopharmacology : official publication of the American College of Neuropsychopharmacology, 39(11), 2646–2653.

202. Koo, J. W., Mazei-Robison, M. S., Chaudhury, D., Juarez, B., LaPlant, Q., Ferguson, D., Feng, J., Sun, H., Scobie, K. N., Damez-Werno, D., Crumiller, M., Ohnishi, Y. N., Ohnishi, Y. H., Mouzon, E., Dietz, D. M., Lobo, M. K., Neve, R. L., Russo, S. J., Han, M. H., & Nestler, E. J. (2012). BDNF is a negative modulator of morphine action. Science (New York, N.Y.), 338(6103), 124–128.

203. Koo, J., Labonté, B., Engmann, O., Calipari, E., Juarez, B., Lorsch, Z., Walsh, J., Friedman, A., Yorgason, J., Han, M.-H., et al. (2016). Essential Role of Mesolimbic Brain-Derived Neurotrophic Factor in Chronic Social Stress–Induced Depressive Behaviors. Biol Psychiat 80, 469–478.

204. Koob GF, Le Moal M. (2008) Addiciton and the brain antireward system. Annual Review of Psychology. 59, 29-53.

205. Koob, G.F. (2013). Addiction is a Reward Deficit and Stress Surfeit Disorder. Frontiers in psychiatry, 4,72.

206. Koós, T. and Tepper, J. M. (1999) Inhibitory control of neostriatal projection neurons by GABAergic interneurons. Nat. Neurosci. 2, 467–72.

207. Kotyuk, E., Magi, A., Eisinger, A., Király, O., Vereczkei, A., Barta, C., Griffiths, M. D., Székely, A., Kökönyei, G., Farkas, J., Kun, B., Badgaiyan, R. D., Urbán, R., Blum, K., & Demetrovics, Z. (2020). Co-occurrences of substance use and other potentially addictive behaviors: Epidemiological results from the Psychological and Genetic Factors of the Addictive Behaviors (PGA) Study. Journal of behavioral addictions, 9(2), 272–288.

208. Kourkoumpetis, T., & Sood, G. (2019). Pathogenesis of Alcoholic Liver Disease: An Update. Clinics in liver disease, 23(1), 71–80.

209. Kovács, I., Gál, B. I., Horváth, Z., Demeter, I., Rózsa, S., Janka, Z., Urbán, R., Demetrovics, Z., & Andó, B. (2022). Externalizing personality characteristics define clinically relevant subgroups of alcohol use disorder. PloS one, 17(3), e0265577.

210. Kranzler, H. R., Burleson, J. A., Del Boca, F. K., Babor, T. F., Korner, P., Brown, J., & Bohn, M. J. (1994). Buspirone treatment of anxious alcoholics. A placebo-controlled trial. Archives of general psychiatry, 51(9), 720–731.

211. Kravitz AV, Freeze BS, Parker PR, Kay K, Thwin MT, Deisseroth K, et al. (2010). Regulation of parkinsonian motor behaviours by optogenetic control of basal ganglia circuitry. Nature. 466, 622–626.

212. Krishnan V, Han MH, Graham DL, Berton O, Renthal W, Russo SJ, Laplant Q, Graham A, Lutter M, Lagace DC, Ghose S, Reister R, Tannous P, Green TA, Neve RL, Chakravarty S, Kumar A, Eisch AJ, Self DW, Lee FS, et al. (2007). Molecular adaptations underlying susceptibility and resistance to social defeat in brain reward regions. Cell. 131:391–404.

213. Kupchik, Y. M., & Kalivas, P. W. (2017). The Direct and Indirect Pathways of the Nucleus Accumbens are not What You Think. Neuropsychopharmacology : official publication of the American College of Neuropsychopharmacology, 42(1), 369–370.

214. Kalivas, P. W. (2015). Coding the direct/indirect pathways by D1 and D2 receptors is not valid for accumbens projections. Nature neuroscience, 18(9), 1230–1232.

215. Kupchik, Y. M., Brown, R. M., Heinsbroek, J. A., Lobo, M. K., Schwartz, D. J., & Kalivas, P. W. (2015). Coding the direct/indirect pathways by D1 and D2 receptors is not valid for accumbens projections. Nature neuroscience, 18(9), 1230–1232.

216. Kupferschmidt, D. A., Cody, P. A., Lovinger, D. M., & Davis, M. I. (2015). Brain BLAQ: Post-hoc thick-section histochemistry for localizing optogenetic constructs in neurons and their distal terminals. Frontiers in neuroanatomy, 9, 6.

217. Lapper SR, Smith Y, Sadikot AF, Parent A, Bolam JP. (1992) Cortical input to parvalbumin-immunoreactive neurones in the putamen of the squirrel monkey. Brain Res. 580, 215–224.

218. Lau T, Gage GJ, Berke JD, and Zochowski M (2010) Local dynamics of gap-junction-coupled interneuron networks. Phys Biol 7, 16015.

219. LeBeau, F. E., Traub, R. D., Monyer, H., Whittington, M. A., & Buhl, E. H. (2003) The role of electrical signaling via gap junctions in the generation of fast network oscillations. Brain research bulletin, 62, 3–13.

220. Lee F. J., Pei L., Moszczynska A., Vukusic B., Fletcher P. J., Liu F. (2007). Dopamine transporter cell surface localization facilitated by a direct interaction with the dopamine D2 receptor. EMBO J. 26 2127–2136

221. Lee, K., Holley, S.M., Shobe, J.L., Chong, N.C., Cepeda, C., Levine, M.S., Masmanidis, S.C. (2017) Parvalbumin Interneurons Modulate Striatal Output and Enhance Performance during Associative Learning. Neuron, 93, 1451-63.

222. Leggio, G. M., Camillieri, G., Platania, C. B., Castorina, A., Marrazzo, G., Torrisi, S. A., Nona, C. N., D'Agata, V., Nobrega, J., Stark, H., Bucolo, C., Le Foll, B., Drago, F., & Salomone, S. (2014). Dopamine D3 receptor is necessary for ethanol consumption: an approach with buspirone. Neuropsychopharmacology: official publication of the American College of Neuropsychopharmacology, 39(8), 2017–2028.

223. Leggio, G. M., Di Marco, R., Gulisano, W., D'Ascenzo, M., Torrisi, S. A., Geraci, F., Lavanco, G., Dahl, K., Giurdanella, G., Castorina, A., Aitta-Aho, T., Aceto, G., Bucolo, C., Puzzo, D., Grassi, C., Korpi, E. R., Drago, F., & Salomone, S. (2019). Dopaminergic-GABAergic interplay and alcohol binge drinking. Pharmacological research, 141, 384–391.

224. Leggio, G. M., Torrisi, S. A., Castorina, A., Platania, C. B., Impellizzeri, A. A., Fidilio, A., Caraci, F., Bucolo, C., Drago, F., & Salomone, S. (2015). Dopamine D3 receptor-dependent changes in alpha6 GABAA subunit expression in striatum modulate anxiety-like behaviour: Responsiveness and tolerance to diazepam. European neuropsychopharmacology : the journal of the European College of Neuropsychopharmacology, 25(9), 1427–1436.

225. Lerner TN, Shilyansky C, Davidson TJ, Evans KE, Beier KT, Zalocusky KA, Crow AK, Malenka RC, Luo L, Tomer R, et al. (2015). Intact-Brain Analyses Reveal Distinct Information Carried by SNc Dopamine Subcircuits. Cell 162, 635–647.

226. Lesscher H.M., van Kerkhof L.W., and Vanderschuren J.M. (2010) Inflexible and indifferent alcohol drinking in male mice. Alcohol. Clin. Exp. Res. 34, 1219-25.

227. Levchuk, L. A., Meeder, E. M. G., Roschina, O. V., Loonen, A. J. M., Boiko, A. S., Michalitskaya, E. V., Epimakhova, E. V., Losenkov, I. S., Simutkin, G. G., Bokhan, N. A., Schellekens, A. F. A., & Ivanova, S. A. (2020). Exploring Brain Derived Neurotrophic Factor and Cell Adhesion Molecules as Biomarkers for the Transdiagnostic Symptom Anhedonia in Alcohol Use Disorder and Comorbid Depression. Frontiers in psychiatry, 11, 296.

228. Li Z., Chen Z., Fan G., Li A., Yuan J., Xu T. (2018). Cell-type-specific afferent innervation of the nucleus accumbens core and shell. Front. Neuroanat. 12:84.

229. Li, X., Peng, X. Q., Jordan, C. J., Li, J., Bi, G. H., He, Y., Yang, H. J., Zhang, H. Y., Gardner, E. L., & Xi, Z. X. (2018). mGluR5 antagonism inhibits cocaine reinforcement and relapse by elevation of extracellular glutamate in the nucleus accumbens via a CB1 receptor mechanism. Scientific reports, 8(1), 3686.

230. Lipton DM, Gonzales BJ, Citri A. (2019). Dorsal Striatal Circuits for Habits, Compulsions and Addictions. Front Syst Neurosci. 13, 28.

231. Lobo, M. K., Covington, H. E., 3rd, Chaudhury, D., Friedman, A. K., Sun, H., Damez-Werno, D., Dietz, D. M., Zaman, S., Koo, J. W., Kennedy, P. J., Mouzon, E., Mogri, M., Neve, R. L., Deisseroth, K., Han, M. H., & Nestler, E. J. (2010). Cell type-specific loss of BDNF signaling mimics optogenetic control of cocaine reward. Science (New York, N.Y.), 330(6002), 385–390.

232. Lobo, M., Covington, H., Chaudhury, D., Friedman, A., Sun, H., Damez-Werno, D., Dietz, D., Zaman, S., Koo, J., Kennedy, P., et al. (2010). Cell Type–Specific Loss of BDNF Signaling Mimics Optogenetic Control of Cocaine Reward. Science, 330, 385–390.

233. Löf, E., Ericson, M., Stomberg, R., & Söderpalm, B. (2007). Characterization of ethanol-induced dopamine elevation in the rat nucleus accumbens. European journal of pharmacology, 555(2-3), 148–155.

234. Logrip, M. L., Barak, S., Warnault, V., & Ron, D. (2015). Corticostriatal BDNF and alcohol addiction. Brain research, 1628(Pt A), 60–67.

235. Logrip ML, Janak PH, Ron D. (2006). Dynorphin is a downstream effector of striatal BDNF regulation of ethanol intake. Faseb J. 2008;22, :2393–2404.

236. Logrip, M. L., Janak, P. H., & Ron, D. (2008). Dynorphin is a downstream effector of striatal BDNF regulation of ethanol intake. FASEB journal : official publication of the Federation of American Societies for Experimental Biology, 22(7), 2393–2404

237. Logrip, M. L., Janak, P. H., & Ron, D. (2009). Escalating ethanol intake is associated with altered corticostriatal BDNF expression. Journal of neurochemistry, 109(5), 1459–1468.

238. Lovinger D. M. (1997). Serotonin's role in alcohol's effects on the brain. Alcohol health and research world, 21(2), 114–120.

239. Lovinger D. M. (2008). Communication networks in the brain: neurons, receptors, neurotransmitters, and alcohol. Alcohol research & health : the journal of the National Institute on Alcohol Abuse and Alcoholism, 31(3), 196–214.

240. Lovinger DM (2010). Neurotransmitter Roles in Synaptic Modulation, Plasticity and Learning in the Dorsal Striatum. Neuropharmacology 58, 951–961.

241. Lovinger, D. M., & Abrahao, K. P. (2018). Synaptic plasticity mechanisms common to learning and alcohol use disorder. Learning & memory (Cold Spring Harbor, N.Y.), 25(9), 425–434.

242. Lovinger, D. M., & Alvarez, V. A. (2017). Alcohol and basal ganglia circuitry: Animal models. Neuropharmacology, 122, 46–55.

243. Lovinger, D. M., & Roberto, M. (2013). Synaptic effects induced by alcohol. Current topics in behavioral neurosciences, 13, 31–86.

244. Lovinger DM, Roberto M. (2013). Synaptic effects induced by alcohol. Curr Top Behav Neurosci., 13, 31–86.

245. Lu X. Y., Lu, J., Cheng, Y., Wang, X., Woodson, K., Kemper, C., Disney, E., & Wang, J. (2019). Alcohol intake enhances glutamatergic transmission from D2 receptor-expressing afferents onto D1 receptor-expressing medium spiny neurons in the dorsomedial striatum. Neuropsychopharmacology : official publication of the American College of Neuropsychopharmacology, 44(6), 1123–1131.

246. Luikart BW, Nef S, Shipman T, Parada LF. (2003). In vivo role of truncated trkb receptors during sensory ganglion neurogenesis. Neuroscience, 117, 847–58.

247. Luk KC, Sadikot AF. (2001). GABA promotes survival but not proliferation of parvalbumin-immunoreactive interneurons in rodent neostriatum: an in vivo study with stereology. Neuroscience. 104, 93–103.

248. Lüscher, C., and Malenka, R.C. (2011). Drug-Evoked Synaptic Plasticity in Addiction: From Molecular Changes to Circuit Remodeling. Neuron, 69, 650–663.

249. Ma, T., Barbee, B., Wang, X., & Wang, J. (2017). Alcohol induces input-specific aberrant synaptic plasticity in the rat dorsomedial striatum. Neuropharmacology, 123, 46–54.

250. Ma, T., Cheng, Y., Hellard, E.R., Wang, X., Lu, J., Gao, X., Huang, C.C.Y., Wei, X-Y., Ji, J-Y., and Wang, J. (2018) Bidirection and long-lasting control of alcohol-seeking behavior by corticostriatal LTP and LTD. Nat. Neurosci. 21, 373-383.

251. MacAskill A. F., Little J. P., Cassel J. M., Carter A. G. (2012). Subcellular connectivity underlies pathway-specific signaling in the nucleus accumbens. Nat. Neurosci. 15 1624–1626.

252. Madisen, L. et al. (2010) A robust and high-throughput Cre reporting and characterization system for the whole mouse brain. Nat. Neurosci. 13, 133–40.

253. Magazanik LG, Buldakova SL, Samoilova MV, Gmiro VE, Mellor IR, Usherwood PN (1997) Block of open channels of recombinant AMPA receptors and native AMPA/ ainite receptors by adamantane derivatives. J Physiol 505:655–663.

254. Maisto, S. A., Aldalur, A., Abar, B., Stecker, T., Chiang, A., & Conner, K. (2022). Heterogeneity in Alcohol-Related Severity and Interests in Going to Treatment in Community Adults with Alcohol Use Disorder (AUD). Substance use & misuse, 57(10), 1626–1632.

255. Malach R, Graybiel AM. (1986). Mosaic architecture of the somatic sensory-recipient sector of the cat's striatum. J Neurosci. 6, 3436–3458.

256. Malec, E., Malec, T., Gagné, M. A., & Dongier, M. (1996). Buspirone in the treatment of alcohol dependence: a placebo-controlled trial. Alcoholism, clinical and experimental research, 20(2), 307–312.

257. Malec, T. S., Malec, E. A., & Dongier, M. (1996). Efficacy of buspirone in alcohol dependence: a review. Alcoholism, clinical and experimental research, 20(5), 853–858.

258. Mallet, N., Le Moine, C., Charpier, S., and Gonon, F. (2005) Feedforward inhibition of projection neurons by fast-spiking GABA interneurons in the rat striatum in vivo. J. Neurosci. 25, 3857–69.

259. Mallet, N., Micklem, B.R., Henny, P., Brown, M.T., Williams, C., Bolam, J.P., Nakamura, K.C., and Magill, P.J. (2012) Dichotomous organization of the external globus pallidus. Neuron. 74, 1075-86.

260. Mann-Metzer, P. and Yarom, Y. (1999) Electrotonic coupling interacts with intrinsic properties to generate synchronized activity in cerebellar networks of inhibitory interneurons. J. Neurosci. 19, 3298-3306.

261. Marino, M., Misuri, L., & Brogioli, D. (2014). A new open source software for the calculation of the liquid junction potential between two solutions according to the stationary Nernst-Planck equation. arXiv: Chemical Physics.

262. Martin, M., Chen, B., Hopf, W., Bowers, S., and Bonci, A. (2006). Cocaine self-administration selectively abolishes LTD in the core of the nucleus accumbens. Nat Neurosci, 9, nn1713.

263. Martinez-Castillo, M., Altamirano-Mendoza, I., Sánchez-Valle, S., García-Islas, L., Sánchez-Barragán, M., Hernández-Santillán, M., Hernández-Barragán, A., Pérez-Hernández, J. L., Higuera-de la Tijera, F., & Gutierrez-Reyes, G. (2023). Immune dysregulation and pathophysiology of alcohol consumption and alcoholic liver disease. Revista de gastroenterologia de Mexico (English), S2255-534X(23)00026-9. Advance online publication.

264. Martiros, N., Burgess, A. A., & Graybiel, A. M. (2018). Inversely Active Striatal Projection Neurons and Interneurons Selectively Delimit Useful Behavioral Sequences. Current biology : CB, 28(4), 560–573.e5.

265. Martos YV, Braz BY, Beccaria JP, Murer MG, Belforte JE. (2017). Compulsive social behavior emerges after selective ablation of striatal cholinergic interneurons. J Neurosci. 37(11), 2849–2858.

266. Matamales M, Bertran-Gonzalez J, Salomon L, Degos B, Deniau JM, Valjent E, et al. (2009). Striatal medium-sized spiny neurons: identification by nuclear staining and study of neuronal subpopulations in BAC transgenic mice. PLoS One. 4, e4770.

267. Mateo Y., Johnson K. A., Covey D. P., Atwood B. K., Wang H. L., Zhang S., et al. (2017). Endocannabinoid actions on cortical terminals orchestrate local modulation of dopamine release in the nucleus accumbens. Neuron 96 1112–1126.

268. Mathur, B. N., Capik, N. A., Alvarez, V. A., & Lovinger, D. M. (2011). Serotonin induces long-term depression at corticostriatal synapses. The Journal of neuroscience : the official journal of the Society for Neuroscience, 31(20), 7402–7411.

269. Mato, S., Robbe, D., Puente, N., Grandes, P., & Manzoni, O. J. (2005). Presynaptic homeostatic plasticity rescues long-term depression after chronic Delta 9-tetrahydrocannabinol exposure. The Journal of neuroscience : the official journal of the Society for Neuroscience, 25(50), 11619–11627.

270. Maurage, P., Pabst, A., Lannoy, S., D'Hondt, F., de Timary, P., Gaudelus, B., & Peyroux, E. (2021). Tackling heterogeneity: Individual variability of emotion decoding deficits in severe alcohol use disorder. Journal of affective disorders, 279, 299–307

271. McCarty, D., Argeriou, M., Huebner, R. B., & Lubran, B. (1991). Alcoholism, drug abuse, and the homeless. The American psychologist, 46(11), 1139–1148.

272. McCutcheon, J. E., Loweth, J. A., Ford, K. A., Marinelli, M., Wolf, M. E., & Tseng, K. Y. (2011). Group I mGluR activation reverses cocaine-induced accumulation of calcium-permeable AMPA receptors in nucleus accumbens synapses via a protein kinase C-dependent mechanism. The Journal of neuroscience : the official journal of the Society for Neuroscience, 31(41), 14536–14541.

273. McGinn, M. A., Pantazis, C. B., Tunstall, B. J., Marchette, R. C. N., Carlson, E. R., Said, N., Koob, G. F., & Vendruscolo, L. F. (2021). Drug addiction co-morbidity with alcohol: Neurobiological insights. International review of neurobiology, 157, 409–472.

274. McGough NN, He DY, Logrip ML, Jeanblanc J, Phamluong K, Luong K, Kharazia V, Janak PH, Ron D. (2004). RACK1 and brain-derived neurotrophic factor: a homeostatic pathway that regulates alcohol addiction. J Neurosci. 24, 10542–10552.

275. McHugh, R. K., & Weiss, R. D. (2019). Alcohol Use Disorder and Depressive Disorders. Alcohol research : current reviews, 40(1), arcr.v40.1.01.

276. Miczek, K. A., Nikulina, E. M., Shimamoto, A., & Covington, H. E., 3rd (2011). Escalated or suppressed cocaine reward, tegmental BDNF, and accumbal dopamine caused by episodic versus continuous social stress in rats. The Journal of neuroscience : the official journal of the Society for Neuroscience, 31(27), 9848–9857.

277. Middleton F. A., Strick P. L., (2000). Basal ganglia and cerebellar loops: Motor and cognitive circuits. Brain Res. Brain Res. Rev. 31, 236–250.

278. Miguez, M. J., Bueno, D., Espinoza, L., Chan, W., & Perez, C. (2020). Among Adolescents, BDNF and Pro-BDNF Lasting Changes with Alcohol Use Are Stage Specific. Neural plasticity, 3937627.

279. Mo, M., Fu, X. Y., Zhang, X. L., Zhang, S. C., Zhang, H. Q., Wu, L., Li, J. L., & Zhou, L. (2021). Association of Plasma Pro-Brain-Derived Neurotrophic Factor (proBDNF)/Mature Brain-Derived Neurotrophic Factor (mBDNF) Levels with BDNF Gene Val66Met Polymorphism in Alcohol Dependence. Medical science monitor : international medical journal of experimental and clinical research, 27, e930421.

280. Moffat, J. J., Sakhai, S. A., Hoisington, Z. W., Ehinger, Y., & Ron, D. (2023). The BDNF Val68Met polymorphism causes a sex specific alcohol preference over social interaction and also acute tolerance to the anxiolytic effects of alcohol, a

phenotype driven by malfunction of BDNF in the ventral hippocampus of male mice. Psychopharmacology, 240(2), 303–317.

281. Monteiro, P., Barak, B., Zhou, Y., McRae, R., Rodrigues, D., Wickersham, I. R., & Feng, G. (2018). Dichotomous parvalbumin interneuron populations in dorsolateral and dorsomedial striatum. The Journal of physiology, 596(16), 3695–3707.

282. Morella, I., Hallum, H., & Brambilla, R. (2020). Dopamine D1 and Glutamate Receptors Co-operate With Brain-Derived Neurotrophic Factor (BDNF) and TrkB to Modulate ERK Signaling in Adult Striatal Slices. Frontiers in cellular neuroscience, 14, 564106.

283. Morris, D. H., Treloar, H., Tsai, C. L., McCarty, K. N., & McCarthy, D. M. (2016). Acute subjective response to alcohol as a function of reward and punishment sensitivity. Addictive behaviors, 60, 90–96.

284. Munoz, B., Fritz, B.M., Yin, F., and Atwood, B.K. (2018) Alcohol exposure disrupts mu opioid receptor-mediated long-term depression at insular cortex inputs to dorsolateral striatum. Nat. Commun. 9, 1318.

285. Muramatsu M, Lapiz MD, Tanaka E, Grenhoff J. (1998). Serotonin inhibits synaptic glutamate currents in rat nucleus accumbens neurons via presynaptic 5-HT1B receptors. Eur J Neurosci. 10, 2371–2379.

286. Mustonen, H., Kiviluoto, T., Paimela, H., Puolakkainen, P., and Kivilaakso, E. (2005) Calcium signaling is involved in ethanol-induced volume decrease and gap junction closure in cultured rat gastric mucosal cells. Dig. Dis. Sci. 50, 103-10.

287. Nakanishi, S., Hikida, T., & Yawata, S. (2014). Distinct dopaminergic control of the direct and indirect pathways in reward-based and avoidance learning behaviors. Neuroscience, 282, 49–59.

288. Nam, H. W., Bruner, R. C., & Choi, D. S. (2013). Adenosine signaling in striatal circuits and alcohol use disorders. Molecules and cells, 36(3), 195–202.

289. Narahashi, T., Kuriyama, K., Illes, P., Wirkner, K., Fischer, W., Mühlberg, K., Scheibler, P., Allgaier, C., Minami, K., Lovinger, D., Lallemand, F., Ward, R. J., DeWitte, P., Itatsu, T., Takei, Y., Oide, H., Hirose, M., Wang, X. E., Watanabe, S., Tateyama, M., … Sato, N. (2001). Neuroreceptors and ion channels as targets of alcohol. Alcoholism, clinical and experimental research, 25(5 Suppl ISBRA), 182S–188S.

290. Narita M, Aoki K, Takagi M, Yajima Y, Suzuki T. (2003). Implication of brain-derived neurotrophic factor in the release of dopamine and dopamine-related behaviors induced by methamphetamine. Neuroscience. 119:767–775.

291. Navabpour, S., Rezayof, A., & Ghasemzadeh, Z. (2021). Activation of VTA/CeA/mPFC cannabinoid CB1 receptors induced conditioned drug effects via interacting with hippocampal CAMKII-CREB-BDNF signaling pathway in rats. European journal of pharmacology, 909, 174417.

292. Nees, F., Witt, S. H., Dinu-Biringer, R., Lourdusamy, A., Tzschoppe, J., Vollstädt-Klein, S., Millenet, S., Bach, C., Poustka, L., Banaschewski, T., Barker, G. J., Bokde, A. L., Bromberg, U., Büchel, C., Conrod, P. J., Frank, J., Frouin, V., Gallinat, J., Garavan, H., Gowland, P., … IMAGEN consortium (2015). BDNF Val66Met and reward-related brain function in adolescents: role for early alcohol consumption. Alcohol (Fayetteville, N.Y.), 49(2), 103–110.

293. Nelson A. B., Hammack N., Yang C. F., Shah N. M., Seal R. P., Kreitzer A. C. (2014). Striatal cholinergic interneurons Drive GABA release from dopamine terminals. Neuron 82 63–70.

294. Nestler, E. J., & Carlezon, W. A., Jr (2006). The mesolimbic dopamine reward circuit in depression. Biological psychiatry, 59(12), 1151–1159.

295. Nguyen, D., Fugariu, V., Erb, S., & Ito, R. (2018). Dissociable roles of the nucleus accumbens D1 and D2 receptors in regulating cue-elicited approach-avoidance conflict decision-making. Psychopharmacology, 235(8), 2233–2244.

296. Nicola SM, Surmeier J, Malenka RC. (2000). Dopaminergic modulation of neuronal excitability in the striatum and nucleus accumbens. Annu Rev Neurosci. 23, 185–215.

297. Nikulina, E. M., Arrillaga-Romany, I., Miczek, K. A., & Hammer, R. P., Jr (2008). Long-lasting alteration in mesocorticolimbic structures after repeated social defeat stress in rats: time course of mu-opioid receptor mRNA and FosB/DeltaFosB immunoreactivity. The European journal of neuroscience, 27(9), 2272–2284.

298. Ninan, I., Bath, K. G., Dagar, K., Perez-Castro, R., Plummer, M. R., Lee, F. S., & Chao, M. V. (2010). The BDNF Val66Met polymorphism impairs NMDA receptor-dependent synaptic plasticity in the hippocampus. The Journal of neuroscience : the official journal of the Society for Neuroscience, 30(26), 8866–8870.

299. Nisenbaum, E., and Berger, T. (1992). Functionally distinct subpopulations of striatal neurons are differentially regulated by GABAergic and dopaminergic inputs – I. In vivo analysis. Neuroscience, 48, 561-578.

300. O'Hare JK, Li H, Kim N, Gaidis E, Ade K, Beck J, et al. (2017). Striatal fast-spiking interneurons selectively modulate circuit output and are required for habitual behavior. Elife. 6, e26231.

301. Oran, Y., Bar-Gad, I. (2018). Loss of Balance between Striatal Feedforward Inhibition and Corticostriatal Excitation Leads to Tremor. J Neurosci, 38(7): 1699-1710.

302. Owen, S. F., Berke, J. D., & Kreitzer, A. C. (2018). Fast-Spiking Interneurons Supply Feedforward Control of Bursting, Calcium, and Plasticity for Efficient Learning. Cell, 172(4), 683–695.e15.

303. Pagliusi, M., Jr, Franco, D., Cole, S., Morais-Silva, G., Chandra, R., Fox, M. E., Iñiguez, S. D., Sartori, C. R., & Lobo, M. K. (2022). The BDNF-TrkB Pathway Acts Through Nucleus Accumbens D2 Expressing Neurons to Mediate Stress Susceptible Outcomes. Frontiers in psychiatry, 13, 854494.

304. Palencia, C. A., & Ragozzino, M. E. (2006). The effect of N-methyl-D-aspartate receptor blockade on acetylcholine efflux in the dorsomedial striatum during response reversal learning. Neuroscience, 143(3), 671–678.

305. Papp, E., Borhegyi, Z., Tomioka, R., Rockland, K. S., Mody, I., & Freund, T. F. (2012). Glutamatergic input from specific sources influences the nucleus accumbens-ventral pallidum information flow. Brain structure & function, 217(1), 37–48.

306. Parthasarathy HB, Schall JD, Graybiel AM. (1992). Distributed but convergent ordering of corticostriatal projections: analysis of the frontal eye field and the supplementary eye field in the macaque monkey. J Neurosci. 12:4468–4488.

307. Pasala, S., Barr, T., & Messaoudi, I. (2015). Impact of Alcohol Abuse on the Adaptive Immune System.

308. Pascoli, V., Turiault, M., and Lüscher, C. (2011). Reversal of cocaine-evoked synaptic potentiation resets drug-induced adaptive behaviour. Nature, 481, 71–75.

309. Patton, M. H., Padgett, K. E., McKeon, P. N., Qadir, H., Patton, M. S., Mu, C., Roberts, B. M., & Mathur, B. N. (2019). TrkB-dependent disinhibition of the nucleus accumbens is enhanced by ethanol. Neuropsychopharmacology : official publication of the American College of Neuropsychopharmacology, 44(6), 1114–1122.

310. Patton, M. H., Roberts, B.M., Lovinger, D.M., Mathur, B.N. (2016) Ethanol Disinhibits Dorsolateral Striatal Medium Spiny Neurons Through Activation of A Presynaptic Delta Opioid Receptor. Neuropsychopharmacology 41, 1831-40.

311. Patton, M. S., Heckman, M., Kim, C., Mu, C., & Mathur, B. N. (2021). Compulsive alcohol consumption is regulated by dorsal striatum fast-spiking interneurons.

Neuropsychopharmacology : official publication of the American College of Neuropsychopharmacology, 46(2), 351–359.

312. Patton, M. S., Sheats, S. H., Siclair, A. N., & Mathur, B. N. (2023). Alcohol potentiates multiple GABAergic inputs to dorsal striatum fast-spiking interneurons. Neuropharmacology, 232, 109527.

313. Pattwell, S. S., Bath, K. G., Perez-Castro, R., Lee, F. S., Chao, M. V., & Ninan, I. (2012). The BDNF Val66Met polymorphism impairs synaptic transmission and plasticity in the infralimbic medial prefrontal cortex. The Journal of neuroscience : the official journal of the Society for Neuroscience, 32(7), 2410–2421.

314. Pautassi RM, Suárez AB, Hoffmann LB, Rueda AV, Rae M, Marianno P, Camarini R. (2017). Effects of environmental enrichment upon ethanol-induced conditioned place preference and pre-frontal BDNF levels in adolescent and adult mice. Sci Rep. 7(1), 8574.

315. Peciña, M., Martínez-Jauand, M., Love, T., Heffernan, J., Montoya, P., Hodgkinson, C., Stohler, C. S., Goldman, D., & Zubieta, J. K. (2014). Valence-specific effects of BDNF Val66Met polymorphism on dopaminergic stress and reward processing in humans. The Journal of neuroscience : the official journal of the Society for Neuroscience, 34(17), 5874–5881.

316. Pena-Bravo, J. I., Penrod, R., Reichel, C. M., & Lavin, A. (2019). Methamphetamine Self-Administration Elicits Sex-Related Changes in Postsynaptic Glutamate Transmission in the Prefrontal Cortex. eNeuro, 6(1), ENEURO.0401-18.2018.

317. Pennartz CM, Ito R, Verschure PF, Battaglia FP, Robbins TW. (2011). The hippocampalstriatal axis in learning, prediction and goal-directed behavior. Trends Neurosci. 34, 548–559.

318. Pezze M. A., Feldon J. (2004). Mesolimbic dopaminergic pathways in fear conditioning. Prog. Neurobiol. 74 301–320.

319. Pfeuty, B., Mato, G., Golomb, D., & Hansel, D. (2003). Electrical synapses and synchrony: the role of intrinsic currents. J. Neurosci. 23, 6280–6294.

320. Phillips, K., Keane, K., & Wolfe, B. E. (2014). Peripheral brain derived neurotrophic factor (BDNF) in bulimia nervosa: a systematic review. Archives of psychiatric nursing, 28(2), 108–113.

321. Phillipson, O. T., & Griffiths, A. C. (1985). The topographic order of inputs to nucleus accumbens in the rat. Neuroscience, 16(2), 275–296.

322. Pickard H. (2022). Is addiction a brain disease? A plea for agnosticism and heterogeneity. Psychopharmacology, 239(4), 993–1007.

323. Pickel V. M., Chan J., Kearn C. S., Mackie K. (2006). Targeting dopamine D2 and cannabinoid-1 (CB1) receptors in rat nucleus accumbens. J. Comp. Neurol. 495 299–313.

324. Pietrucci, C. L., Milton, L. K., Greaves, E., Stefanidis, A., van den Buuse, M., Oldfield, B. J., & Foldi, C. J. (2022). The BDNF Val66Met Polymorphism Does Not Increase Susceptibility to Activity-Based Anorexia in Rats. Biology, 11(5), 623.

325. Pozhidayeva, D. Y., Farris, S. P., Goeke, C. M., Firsick, E. J., Townsley, K. G., Guizzetti, M., & Ozburn, A. R. (2020). Chronic Chemogenetic Stimulation of the Nucleus Accumbens Produces Lasting Reductions in Binge Drinking and Ameliorates Alcohol-Related Morphological and Transcriptional Changes. Brain sciences, 10(2), 109.

326. Prado VF, Janickova H, Al-Onaizi MA, Prado MA. (2017). Cholinergic circuits in cognitive flexibility. Neuroscience. 345, 130–141.

327. Puddephatt, J. A., Irizar, P., Jones, A., Gage, S. H., & Goodwin, L. (2022). Associations of common mental disorder with alcohol use in the adult general population: a systematic review and meta-analysis. Addiction (Abingdon, England), 117(6), 1543–1572.

328. Purohit, K., Parekh, P. K., Kern, J., Logan, R. W., Liu, Z., Huang, Y., McClung, C. A., Crabbe, J. C., & Ozburn, A. R. (2018). Pharmacogenetic Manipulation of the Nucleus Accumbens Alters Binge-Like Alcohol Drinking in Mice. Alcoholism, clinical and experimental research, 42(5), 879–888.

329. Qi J., Zhang S., Wang H. L., Barker D. J., Miranda-Barrientos J., Morales M. (2016). VTA glutamatergic inputs to nucleus accumbens drive aversion by acting on GABAergic interneurons. Nat. Neurosci. 19 725–733.

330. Raivio, N., Miettinen, P., and Kiianmaa, K. (2014). Innate BDNF expression is associated with ethanol intake in alcohol-preferring AA and alcohol avoiding ANA rats. Brain Research, 1579, 74-83.

331. Ramanathan, S., Hanley, J. J., Deniau, J. M., & Bolam, J. P. (2002). Synaptic convergence of motor and somatosensory cortical afferents onto GABAergic interneurons in the rat striatum. The Journal of neuroscience : the official journal of the Society for Neuroscience, 22(18), 8158–8169.

332. Redlich, R., Schneider, I., Kerkenberg, N., Opel, N., Bauhaus, J., Enneking, V., Repple, J., Leehr, E. J., Grotegerd, D., Kähler, C., Förster, K., Dohm, K., Meinert,

S., Hahn, T., Kugel, H., Schwarte, K., Schettler, C., Domschke, K., Arolt, V., Heindel, W., … Dannlowski, U. (2020). The role of BDNF methylation and Val66 Met in amygdala reactivity during emotion processing. Human brain mapping, 41(3), 594–604.

333. Reidy, J., McHugh, E., & Stassen, L. F. (2011). A review of the relationship between alcohol and oral cancer. The surgeon : journal of the Royal Colleges of Surgeons of Edinburgh and Ireland, 9(5), 278–283.

334. Rhodes JS, Best K, Belknap JK, Finn DA, Crabbe JC. (2005). Evaluation of a simple model of ethanol drinking to intoxication in C57BL/6J mice. Physiol Behav. 84, 53–63.

335. Ribeiro E. A., Nectow A. R., Pomeranz L. E., Ekstrand M. I., Koo J. W., Nestler E. J. (2019). Viral labeling of neurons synaptically connected to nucleus accumbens somatostatin interneurons. PLoS One 14:e0213476.

336. Rice M. E., Cragg S. J. (2008). Dopamine spillover after quantal release: rethinking dopamine transmission in the nigrostriatal pathway. Brain Res. Rev. 58 303–313.

337. Roberts, B. M., White, M. G., Patton, M. H., Chen, R., & Mathur, B. N. (2019). Ensemble encoding of action speed by striatal fast-spiking interneurons. Brain structure & function, 224(7), 2567–2576.

338. Robertson M. J. (1991). Homeless women with children. The role of alcohol and other drug abuse. The American psychologist, 46(11), 1198–1204.

339. Rocco, A., Compare, D., Angrisani, D., Sanduzzi Zamparelli, M., & Nardone, G. (2014). Alcoholic disease: liver and beyond. World journal of gastroenterology, 20(40), 14652–14659.

340. Roltsch Hellard, E., Binette, A., Zhuang, X., Lu, J., Ma, T., Jones, B., Williams, E., Jayavelu, S., & Wang, J. (2019). Optogenetic control of alcohol-seeking behavior via the dorsomedial striatal circuit. Neuropharmacology, 155, 89–97.

341. Ron, D., & Berger, A. (2018). Targeting the intracellular signaling "STOP" and "GO" pathways for the treatment of alcohol use disorders. Psychopharmacology, 235(6), 1727–1743

342. Ross, S., & Peselow, E. (2009). Pharmacotherapy of addictive disorders. Clinical neuropharmacology, 32(5), 277–289.

343. Russo S. J., Nestler E. J. (2013). The brain reward circuitry in mood disorders. Nat. Rev. Neurosci. 14 609–625.

344. Russo, S. J., Dietz, D. M., Dumitriu, D., Morrison, J. H., Malenka, R. C., & Nestler, E. J. (2010). The addicted synapse: mechanisms of synaptic and structural plasticity in nucleus accumbens. Trends in neurosciences, 33(6), 267–276.

345. Russo, S., Mazei-Robison, M., Ables, J., and Nestler, E. (2009). Neurotrophic factors and structural plasticity in addiction. Neuropharmacology, 56, 73–82.

346. Rygula R, Abumaria N, Flügge G, Fuchs E, Rüther E, Havemann-Reinecke U. (2005). Anhedonia and motivational deficits in rats: impact of chronic social stress. Behavioural Brain Research. 162(1), 127–34.

347. Sagarkar, S., Choudhary, A. G., Balasubramanian, N., Awathale, S. N., Somalwar, A. R., Pawar, N., Kokare, D. M., Subhedar, N. K., & Sakharkar, A. J. (2021). LSD1-BDNF activity in lateral hypothalamus-medial forebrain bundle area is essential for reward seeking behavior. Progress in neurobiology, 202, 102048.

348. Saha T. D., Grant B. F., Chou S. P., Kerridge B. T., Pickering R. P. and Ruan W. J. (2018) Concurrent use of alcohol with other drugs and DSM-5 alcohol use disorder comorbid with other drug use disorders: sociodemographic characteristics, severity, and psychopathology. Drug Alcohol. Depend. 187, 261–269.

349. Salamone J. D., Correa M. (2002). Motivational views of reinforcement: implications for understanding the behavioral functions of nucleus accumbens dopamine. Behav. Brain Res. 137 3–25.Salkoff, D. B., Zagha, E., Yuzgec, O., McCormick, D.A. (2015) Synaptic Mechanisms of Tight Spike Synchrony at Gamma Frequency in Cerebral Cortex. J. Neurosci. 35, 10236-51.

350. Sandoval-Rodríguez, R., Parra-Reyes, J. A., Han, W., Rueda-Orozco, P. E., Perez, I. O., de Araujo, I. E., & Tellez, L. A. (2023). D1 and D2 neurons in the nucleus accumbens enable positive and negative control over sugar intake in mice. Cell reports, 42(3), 112190.

351. Schall T. A., Wright W. J., Dong Y. (2021). Nucleus accumbens fast-spiking interneurons in motivational and addictive behaviors. Mol. Psychiatry 26 234–246.

352. Schlösser B, Bruggencate G, Sutor B. (1999). Local disinhibition of neocortical neuronal circuits causes augmentation of glutamatergic and GABAergic synaptic transmission in the rat neostratium in vitro. Exp Neurol. 157, 180–93.

353. Schmid, F., Benzerouk, F., Barrière, S., Henry, A., Limosin, F., Kaladjian, A., & Gierski, F. (2021). Heterogeneity of Executive Function Abilities in Recently Detoxified Patients with Alcohol Use Disorder: Evidence from a Cluster Analysis. Alcoholism, clinical and experimental research, 45(1), 163–173.fostering analysis of adopted men. Archives of general psychiatry, 38(8), 861–868.

354. Schmidt HD, Pierce RC. (2010). Cocaine-induced neuroadaptations in glutamate transmission: potential therapeutic targets for craving and addiction. Ann N Y Acad Sci. 1187, 35–75.

355. Schotanus, S. M., & Chergui, K. (2008). Dopamine D1 receptors and group I metabotropic glutamate receptors contribute to the induction of long-term potentiation in the nucleus accumbens. Neuropharmacology, 54(5), 837–844.

356. Schultz W. (2011). Potential vulnerabilities of neuronal reward, risk, and decision mechanisms to addictive drugs. Neuron. 69, 603–617.

357. Schultz, W. (2016). Reward functions of the basal ganglia. J Neural Transm, 123, 679–693.

358. Schwabe L, Wolf OT. (2009). Stress Prompts Habit Behavior in Humans. European Journal of Neuroscience. 29(22), 7191–7198.

359. Sciamanna G., Ponterio G., Mandolesi G., Bonsi P., Pisani A. (2015) Optogenetic stimulation reveals distinct modulatory properties of thalamostriatal vs corticostriatal glutamatergic inputs to fast spiking interneurons. Sci Rep. 5:16742.

360. Scudder S. L., Baimel C., Macdonald E. E., Carter A. G. (2018). Hippocampal-evoked feedforward inhibition in the nucleus accumbens. J. Neurosci. 38 9091–9104.

361. Sebold, M., Deserno, L., Nebe, S., Schad, D. J., Garbusow, M., Hägele, C., Keller, J., Jünger, E., Kathmann, N., Smolka, M. N., Rapp, M. A., Schlagenhauf, F., Heinz, A., & Huys, Q. J. (2014). Model-based and model-free decisions in alcohol dependence. Neuropsychobiology, 70(2), 122–131.

362. Sebold, M., Nebe, S., Garbusow, M., Guggenmos, M., Schad, D. J., Beck, A., Kuitunen-Paul, S., Sommer, C., Frank, R., Neu, P., Zimmermann, U. S., Rapp, M. A., Smolka, M. N., Huys, Q. J. M., Schlagenhauf, F., & Heinz, A. (2017). When Habits Are Dangerous: Alcohol Expectancies and Habitual Decision Making Predict Relapse in Alcohol Dependence. Biological psychiatry, 82(11), 847–856.

363. Segel, L. D., Klausner, S. C., Gnadt, J. T., & Amsterdam, E. A. (1984). Alcohol and the heart. The Medical clinics of North America, 68(1), 147–161

364. Seiler, J. L., Cosme, C. V., Sherathiya, V. N., Schaid, M. D., Bianco, J. M., Bridgemohan, A. S., & Lerner, T. N. (2022). Dopamine signaling in the dorsomedial striatum promotes compulsive behavior. Current biology : CB, 32(5), 1175–1188.

365. Seroogy, K., Lundgren, K., Tran, T., Guthrie, K., Isackson, P., and Gall, C. (1994). Dopaminergic neurons in rat ventral midbrain express brain-derived neurotrophic factor and neurotrophin-3 mRNAs. J Comp Neurol, 342, 321–334

366. Sesack, S.R., and Grace, A.A. (2010). Cortico-Basal Ganglia reward network: microcircuitry. Neuropsychopharmacology, 35, 27–47.

367. Shin J. H., Adrover M. F., Alvarez V. A. (2017). Distinctive modulation of dopamine release in the nucleus accumbens shell mediated by dopamine and acetylcholine receptors. J. Neurosci. 37 11166–11180.

368. Shobeiri, P., Bagherieh, S., Mirzayi, P., Kalantari, A., Mirmosayyeb, O., Teixeira, A. L., & Rezaei, N. (2022). Serum and plasma levels of brain-derived neurotrophic factor in individuals with eating disorders (EDs): a systematic review and meta-analysis. Journal of eating disorders, 10(1), 105.

369. Siggins GR, Roberto M, Nie Z. (2005). The tipsy terminal: presynaptic effects of ethanol. Pharmacol Ther. 107, 80–98.

370. Simet, S. M., & Sisson, J. H. (2015). Alcohol's Effects on Lung Health and Immunity. Alcohol research : current reviews, 37(2), 199–208.

371. Sjoerds Z, Wit S, Brink W, Robbins TW, Beekman ATF, Pennix BWJH, et al. (2013). Behavioral and neuroimaging evidence for overreliance on habit learning in alcohol-dependent patients. Transl Psychiatry. 3, 1–8.

372. Sjoerds, Z., de Wit, S., van den Brink, W., Robbins, T. W., Beekman, A. T., Penninx, B. W., & Veltman, D. J. (2013). Behavioral and neuroimaging evidence for overreliance on habit learning in alcohol-dependent patients. Translational psychiatry, 3(12), e337.

373. Smart, R. G., & Mann, R. E. (2000). The impact of programs for high-risk drinkers on population levels of alcohol problems. Addiction (Abingdon, England), 95(1), 37–51.

374. Smith A. C. W., Scofield M. D., Heinsbroek J. A., Gipson C. D., Neuhofer D., Roberts-Wolfe D. J., et al. (2017). Accumbens nNOS interneurons regulate cocaine relapse. J. Neurosci. 37 742–756.

375. Smith Y, Raju DV, Pare JF, Sidibe M. (2004). The thalamostriatal system: a highly specific network of the basal ganglia circuitry. Trends Neurosci. 27, 520–527

376. Snyder GL, Allen PB, Fienberg AA, Valle CG, Huganir RL, Nairn AC, Greengard P. (2000). Regulation of phosphorylation of the GluR1 AMPA receptor in the neostriatum by dopamine and psychostimulants in vivo. J Neurosci. 20, 4480–4488.

377. Snyder, J. L., & Bowers, T. G. (2008). The efficacy of acamprosate and naltrexone in the treatment of alcohol dependence: a relative benefits analysis of randomized controlled trials. The American journal of drug and alcohol abuse, 34(4), 449–461.

378. Soares JM, Sampaio A, Ferreira LM, Santos NC, Marques F, Palha JA, Sousa N. (2012). Stress-induced changes in human decision-making are reversible. Translational Psychiatry. 2:e131.

379. Soares-Cunha, C., Coimbra, B., David-Pereira, A., Borges, S., Pinto, L., Costa, P., Sousa, N., & Rodrigues, A. J. (2016). Activation of D2 dopamine receptor-expressing neurons in the nucleus accumbens increases motivation. Nature communications, 7, 11829.

380. Soares-Cunha, C., Coimbra, B., Sousa, N., & Rodrigues, A. J. (2016). Reappraising striatal D1- and D2-neurons in reward and aversion. Neuroscience and biobehavioral reviews, 68, 370–386.

381. Soares-Cunha, C., de Vasconcelos, N. A. P., Coimbra, B., Domingues, A. V., Silva, J. M., Loureiro-Campos, E., Gaspar, R., Sotiropoulos, I., Sousa, N., & Rodrigues, A. J. (2020). Nucleus accumbens medium spiny neurons subtypes signal both reward and aversion. Molecular psychiatry, 25(12), 3241–3255.

382. Soares-Cunha, C., Domingues, A. V., Correia, R., Coimbra, B., Vieitas-Gaspar, N., de Vasconcelos, N. A. P., Pinto, L., Sousa, N., & Rodrigues, A. J. (2022). Distinct role of nucleus accumbens D2-MSN projections to ventral pallidum in different phases of motivated behavior. Cell reports, 38(7), 110380.

383. Söderpalm, B., & Ericson, M. (2013). Neurocircuitry involved in the development of alcohol addiction: the dopamine system and its access points. Current topics in behavioral neurosciences, 13, 127–161.

384. Söderpalm, B., Löf, E., & Ericson, M. (2009). Mechanistic studies of ethanol's interaction with the mesolimbic dopamine reward system. Pharmacopsychiatry, 42 Suppl 1, S87–S94.

385. Spies, C. D., Sander, M., Stangl, K., Fernandez-Sola, J., Preedy, V. R., Rubin, E., Andreasson, S., Hanna, E. Z., & Kox, W. J. (2001). Effects of alcohol on the heart. Current opinion in critical care, 7(5), 337–343.

386. Stephen Rich, J., & Martin, P. R. (2014). Co-occurring psychiatric disorders and alcoholism. Handbook of clinical neurology, 125, 573–588.

387. Stuber GD, Britt JP, Bonci A. (2012). Optogenetic modulation of neural circuits that underlie reward seeking. Biol Psychiatry. 71(12),1061-7.

388. Stuber GD, Hnasko TS, Britt JP, Edwards RH, Bonci A. (2010). Dopaminergic terminals in the nucleus accumbens but not the dorsal striatum corelease glutamate. J Neurosci. 30, 8229–8233.

389. Stuber GD, Klanker M, de Ridder B, Bowers MS, Joosten RN, Feenstra MG, Bonci A. (2008). Reward-predictive cues enhance excitatory synaptic strength onto midbrain dopamine neurons. Science. 321, 1690–1692.

390. Sun X, Milovanovic M, Zhao Y, Wolf ME. (2008). Acute and chronic dopamine receptor stimulation modulates AMPA receptor trafficking in nucleus accumbens neurons cocultured with prefrontal cortex neurons. J Neurosci. 28, 4216–4230.

391. Sun X, Zhao Y, Wolf ME. (2005). Dopamine receptor stimulation modulates AMPA receptor synaptic insertion in prefrontal cortex neurons. J Neurosci. 25, 7342–7351.

392. Surmeier D. J., Song W. J., Yan Z. (1996). Coordinated expression of dopamine receptors in neostriatal medium spiny neurons. J. Neurosci. 16 6579–6591.

393. Surmeier DJ, Ding J, Day M, Wang Z, Shen W. (2007). D1 and D2 dopamine-receptor modulation of striatal glutamatergic signaling in striatal medium spiny neurons. Trends Neurosci. 30, 228–235.

394. Surtel, A., Klepacz, R., & Wysokińska-Miszczuk, J. (2014). Następstwa uzależnienia od alkoholuobserwowane w jamie ustnej [Alcohol dependence syndrome--symptoms in the oral cavity]. Postepy higieny i medycyny doswiadczalnej (Online), 68, 828–833.

395. Swant, J., Stramiello, M., & Wagner, J. J. (2008). Postsynaptic dopamine D3 receptor modulation of evoked IPSCs via GABA(A) receptor endocytosis in rat hippocampus. Hippocampus, 18(5), 492–502.

396. Szabo, G., & Saha, B. (2015). Alcohol's Effect on Host Defense. Alcohol research : current reviews, 37(2), 159–170.

397. Tai L-H, Lee AM, Benavidez N, Bonci A, Wilbrecht L. (2012). Transient stimulation of distinct subpopulations of striatal neurons mimics changes in action value. Nat Neurosci. 15, 1281.

398. Takada M, Tokuno H, Nambu A, Inase M. (1998). Corticostriatal projections from the somatic motor areas of the frontal cortex in the macaque monkey: segregation versus overlap of input zones from the primary motor cortex, the supplementary motor area, and the premotor cortex. Exp Brain Res. 120, 114–128.

399. Tanahira, C. et al. (2009) Parvalbumin neurons in the forebrain as revealed by parvalbumin-Cre transgenic mice. Neurosci. Res. 63, 213–23.

400. Taverna S., Canciani B., Pennartz C. M. (2007). Membrane properties and synaptic connectivity of fast-spiking interneurons in rat ventral striatum. Brain Res. 1152 49–56.

401. Tecuapetla F, Patel JC, Xenias H, English D, Tadros I, Shah F, et al. (2010). Glutamatergic signaling by mesolimbic dopamine neurons in the nucleus accumbens. J Neurosci. 30, 7105–7110.

402. Tepper JM, Koós T, Wilson CJ. (2004). GABAergic microcircuits in the neostriatum. Trends Neurosci. 27, 662–9.

403. Terracciano, A., Tanaka, T., Sutin, A. R., Deiana, B., Balaci, L., Sanna, S., Olla, N., Maschio, A., Uda, M., Ferrucci, L., Schlessinger, D., & Costa, P. T., Jr (2010). BDNF Val66Met is associated with introversion and interacts with 5-HTTLPR to influence neuroticism. Neuropsychopharmacology : official publication of the American College of Neuropsychopharmacology, 35(5), 1083–1089.

404. Thomas, M., Beurrier, C., Bonci, A., and Malenka, R. (2001). Long-term depression in the nucleus accumbens: a neural correlate of behavioral sensitization to cocaine. Nat Neurosci, 4, nn757.

405. Threlfell, S., Lalic, T., Platt, N. J., Jennings, K. A., Deisseroth, K., & Cragg, S. J. (2012). Striatal dopamine release is triggered by synchronized activity in cholinergic interneurons. Neuron, 75(1), 58–64

406. Ting, J. T., Daigle, T. L., Chen, Q., and Feng, G. (2014) Acute brain slice methods for adult and aging animals: application of targeted patch clamp analysis and optogenetics. Methods Mol. Biol. 1183, 221–42.

407. Ting, J.T., Lee, B.R., Chong, P., Soler-Llavina, G., Cobbs, C., Koch, C., Zeng, H., and Lein, E. (2018) Preparation of Acute Brain Slices Using an Optimized N-Methyl-D-glucamine Protective Recovery Method. J. Vis. Exp. 132.

408. Traub, R.D., Whittington, M.A., Buhl, E.H., LeBeau F.E., Bibbig, A., Boyd, S., Cross, H., and Baldeweg, T. (2001) A possible role for gap junctions in generation of very fast EEG oscillations preceding the onset of, and perhaps initiating, seizures. Epilepsia 42, 153-70.

409. Tritsch, N. X., Oh, W. J., Gu, C., & Sabatini, B. L. (2014). Midbrain dopamine neurons sustain inhibitory transmission using plasma membrane uptake of GABA, not synthesis. eLife, 3, e01936.

410. Trouche S., Koren V., Doig N. M., Ellender T. J., El-Gaby M., Lopes-Dos-Santos V., et al. (2019). A hippocampus-accumbens tripartite neuronal motif guides appetitive memory in space. Cell 176 1393–1406 e16

411. Valjent E, Bertran-Gonzalez J, Herve D, Fisone G, Girault JA. (2009). Looking BAC at striatal signaling: cell-specific analysis in new transgenic mice. Trends Neurosci. 32, 538–547

412. van der Merwe, R. K., Nadel, J. A., Copes-Finke, D., Pawelko, S., Scott, J. S., Ghanem, M., Fox, M., Morehouse, C., McLaughlin, R., Maddox, C., Albert-Lyons, R., Malaki, G., Groce, V., Turocy, A., Aggadi, N., Jin, X., & Howard, C. D. (2023). Characterization of striatal dopamine projections across striatal subregions in behavioral flexibility. The European journal of neuroscience, 10.1111/ejn.15910. Advance online publication.

413. Vaynman, S., Ying, Z., & Gomez-Pinilla, F. (2004). Hippocampal BDNF mediates the efficacy of exercise on synaptic plasticity and cognition. The European journal of neuroscience, 20(10), 2580–2590.

414. Volkow, N. D., & Morales, M. (2015). The Brain on Drugs: From Reward to Addiction. Cell, 162(4), 712–725.

415. Waeiss, R. A., Knight, C. P., Engleman, E. A., Hauser, S. R., & Rodd, Z. A. (2020). Co-administration of ethanol and nicotine heightens sensitivity to ethanol reward within the nucleus accumbens (NAc) shell and increasing NAc shell BDNF is sufficient to enhance ethanol reward in naïve Wistar rats. Journal of neurochemistry, 152(5), 556–569.

416. Wang J, Ben Hamida S, Darcq E, Zhu W, Gibb SL, Lanfranco MF, Carnicella S, Ron D. (2012). Ethanol-mediated facilitation of AMPA receptor function in the dorsomedial striatum: implications for alcohol drinking behavior. Journal of Neuroscience 32, 15124–15132.

417. Wang J, Lanfranco MF, Gibb SL, Yowell QV, Carnicella S, Ron D. (2010). Long-lasting adaptations of the NR2B-containing NMDA receptors in the dorsomedial striatum play a crucial role in alcohol consumption and relapse. Journal of Neuroscience 30, 10187–10198.

418. Wang, H. P., Garcia, J. W., Sabottke, C. F., Spencer, D. J., & Sejnowski, T. J. (2019). Feedforward Thalamocortical Connectivity Preserves Stimulus Timing Information in Sensory Pathways. The Journal of neuroscience : the official journal of the Society for Neuroscience, 39(39), 7674–7688.

419. Wang, J., Bastle, R. M., & Nikulina, E. M. (2017). VTA BDNF enhances social stress-induced compulsive cocaine bingeing. Oncotarget, 8(4), 5668–5669.

420. Wang, J., Bastle, R. M., Bass, C. E., Hammer, R. P., Jr, Neisewander, J. L., & Nikulina, E. M. (2016). Overexpression of BDNF in the ventral tegmental area

enhances binge cocaine self-administration in rats exposed to repeated social defeat. Neuropharmacology, 109, 121–130.

421. Wang, X., Chen, X., Lu, L., & Yu, X. (2021). Alcoholism and Osteoimmunology. Current medicinal chemistry, 28(9), 1815–1828.

422. Wang, Z., Flores, I., Donahue, E. K., Lundquist, A. J., Guo, Y., Petzinger, G. M., Jakowec, M. W., & Holschneider, D. P. (2020). Cognitive flexibility deficits in rats with dorsomedial striatal 6-hydroxydopamine lesions tested using a three-choice serial reaction time task with reversal learning. Neuroreport, 31(15), 1055–1064.

423. Warnault, V., Darcq, E., Morisot, N., Phamluong, K., Wilbrecht, L., Massa, S.M., Longo, F.M., and Ron, D. (2016). The BDNF Valine 68 to Methionine Polymorphism Increases Compulsive Alcohol Drinking in Mice That Is Reversed by Tropomyosin Receptor Kinase B Activation. Biological Psychiatry, 79(6), 463-473.

424. Watanabe, D., Savion-Lemieux, T., and Penhune, V.B. (2007) The effect of early musical training on adult motor performance: evidence for a sensitive period in motor learning. Exp. Brain. Res. 176, 332-340.

425. Wentlandt, K., Kushnir, M., Naus, C. C. G., and Carlen, P. L. (2004) Ethanol inhibits gap-junctional coupling between P19 cells. Alcohol Clin. Exp. Res. 28, 1284-90.

426. Wenzel, J. M., Su, Z. I., Shelton, K., Dominguez, H. M., von Furstenberg, V. A., & Ettenberg, A. (2013). The dopamine antagonist cis-flupenthixol blocks the expression of the conditioned positive but not the negative effects of cocaine in rats. Pharmacology, biochemistry, and behavior, 114-115, 90–96.

427. White, N. M., Packard, M. G., & Hiroi, N. (1991). Place conditioning with dopamine D1 and D2 agonists injected peripherally or into nucleus accumbens. Psychopharmacology, 103(2), 271–276.

428. Wichmann, T., & DeLong, M. R. (1996). Functional and pathophysiological models of the basal ganglia. Current opinion in neurobiology, 6(6), 751–758.Wickens JR, Horvitz JC, Costa RM, Killcross S. (2007). Dopaminergic mechanisms in actions and habits. J Neurosci. 27(31), 8181–8183.

429. Wickens JR. Synaptic plasticity in the basal ganglia. (2009). Behavioural Brain Research. 199, 119–128.

430. Wigger, G. W., Bouton, T. C., Jacobson, K. R., Auld, S. C., Yeligar, S. M., & Staitieh, B. S. (2022). The Impact of Alcohol Use Disorder on Tuberculosis: A Review of the Epidemiology and Potential Immunologic Mechanisms. Frontiers in immunology, 13, 864817.

431. Wilcox, M. V., Cuzon Carlson, V. C., Sherazee, N., Sprow, G. M., Bock, R., Thiele, T. E., Lovinger, D. M., & Alvarez, V. A. (2014). Repeated binge-like ethanol drinking alters ethanol drinking patterns and depresses striatal GABAergic transmission. Neuropsychopharmacology : official publication of the American College of Neuropsychopharmacology, 39(3), 579–594.

432. Wilson CJ, Kawaguchi Y. (1996). The origins of two-state spontaneous membrane potential fluctuations of neostriatal spiny neurons. J Neurosci. 16:2397–2410.

433. Wilson CJ. (1995). The contribution of cortical neurons to the firing pattern of striatal spiny neurons. In: Houk JC, Davis JD, Beiser DG, editors. Models of information processing in the basal ganglia. MIT; Cambridge, MA: pp. 29–50.

434. Wiltschko, A. B., Pettibone, J. R. and Berke, J. D. (2010) Opposite effects of stimulant and antipsychotic drugs on striatal fast-spiking interneurons. Neuropsychopharmacology 35, 1261–70.

435. Witten I. B., Lin S. C., Brodsky M., Prakash R., Diester I., Anikeeva P., et al. (2010). Cholinergic interneurons control local circuit activity and cocaine conditioning. Science 330 1677–1681.

436. Wolf ME, Ferrario CR. (2010). AMPA receptor plasticity in the nucleus accumbens after repeated exposure to cocaine. Neurosci Biobehav Rev. 35, 185–211.

437. Wright W. J., Schluter O. M., Dong Y. (2017). A Feedforward inhibitory circuit mediated by CB1-expressing fast-spiking interneurons in the nucleus accumbens. Neuropsychopharmacology 42 1146–1156.

438. Xia Y, Driscoll JR, Wilbrecht L, Margolis EB, Fields HL, Hjelmstad GO. (2011). Nucleus accumbens medium spiny neurons target non-dopaminergic neurons in the ventral tegmental area. J Neurosci. 31, 7811–7816.

439. Xu, X., Ji, H., Liu, G., Wang, Q., Liu, H., Shen, W., Li, L., Xie, X., Zhou, W., & Duan, S. (2016). A significant association between BDNF promoter methylation and the risk of drug addiction. Gene, 584(1), 54–59.

440. Yamaguchi, T., Goto, A., Nakahara, I., Yawata, S., Hikida, T., Matsuda, M., Funabiki, K., & Nakanishi, S. (2015). Role of PKA signaling in D2 receptor-expressing neurons in the core of the nucleus accumbens in aversive learning. Proceedings of the National Academy of Sciences of the United States of America, 112(36), 11383–11388.

441. Yang, C. H., Yoon, S. S., Hansen, D. M., Wilcox, J. D., Blumell, B. R., Park, J. J., & Steffensen, S. C. (2010). Acupuncture inhibits GABA neuron activity in the

ventral tegmental area and reduces ethanol self-administration. Alcoholism, clinical and experimental research, 34(12), 2137–2146.

442. Yang, J. W., Ma, W., Yang, Y. L., Wang, X. B., Li, X. T., Wang, T. T., Wang, X. P., Gao, W., Li, J. Y., Zhou, X. F., Guo, J. H., & Li, L. Y. (2017). Region-specific expression of precursor and mature brain-derived neurotrophic factors after chronic alcohol exposure. The American journal of drug and alcohol abuse, 43(5), 602–608.

443. Yavas E., Young A. M. (2017). N-Methyl-d-aspartate modulation of nucleus accumbens dopamine release by metabotropic glutamate receptors: fast cyclic voltammetry studies in rat brain slices in vitro. ACS Chem. Neurosci. 8 320–328.

444. Yeterian EH, Van Hoesen GW. (1978). Cortico-striate projections in the rhesus monkey: the organization of certain cortico-caudate connections. Brain Res. 139:43–63.

445. Yin HH, Knowlton BJ, Balleine BW. (2004). Lesions of the dorsolateral striatum preserve outcome expectancy but disrupt habit formation in instrumental learning. Eur J Neurosci. 19, 181–9.

446. Yin HH, Knowlton BJ, Balleine BW. (2006). Inactivation of dorsolateral striatum enhances sensitivity to changes in the action-outcome contingency in instrumental conditioning. Behavioural Brain Res. 166, 189–96.

447. Yin, H. H., Park, B. S., Adermark, L., & Lovinger, D. M. (2007). Ethanol reverses the direction of long-term synaptic plasticity in the dorsomedial striatum. The European journal of neuroscience, 25(11), 3226–3232.

448. Yin, H.H. and Knowlton, B.J. (2006) The role of the basal ganglia in habit formation. Nat. Rev. Neurosci. 7, 464-76.

449. Yu J., Yan Y., Li K. L., Wang Y., Huang Y. H., Urban N. N., et al. (2017). Nucleus accumbens feedforward inhibition circuit promotes cocaine self-administration. Proc. Natl. Acad. Sci. U.S.A. 114 E8750–E8759.

450. Yu, J., Ishikawa, M., Wang, J., Schlüter, O. M., Sesack, S. R., & Dong, Y. (2019). Ventral Tegmental Area Projection Regulates Glutamatergic Transmission in Nucleus Accumbens. Scientific reports, 9(1), 18451.

451. Zahm D. S., Brog J. S. (1992). On the significance of subterritories in the "accumbens" part of the rat ventral striatum. Neuroscience 50 751–767.

452. Zhang H., Sulzer D. (2004). Frequency-dependent modulation of dopamine release by nicotine. Nat. Neurosci. 7 581–582.

453. Zhang M, Zhao Z, He P, and Wang J (2014) Effect of gap junctions on the firing patterns and synchrony for different external inputs in the striatal fast-spiking neuron network. Biomed Mater Eng 24, 2635–44.

454. Zhang, X-J., Zhizhong, L., Han, Z., Sultan, K.T., Huang, K., and Shi, S-H. (2017) Precise inhibitory microcircuit assembly of developmentally related neocortical interneurons in clusters. Nat. Commun. 8, 16091.

455. Zhou F. M., Wilson C. J., Dani J. A. (2002). Cholinergic interneuron characteristics and nicotinic properties in the striatum. J. Neurobiol. 53 590–605.

456. Zhou, K., Xu, H., Lu, S., Jiang, S., Hou, G., Deng, X., He, M., & Zhu, Y. (2022). Reward and aversion processing by input-defined parallel nucleus accumbens circuits in mice. Nature communications, 13(1), 6244.

457. Zhou, L., Xiong, J., Ruan, C. S., Ruan, Y., Liu, D., Bao, J. J., & Zhou, X. F. (2018). ProBDNF/p75NTR/sortilin pathway is activated in peripheral blood of patients with alcohol dependence. Translational psychiatry, 7(11), 2.

458. Zhuang, X., Masson, J., Gingrich, J. A., Rayport, S., & Hen, R. (2005). Targeted gene expression in dopamine and serotonin neurons of the mouse brain. Journal of neuroscience methods, 143(1), 27–32.